Application of Genetic Algorithms in the Optimization of a Solar Tunnel Fish Dryer Design and Performance

MICHAEL GARETH MUTHINI KITUU

(AGRICULTURAL ENGINEERING)

JOMO KENYATTA UNIVERSITY OF AGRICULTURE AND TECHNOLOGY

2011

Application of Genetic Algorithms in the Optimization of a Solar Tunnel Fish Dryer Design and Performance

Michael Gareth Muthini Kituu

A thesis submitted in fulfilment for the degree of Doctor of Philosophy in Agricultural Engineering in the Jomo Kenyatta University of Agriculture and Technology

2011

DECLARATION

This thesis is my original work and has not been presented for a degree in any other university.

Signature ..... Date .....

Michael Gareth Muthini Kituu

Signature ..... Date .....

Professor Douglas Shitanda

JKUAT, Kenya

Signature ..... Date .....

Professor Christopher Kanali

JKUAT Kenya

Signature ..... Date .....

Professor Joseph Mailutha

JKUAT Kenya

Signature ..... Date .....

Professor Charles Njoroge

JKUAT Kenya

DEDICATION

I dedicate this thesis to Jesus Christ. I further dedicate it to my father's family, my wife Angeline and my children Alice and Cornelius, who have all been and continue to be a source of encouragement in my life.

ACKNOWLEDGMENT

I thank God Almighty for enabling me to carry out this study in good health. I also extend my warm regards to Prof. D. Shitanda for co–sponsoring this research, through VicRes research project. Further, I acknowledge my supervisors: Prof. D. Shitanda, Prof. C. L. Kanali and Prof. J. T. Mailutha all from Biomechanical and Environmental Engineering Department (BEED), and Prof. C. K. Njoroge of Food Science and Technology Department (FSTD), all of the Jomo Kenyatta University of Agriculture and Technology (JKUAT) for working tirelessly and closely with me, and positive criticism in this study positively, throughout the research period. In addition, I highly regard the contribution to this work by Mr J. K. Wainaina of the Institute of Computer Science and Information Technology for his valuable assistance in programming in Visual Basic 6. I appreciate the input by Dr. P. G. Home (BEED, JKUAT) for convening regular progress seminars from which I learnt a lot, and this enabled me to perfect the quality of the study.

Angel Martin, a chemical engineer at the University of Valladolid in Spain developed and freely availed a Genetic Algorithm named Goal, which was very useful in this study. The technicians at BEED, JKUAT especially Moses K. Muuo, L. O Mulamu, Mr Francis K. Kigira, Mr. Benjamin K. Maritim, and Mr. Patrick Kavangi of Horticulture Laboratory and Mr Paul Karanja of Food Science Laboratory assisted me during experimental data acquisition, even at odd working hours, and at times over the weekend. The librarian and her staff at South Eastern University College assisted me with exemplary printing and photocopying services.

The list is endless and I want to thank those who contributed to the success of this work. To all I say thank you very much and May the Lord bless you in a Mighty Way.

TABLE OF CONTENTS

LIST OF TABLES

LIST OF FIGURES

LIST OF PLATES

LIST OF APPENDICES

LIST OF ABBREVIATIONS AND SYMBOLS

A_b	Albedo of the surrounding area(dimensionless)
A_c	Collector plate surface area (m^2)
a_c	Drying chamber width (m)
A_f	Cross–sectional area of flow (m^2)
$a_i (i=0,1,2,...)$	Coefficients
a_j	Parameter defining sine wave in solar energy harnessing models
ANOVA	Analysis of variance
a_x	Coefficient
a^*	Value representing green–red spectrum in food colour measurements
B	Half of thickness of drying slab (m)
BEED	Biomechanical and Environmental Engineering Department
b_c	Drying chamber height (m)
b_f	Breadth of flow area (m)
b_j	Parameter defining sine wave in solar energy harnessing models
b_p	Biochemical properties (dimensionless)
b_x	Coefficient
b^*	Value representing blue–yellow spectrum in food colour measurements
C	Value of the colour parameter (L^*, a^*, b^*) at time t (hrs)
C_o	Initial value of the colour parameter (L^*, a^*, b^*)
C_p	Specific heat of humid air (J/kg–K)
C_{pa}	Specific heat capacity of air (J/kg–K)
c_{pv}	Specific heat of vapor (J kg^{-1} K^{-1})
c_{pw}	Specific heat of water (J kg^{-1} K^{-1}))
C_{ps}	Specific heat of dry fish (J kg^{-1} K^{-1})
d	Half thickness of the drying material (m)
d_d	Depth of the drying chamber (m)
d_e	Equivalent diameter of the air flow (m)
D_f	Effective diffusivity of fish (m^2/s)

D_{sf}	Effective diffusivity associated with shrinkage (m^2/s)
D_o	Pre–exponential factor for Arrhenius equation (m^2/s)
D_h	Hydraulic diameter (m)
d	Thickness of drying fish (m)
d_o	Initial thickness of the drying fish (m)
d_1	Fish drying process characteristics (dimensionless)
d_2	Dryer design characteristics (dimensionless)
d_s	Shrinkage dependent thickness of drying fish (m)
d_t	Depth of air heating chamber (m)
E	Activation Energy (J/mol).
F	Collector efficiency factor (dimensionless)
f	Function of the quality of the drying fish (dimensionless)
f_1	Function of the fish dryer design parameters (dimensionless)
f_2	Function of the fish drying process characteristics (dimensionless)
f_3	Function of the energy harnessing characteristics (dimensionless)
f_4	Function of the drying process characteristics (dimensionless)
GA	Genetic algorithm
GAs	Genetic Algorithms
G_a	Air mass flow rate per unit cross–sectional area ($kg/s–m^2$)
GIU	Graphic use interface
H_{act}	Actual value of H_q (MJ/m^2)
H_{asl}	Altitude (m)
h_b	Convective heat transfer coefficient between the rear plate and the air($W/m^2–K$)
h_c	Convective heat transfer coefficient between fish and air ($W/m^2–K$)
H_d	Daily diffuse solar radiation (MJ/m^2)
H^*	Hue angle (degrees)
h_{eq}	Equivalent heat transfer coefficient ($W/m^2–K$)
h_{fq}	Latent heat of vaporisation of the moisture (J/kg)
H_g	Daily global solar radiation (MJ/m^2)
h_m	mass transfer coefficient (m/s)
H_o	Daily extra–terrestrial energy incident on a horizontal surface (MJ/m^2)
H_p	Humidity of air at the plenum chamber(kg/kg)

H_r	Hour of the day in 24 hour time format
H_{sim}	Simulated value of H_g (MJ/m^2)
h_w	Wind heat transfer coefficient (W/m^{2}K)
I_b	Direct solar radiation (W/m^2)
I_d	Diffuse radiation (W/m^2)
I_c	Solar radiation absorbed by a collector plate per unit area per unit time (W/m^2)
I_g	Global solar radiation at a particular point on the ground (W/m^2)
I'_{sc}	Solar energy flux on the earth's surface at the nth day of the year (W/m^2)
I_{sc}	Solar constant (W/m^2).
JKUAT	Jomo Kenyatta University of Agriculture and Technology
K	Drying rate constant for fish (s^{-1})
K_b	Thermal conductivity of the bottom insulation (Wm^{-1}K^{-1})
k_e	Conductivity of heating chamber wall insulating material (Wm^{-1}K^{-1})
k_c	Extinction coefficient for the cover plate (m^{-1})
k_s	Shrinkage–dependent drying rate constant (s^{-1})
k_t	Cloudiness ratio
K_v	Thermal conductivity of humid air(Wm ^{1}s^{-1})
L	Collector plate length (m)
L_{cd}	Ratio of collector length–to–equivalent diameter
L_1	Side wall insulating material depth (m)
L_2	Length of drying chamber (m)
L_f	Length of flow area (m)
L^*	Value representing light–dark spectrum in the colour measurements
M	Moisture content of drying fish, dry basis (kg H_2O/kg dry matter)
$\dot{m}_a$	Air flow rate (kg/s)
M_e	Equilibrium moisture content, dry basis (kg H_2O/kg dry matter)
M_o	Initial moisture content, dry basis (kg H_2O/kg dry matter)
MR	Moisture ratio (dimensionless)
n	The day of the year, number of solutions
N_c	Number of covers (dimensionless)
N_m	Normality of standard nitrogen (N)

NOSTD	Non–optimised solar tunnel dryer
N_u	Nusselt number (dimensionless)
OS	Open solar drying
OSTD	Optimised solar tunnel dryer
P_r	Prandtl number (dimensionless)
$P_{(T)}$	Partial vapour pressure of air (Pa)
q_i	Quality attributes of fish
R	Universal gas constant (J/K–mol)
R_b	Tilt factor for beam radiation(dimensionless)
R_d	Tilt factor for diffuse radiation(dimensionless)
R_e	Reynolds Number(dimensionless)
Rh	Relative humidity
R_r	Tilt factor for reflected radiation (dimensionless)
RhNOSTD	Relative humidity measured during testing of NOSTD
RhOSTD	Relative humidity measured during testing of OSTD
$\overline{S}_a$	Daily mean actual sunshine hours
$\overline{S}_p$	Daily mean possible sunshine hours
T	Temperature of the drying fish (K)
t	Drying time (s)
$T_{a(x)}$	Air temperature at a point at distance x from the inlet(K)
T_{av}	Average of T_c and T_b (K)
T_b	Temperature of the bottom plate (K)
TBARS	Thiobarbituric acid reactive substances (µg(MA)/kg)
t_b	Thickness of the bottom insulation (m)
T_c	Heating chamber bottom plate temperature (K)
t_c	Thickness of the cover plate (m)
T_e	Exit temperature (K)
t_e	Thickness of heating chamber wall insulation (m)
T_m	Mean plate temperature (K)
T_i	Inlet air temperature (K)
TiNOSTD	Inlet temperatures measured during testing of NOSTD

$TiOSTD$	Inlet temperatures measured during testing of NOSTD
$TpNOSTD$	Plenum temperatures measured during testing of NOSTD
$TpNOSTD$	Plenum temperatures measured during testing of NOSTD
T_p	Plenum chamber air temperature (K)
t_p	Textural properties (dimensionless)
$TVB–N$	Total volatile base nitrogen (mg/100g)
T_∞	Ambient air temperature (K)
U	x,y or z
U_b	Bottom heat loss coefficient ($W/m^2–K$)
U_e	Edge heat loss coefficient ($W/m^2–K$)
U_L	Overall heat loss coefficient ($W/m^2–K$)
U_t	Top heat loss coefficient ($W/m^2–K$)
v_w	Wind velocity (m/s)
v_{sa}	Drying air velocity (m/s)
w	Collector plate width (m)
W_2	Width of drying chamber (m)
x	Distance of point P(x) from the inlet (m) in the three dimensional space
x_i	Solar energy harnessing parameters
y_i	Conditions of the drying air
Z	Height above the base within a drying matrix (m)
z_i	Characteristics of the drying fish
α	Absorptivity of the absorber plate ($W/m^2–K$)
α_a	Thermal diffusivity(m^2s^1)
β	Collector plate tilt angle (degrees)
β'	Volume shrinkage coefficient (dimensionless)
β'_s	Linear shrinkage coefficient (dimensionless)
δ	Angle of declination (degrees)
ε	Porosity (dimensionless)
ε_b	Emissivity of the rear plate (dimensionless)
ε_g	Emissivity of glass (dimensionless)

ε_p	Emissivity of absorber plate (dimensionless)
ε_r	Residual error (%)
φ	Latitude (degrees)
η	Collector efficiency (%)
η_1	Refractive index of air (dimensionless)
η_2	Refractive index of cover material (dimensionless)
μ	Dynamic viscosity ($kgm^{-1}s^{-1}$).
θ_i	Angle of incidence of solar beam on a the cover glass (degrees)
θ_2	Angle of refraction of a solar beam incident on a the cover glass (degrees)
ρ_a	Density of drying air (kgm^{-3})
ρ	True density of fish (kg/m^3)
ρ_b	Apparent density of fish (kg/m^3)
ρ_{bo}	Dry solid apparent density (kg/m^3)
$\rho_{d(f)}$	Density of the drying material (kg/m^3)
ρ_d	Diffuse reflectance of the covers of the cover plate (dimensionless)
ρ_z	Dry solid true density (kg/m^3)
ρ_w	Enclosed water density ($kg.m^3$)
σ	Stefan–Boltzmann constant ($W/m^2–K$)
τ	Transmissivity of the collector cover material(dimensionless)
υ	Kinetic viscosity (m^2s)
υ	Specific volume (m^3/kg)
ς_c	Number of data within a certain residual error interval
ς_t	Total trial data used in determination of residual error interval
ω	Hour angle (degrees)
ω_s	Sunset or sunrise hour angle (degrees)
ψ_m	Actual data values used in residual error analysis
ψ_p	Predicted data values used in residual error analysis

ABSTRACT

The fish industry in Kenya, with a production of over 350,000 metric tonnes earns USD 105 million which accounts for about 5% of the national Gross Domestic Product, provides 3% of skilled and unskilled employment. However, this industry is threatened as the fish is harvested at high moisture content of about 5kg/kg, dry basis, and at this moisture content, if not preserved, fish undergoes spontaneous spoilage in 24 hours. At the artisanal fishermen level, the most viable preservation option is solar drying, in which fish is enclosed in a solar dryer, shielding it from contamination, and destruction. Depending on the conditions in the dryer, fish can either be over-dried or under-dried, resulting in heavy losses at household and national level, and therefore, a conducive environment must be provided within the dryer to avoid destruction of fish during drying.

Based on the above observations, studies were conducted with the objective of optimising the design parameters and performance of a solar tunnel dryer, using genetic algorithms. This involved, initially, developing computer simulation models for prediction of global solar radiation incident on the dryer, the amount of solar energy harnessed and the drying of fish. The models were then validated, based on actual data, and thereafter were used in the optimisation process. The original (non–optimised) solar dryer was then modified based on the obtained optimised design parameters. The optimised solar tunnel dryer was then tested to evaluate its performance in the harnessing of solar energy and the drying of tilapia fish.

The results of a two–way Student's t–test at 5% level of significance, show that there were no significant differences between simulated and actual data for global solar radiation (t_{stat} = *0.17*, t_{crit} = *1.65*), plenum chamber temperature (t_{stat} = *0.55*, t_{crit} = *1.72*) and for moisture ratio of the drying fish (t_{stat} = *0.96*, t_{crit} = *2.06*). The subsequent performances of the models in the prediction of the above parameters were 78.4, 83.3 and 81%, respectively, at 10% absolute residual error interval. This implies that the developed models can be used to predict the global solar radiation, the harnessed energy and the drying of fish in a solar tunnel dryer.

The optimization process resulted in the heating chamber dimensions of 2.44m long, 1.22m wide and 0.11m high as compared with the non–optimised of 2.44m long, 1.22m wide and 0.54m high. Higher temperatures (14.2 to 57.6^{o}C) in the plenum chamber were obtained for the optimised solar tunnel dryer (*OSTD)* as compared with those (12.1 to 42.5^{o}C) for the non-optimised solar tunnel dryer (*NOSTD)*. This indicates that the *OSTD* harnessed more energy than the *NOSTD*. The results further show that the *OSTD* took 15 hours as compared to 28 hours for the *NOSTD* to dry fish to equilibrium moisture. A two–factor Analysis of Variance at 5% level of significance confirmed the existence of significant difference in plenum temperatures developed by the two dyers (*F=36.83,* $F_{crit,\alpha=0.95}$ = *3.26*).

The mean values of protein, fat, carbohydrates and ash content of fish dried under *NOSTD* and *OSTD* were 69.60%, 8.00%, 1.01µg/g and 8.41% (for *OSTD* only), respectively, 69.70%, 5.92%, 1.00 µg/g and 17.6%, (for *NOSTD* only), respectively, and 71.10%, 7.3%, 0.73 µg/g and 18.11% (for open sun drying, *Osd*), respectively.

This indicates that the drying process had no significant influence on the nutritive value of fish dried in both the *OSTD* and *NOSTD* solar dryers. In addition, based on TBARS analysis, the quality of fish dried in the *OSTD* was found to be acceptable at 2.3µg(MA)/kg, while that for *NOSTD* (5.3µg(MA)/kg) was close to the unacceptable level of 6 µg(MA)/kg, though within the acceptable range. Finally, the TVB–N results show "very good" putrefaction values (11.14–12.74mg/100g) and these were not significantly different for the two treatments.

Based on these results, it is recommended that appropriate designs and optimisation principles and models for solar dryers should always be developed and adopted as has been established in this study. This would result in effective and efficient energy harnessing and quality enhancement of solar dried food material, with the possibility of reducing food losses, improving food security and raising the level of income at farm level.

CHAPTER ONE

INTRODUCTION

1.1. Background information

About 80% of the agricultural production in Kenya is rural based where most (75%) farmers rely on open sun drying, and fossil and biomass fuels as the main sources of energy for drying of the produce (Omiti *et al*., 2007). Electricity is normally required in agricultural processing industries as a supplement to fossil fuel. Recently, the prices of fossil fuel and electricity have more than doubled, thereby becoming unaffordable to most small–scale farmers (KNBS, 2008). In addition, biomass fuel contributes a significant 68% of the total energy consumption in Kenya (Kalua, 2008; Karekezi and Kithyoma, 2003; Malo *et al*., 2008). Kenyan forest cover has dwindled from 30% in 1900 to 3% at independence, and subsequently to less than 1.7% over the last 45 years (Southall, 2005; Akotsi *et al*., 2006), which is way below sustainable levels of 12% (Wamwachai, 2009), further exacerbating the problem of energy scarcity for drying of agricultural produce in the rural areas. Therefore, there is need for provision of alternative sources of energy for drying and preservation of agricultural and livestock produce such as fish in rural areas of Kenya.

The fish industry is important in Kenya as it provides about 3% employments, which constitutes skilled and unskilled labour, and is rural based. In addition, fish contributes to about 14% of the total protein supply, which together with chicken are

classified as safe proteins (Tidwell and Allan, 2001; Doyle, 2007), and therefore measures must be taken to reduce significantly its spoilage. Further, the annual production of fish in Kenya is over 350,000 metric tonnes, and this earns the country about US$105million, which constitutes about 5% of the national Gross Domestic Product (Orengoh and Kisumo, 2007; Abila, 2003). In spite of the above, the annual fish harvest fluctuates seasonally, with periods of high and low supply (Shitanda, 2006). During the periods of high supply, a lot of fish is spoilt and wasted due to poor drying and preservation at artisanal fishermen level, while acute shortage and increased prices of fish are experienced in periods of low harvest.

According to Orengoh and Kisumo (2007), 50% of total annual fish harvest in Kenya goes to waste due to use of poor traditional drying and storage techniques. This is because fish is harvested at an averagely high moisture content of 5 kg/kg dry basis, d.b, (Garg and Prakash, 2000; Kituu *et al*., 2009), and if not properly dried and safely preserved, it undergoes rapid spoilage, even without external contamination, in less than 24 hours (Gram and Delgaard, 2002; Abila, 2003). Furthermore, the landing sites for fish are usually far from market places and consumption points, and this leads to large amounts of fish being spoilt and wasted**.** In order to reduce the wastage and spoilage of fish during periods of oversupply, and to enhance long storage, it is necessary to adopt appropriate as well as affordable drying techniques for safe preservation of fish, especially at the artisanal fishermen level. This will enable the fishermen supply sufficient fish during periods of shortage, in order for them to take advantage of the high prices prevailing during these periods.

The traditional techniques commonly used to dry fish for effective preservation in Kenya include dry salting, open sun drying, deep frying and smoking (Shitanda, 2006). Open sun drying is used to dry about 50% of the fish in Kenya (Abila, 2003). This method is the most widespread at the artisanal fishermen level. However, this method exposes fish to contaminants such as dust and excreta from birds and animals. The fish is also subjected to destruction by birds, blowflies' larvae and animals (Jian and Pathare, 2007; Gewali *et al.*, 2005; Perumal, 2007). The open sun drying is usually slow, and it requires intensive labour and large areas. In most cases, the fish dries to unstable moisture content that is conducive for the proliferation of micro–organisms. This way the fish becomes a source of food poisoning. In addition, the direct exposure of fish to sunlight destroys light sensitive nutrients (Suzuki *et al*., 1988). According to Delgado *et al.* (2005), deep frying causes environmental degradation, since it uses vast quantities of biomass. In addition, smoking introduces significant quantities of known health–damaging pollutants, including several carcinogenic compounds such as polycyclic aromatic hydrocarbons, benzene, aldehydes, respirable particulate matter, carbon monoxide [CO], nitrogen oxides [NOx], and other free radicals in fish (Naeher *et al*., 2007). Thus, there is need to develop suitable technologies for drying of fish to enhance safe preservation.

Solar drying of fish would offer alternative methods to smoking and deep frying. Solar dryers shield fish from agents of contamination and destruction, and they provide a conducive atmosphere which results in high drying rates as compared to

open sun drying (Bala and Mondol, 2001). In addition, solar dryers can be affordable depending on design and fabrication material, they offer effective drying for safe preservation of fish, and are environmentally friendly (Jairaj *et al*., 2009; Perumal, 2007). This technology is suited for use in most rural areas in Kenya as there is abundant supply of sunshine (Rabah, 2005), and the forests in these areas are highly depleted. Further, most of these regions are not supplied with electricity, and poverty levels prohibit the use fossil fuels for drying of agricultural produce.

Recently, various solar dryer technologies such as box, tent and green house dryers have been introduced in Kenya for drying of agricultural produce (Kerr, 1998). Other solar dryers found mainly in Asian countries include the cabinet dryers, the batch dryers and green house dryers (Whitfield, 2000). Nevertheless, these technologies lack design and performance concepts that can be used for development of better drying systems. Hence, there is need to gather and develop such concepts, which would be useful in the design and development of optimal drying systems. Solar tunnel dryers have been employed to dry fruits and vegetables with success in developed countries (Reza *et al.*, 2009; Bala and Mondol, 2001). However, these dryers have not been utilised for drying of agricultural produce such as fish in Kenya.

Several authors have developed, and analysed models for thin layer drying of biological products, using conventional or solar tunnel dryers (Joshi *et al*., 2005; Mujaffar and Sankat, 2005), some of which subject fish to direct contact with sunlight. The solar tunnel dryer provides a hygienic and environmentally friendly

atmosphere for drying fish. This is because it protects the fish from contaminants and sunlight. It is also possible to control the temperature and humidity within it during drying. Nonetheless, it is possible for the fish undergoing drying in the solar tunnel dryer to get spoilt, or be over–dried, if the harnessed solar energy is not regulated. Hence, thorough analysis of available solar energy and its harnessing by the solar tunnel dryer form important components of an effective and efficient solar tunnel dryer design.

In spite of the abundance of solar energy in the tropics**,** the determination of the quantity of energy available at any given location continues to pose various challenges. This is because the quantity of solar energy available within these regions is dependent on the latitude, altitude, the hour of the day, day of the year and the clearness of the sky (Al–Ajlan *et al*., 2003; Jin *et al*., 2005). The values of these parameters need to be determined for effective evaluation of the incident solar radiation, which is an important input in solar drying process. In addition, normally the amount of global solar insolation at a particular place is determined through measurement. This process is tedious and many consumers of such information lack the tools to carry out physical measurements. Further, the common practice has been to develop models which can predict the energy incident at a particular location at any time (Al–Ajlan *et al.*, 2003; Jin *et al.*, 2005; Alfayo and Uiso, 2002; Mechlouch and Brahim, 2008). Accurate determination of solar energy would lead to design and development of efficient solar energy harnessing systems such as solar dryers.

However, the challenge in Sub–Saharan Africa is that the exact science of the simulation and application of solar energy in the design of solar drying systems has not been adequately developed.

In order to develop optimal fish dryer systems, it is necessary that proper relationships are established that link the incident solar energy to the dryer design parameters, and the energy harnessed. The energy harnessed should also be appropriately related to the drying process. In addition, the relationships linking the incident solar energy to the dryer design parameters and the drying process should be optimised using effective optimisation tools such as genetic algorithms.

1.2. The problem

Despite the low harvest of fish in Kenya, 50% of the harvest is lost through spoilage, due to poor fish preservation and processing methods at artisanal level, among them smoking, deep frying, and salting, open sun–drying and occasionally unprofessionally designed solar dryer. In addition, a solar tunnel dryer design, which introduces dark chamber drying for preservation of ultra-violet sensitive nutrients in fish, was recently introduced in Kenya. Although the dryer offers the possibility of incorporation of temperature regulation mechanism for in order to produce high quality dried fish, its performance in the drying of fish is unknown, as its design is haphazard and has minimal engineering theoretical backing. Further, the optimal design which would be based on energy harnessing, design parameters, drying fish

characteristics and the quality attributes of the dried fish products is lacking. While the dryer is an engineering facility, which would present complex objective function, requiring heuristic approach to optimisation, there have been no attempts to utilise heuristic schemes in general and genetic algorithms in particular in optimising the system.

Based on the above observations, the following design and optimisation questions were considered of interest in this study: Is it possible to establish the relationships between solar energy reception, solar energy harnessing by a solar tunnel dryer, dryer design parameters, drying characteristics of fish and the quality attributes of fish, namely moisture content, nutritional content, rancidity, putrefaction and colour? Is it possible to develop and validate a computer simulation model for the above relationships? Is it possible to apply genetic algorithms and the developed computer simulation model in the optimisation of a solar tunnel dryer, and develop and evaluate the performance of the optimised solar tunnel dryer in the drying of fish?

1.3. Hypothesis

This research work focused on the optimisation of the design and performance of a solar tunnel dryer for drying of fish using genetic algorithms. In particular, the hypothesis of this study were that

1. It is possible to establish relations which link the energy incident on a solar tunnel dryer, the energy harnessed by the dry based on both environmental

and dryer design parameters, the drying characteristics of fish and the quality attributes of the dried fish.

2. A computer model to simulate the established relationships can be developed and validated.
3. An optimised solar tunnel fish dryer can be artificially bred by executing a genetic algorithm, using the developed computer simulation model.
4. The optimised solar tunnel fish dryer can be developed and its performance in the drying of fish established against open sun drying and the non-optimised solar tunnel dryer.

1.4. Justification

Based on a per capita consumption of fish at 12kg (Chukwu and Shaba, 2009), the annual demand for fish in Kenya, with a population exceeding 38,610,097 by 2009 (KNBS, 2010) is more than 463,000 metric tonnes. Thus, the total annual production of fish at 350,000 metric tonnes (Orengoh and Kisumo, 2007; Abila, 2003) is grossly insufficient for local consumption. In addition, 50% of this harvest goes to waste due to poor handling, while 30% is exported (Orengoh and Kisumo, 2007; Ogunja *et al.*, 1992; Gitonga *et al.*, 2003), leaving roughly 70,000 metric tonnes for local consumption, which is grossly insufficient for Kenyans. In addition, due to rapid spontanesous spoilage of the unpreserved fish, under high tropical temperature, as is prevalent in Kenya, the sector is threatened, with the possibility of food insecurity and excessive financial losses by artisanal fishermen.

At the artisanal fishermen level, fish is preserved by either deep frying, smoking or open sun drying. These three preservation methods lead to environmental degradation, contaminate the fish and render it unsafe for human consumption. Solar drying is a viable option, but most solar dryers are not designed specifically for fish, and therefore using them in the drying of fish destroys fragile nutrients in the fish. Further, the possibility of fish in the dryer over–drying due to excessive harnessed heat or under–drying due to low temperatures is real, and this results in poor quality dried fish. A solar tunnel dryer, which has a dark drying chamber is able to preserve the light sensitive nutrients in the fish, and offers the possibility of incorporation of temperature regulation mechanism in the design. However, the optimal performance of the dryer is unknown, having been constructed using haphazard construction procedures which disregarded basic scientific approach to optimal design. Furthermore, these being an engineering facility, with complex objective functions, there have been no attempts in applying the well known heuristic optimisation tools, and in particular Genetic Algorithms (GA(s)) in the optimisation of solar tunnel dryer design. Based on these observations, these studies were undertaken with the aim of applying scientific procedures in simulation, design, development and performance evaluation of an optimised solar tunnel dryer for use in the drying of fish.

1.5. Objectives

The foregoing information shows that the fish industry can significantly contribute to Kenya's economy, health and food security only if affordable and optimised drying

and preservation technologies are available. In an attempt to avail these technologies, this study in general aimed at developing an optimised solar tunnel dryer for drying of fish.

1.5.1. Broad objective

The broad objective of the study was to apply genetic algorithms in the optimisation of the design and performance of a solar tunnel fish dryer.

1.5.5. Specific objectives

The specific objectives were as follows:

1. To establish the relationships between the incident solar energy, solar tunnel dryer design parameters and the drying characteristics of fish.
2. To develop a computer model for simulating the energy harnessed by the solar tunnel dryer and the drying process of fish.
3. To validate the performance of the developed computer simulation model using the non–optimised solar tunnel dryer.
4. To optimise the design parameters of the solar tunnel dryer using a Genetic Algorithm.
5. To develop the optimised solar tunnel dryer and evaluate its performance in the drying of fish, against that for the non–optimised solar tunnel dryer and for open sun drying.

1.6. Scope of Study

This study concentrated on the increasing knowledge on the application of genetic algorithms in the optimisation of solar drying systems. It sought to advance the study of these systems through development of simulation models, and validation of the models to predict the behaviour of solar tunnel drying systems in the drying of fish. The study was however confined to solar tunnel dryers, and their application in the drying of fish at artisanal fishermen level. This is due to the problems experienced by the fishermen in processing of their fish, the heavy losses they incur in spoilt fish, and the potential benefits in fishermen income, food security, employment and national income. In addition, when fish at the artisanal fishermen level is subjected to open solar drying or conventional solar dryers, they often get spoilt through overheating on the one hand and under–heating heating on the other hand. The study was also limited to optimising the energy harnessing section of the solar tunnel dryer. This is because the drying of fish at the artisanal fishermen is basically a thin layer drying process. However, the thickness of the drying bed and the drying time to attain equilibrium moisture content was also optimised. This study eventually applied genetic algorithm in combination with the developed model to optimise the solar tunnel fish dryer. Finally, the study developed the optimised solar tunnel dryer, evaluated the ability of the dryer to harness energy and to dry fish, and the quality attributes of the fish dried in the optimised dryer.

CHAPTER TWO

LITERATURE REVIEW

2.1. Solar Drying

Solar energy is one of the most promising renewable energy sources in the world because of its abundance, inexhaustible and non–pollutant in nature compared with higher prices and shortage of fossil fuels (Basunia and Abe, 2001). Sun–drying of fish is an old traditional practice done in many parts of the world (Sablani *et al.*, 2003; Moradi and Zomorodian, 2009). A major problem with the traditional sun drying of sardines is the loss of dried products due to rats, cats, dogs and bird, which may reach up to 50% and the infestation with insects (Sacilic *et al.*, 2006; Purohit *et al.*, 2006). The other disadvantage of open sun–drying include destruction of the fish by birds, animals and man, fungal growth and mycotoxins, loss of both nutrients and quality, intensive labour and a large area requirements. These factors reduce fishermen revenues from sardines. In Kenya, fish is traditionally dried by spreading out on sand along the beaches for about 4–5 days in dry and hot periods. Further, the use of solar dryers would enclose fish from contaminating agents such as rain, blow flies, dust, birds and animal excreta (Sacilic *et al.*, 2006). It is therefore important that any technology introduced in the drying of fish is able to maintain the appropriate environment which promotes safe drying of the fish.

2.2. Solar dryers

Solar drying can be considered as an elaboration of sun drying and is an efficient system of utilizing solar energy. The introduction of solar drying system is one of the most promising alternatives to reduce post harvest losses for biological products. Ekechukwe and Norton (1999), Oyero *et al*. (2007) and Sablani *et al*. (2002) have given the advantages of solar–drying, compared with open sun–drying as reduced drying time, retarded microorganisms and insect activity due to the higher temperatures attainable in solar dryer, safeguarding the product from wind–borne dust, contamination and destruction by animals, and the ability to dry products to lower moisture contents which increases the storage life (Ebuy, 2007; Ojutiku *et al*., 2009). Other advantages include the solar dried fish having much better colour and texture as compared to open sun dried fish, the smaller area of land required by solar dryers for the same quantity of dried fish, protection of drying fish from sudden down pours of rain, improved throughput due to increased drying temperatures, and the high quantity and quality of dry fish because fungi; insects and rodents are unlikely to infest the fish during drying (Jairaj *et al*., 2009; Fudholi *et al*., 2010; Ebuy, 2007; Purohit *et al*., 2006). However, the availability of solar dryers' technology is not widespread in Kenya, and in order to encourage its adoption, attempts should be made to provide technically sound, well constructed and optimized designs of solar dryers for use by the fishing communities in the country.

The various approaches in the classification of solar dryers are based on the mode of exposure of drying material to solar radiation, the type of air flow through the material and the circulating air temperatures (Jairaj *et al.*, 2009; Fudholi *et al.*, 2010). For classification under air flow pattern, there are natural, forced or hybrid convection solar dryers. In addition, in the natural circulation mode, air is heated and circulated through the fish naturally by buoyant force or as a result of wind pressure caused by a wind powered fan located at the chimney or a combination of both (Fudholi *et al*., 2010). On the other hand, in the forced circulation mode, heated air is circulated through the fish using solar, or electricity drive fans or pumps (Ebuy, 2007; Jairaj *et al*., 2009). Further, Jairaj *et al*. (2009) and Fudholi *et al*. (2010) stated that the natural and forced convection solar dryers can be grouped into direct, indirect or mixed mode solar dryers, based on the mode of exposure of the drying material to solar energy.

In the direct type of solar dryer, fish is exposed directly to solar radiation or a combination of direct solar radiation and reflected radiation, while in the indirect type of solar dryer, it is shielded from direct exposure to solar radiation, and the drying energy is supplied using heated air (Jairaj *et al*., 2009; Fudholi *et al*., 2010). Furthermore, the mixed type of solar dryer exposes the drying fish directly to solar radiation and also allows hot air to flow through the fish. Moreover, an indirect solar dryer basically consists of two major components: an air heater, which is used to raise the temperature of the drying air and a drying chamber which is the enclosure

that accommodates the drying fish. A chimney is usually incorporated in natural convection indirect dryers to increase the air–flow through the fish drying bed (Ebuy, 2007).

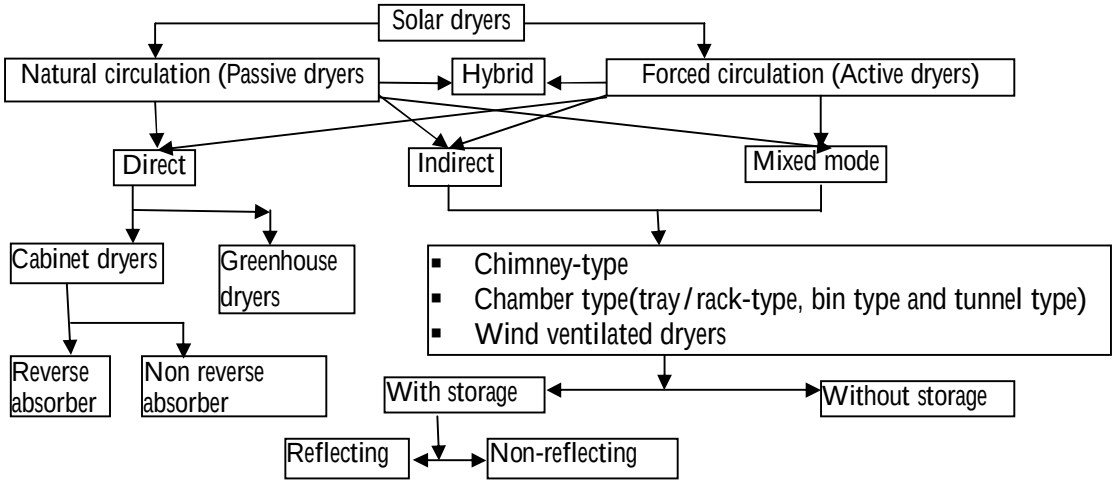

Figure 2.1: Classification of solar dryers. (Jairaj *et al*., 2009; Purohit *et al*., 2006)

Classification of dryers is finally based on circulated air temperature mode. The air entering the drying chamber of a solar dryer can be either at the ambient temperature or at higher temperature. The air temperature rise is achieved by the passage of air through a solar collector prior to the drying chamber, which is the principle of the design of solar tunnel dryers. If the collector and the drying chamber are combined, the dryer is termed integral ducting dryer. Dryers that employ a separate solar collector and drying chamber are termed separate ducting dryers (Fudholi *et al*., 2010) as in solar tunnel dryers.

2.3. Fish drying methods

2.3.1. General methods of drying of fish

Methods of drying fish vary between different countries and within the same country depending on the species of fish used, the type of product desired and the types of energy resources available and their level of utilisation (Chukwu and Shaba, 2009). In most of the developing countries, sun drying has been used from the ancient times, but this traditional drying method has many disadvantages as stated in section 1.1. Non–uniform and/or insufficient drying of the fish also lead to deterioration during storage. Other drying technologies (viz., conveyor, drum, foam mat, fluidized bed, kiln, pneumatic, rotary, spray, vacuum, radiant, microwave, dielectric) are modern, expensive and technically unviable for artisanal fishermen set–up commonly found in developing country like Kenya, where electricity utility facilities are simply not available.

2.3.2. Solar drying of fish

Palaniappan (2009) classified fish as a highly perishable food product which can be stored only under refrigeration or when dried, and stated the problem affecting the quality of the dried fish as environmental contamination in drying. He suggested the use of hygienic solar drying systems in the drying of fish, which shield the fish from the surroundings in order to improve its quality.

Oyero *et al*. (2007) and Oluwasesan (2008), reported drying of fish in a solar tent dryer, and natural and forced convection solar cabinet dryers where they noted that temperatures above 40^{o}C caused case hardening on dried fish, and that the tent and box dryer subjects the drying fish to undesirable ultra–violet radiation. Sablani *et al*. (2002) further reported a solar tent and dome solar dryers for drying of fish at the artisanal fishermen level, with the resulting quality being good with respect to odour, rancidity and microbial or insect attack compared to open sun drying. However, control of temperature and elimination of influence of ultra violet light on the drying fish is difficult under the solar tent and dome dryers.

2.3.3. Influence of drying temperatures on the quality of fish

Fish and its products are easily putrefied by the proliferation of micro-organisms, due to high nutrient and water content (Zhang *et al*., 2002; Bille and Shemkai, 2006), and therefore, fast reduction of moisture content is crucial in its preservation. The temperatures used in the dehydration process can encourage the proliferation of micro-organisms, in addition to denaturing of the proteins and introducing structural changes in the fish product, and therefore producing a tough end product. The commonest and most dangerous micro-organisms prevalent in fish during processing are *Staphylococcus aureus, Clostridium botulinum, Salmonella* and *Escherichia Colli*. Table 2.1 shows the conditions under which each of these micro-organisms thrives during the drying of fish.

Table 2.1: Conditions favourable to micro-organisms proliferation

Micro-Organism	Exposure temperature (^oC)	Exposure before development (Hrs)	Maximum activity (a_w)	Maximum Temperature (^oC)	Remarks
staphylococ	>21	3	0.85	48.0	Anaerobic
Clostridium	>21	2	0.97	45.0	Anaerobic
Salmonella	>21	3	0.95	46.2	Anaerobic
E.Colli	>21	3	0.94	49.9	Anaerobic

Source: Lalitha and Surendran (2002), Himelbloom and Crapo (1998)

Mujaffar and Sankat (2005) reported that in drying of fish, increasing the temperature to between 40 and 50°C resulted in a noticeable increase in moisture loss, while fish slabs at 60°C dried marginally faster than those at 50°C, probably due to crusting, and the increase in temperature is not justified. Besides, they also noted that drying fish at temperatures above 60°C develops an undesirable aroma of cooked fish, which is not noticeable at 50^oC. Table 2.1 shows that increasing drying air temperatures to 50^oC, inhibits the development of most pathogenic micro-organisms in fish. Besides, micro-organic activity in fish processing ceases at 15% moisture content (Panduro *et al*., 2004).

Although Supranto *et al*. (2008) state that drying can proceed at 70^oC to 80^oC, partial cooking would result, and introduce aroma in the dried product. Control of toxicants is therefore a major factor in the design temperatures for the solar tunnel dryer. To limit the growth of *Escherichia colli*, which would also limit the growth of the other types of bacterial, the temperature in the drying chamber would need to be less than

60^{o}C (Codex Alimentarius, 1979). This combined with aerobic drying, and consequently reducing the moisture content to about 15% would reduce spoilage of fish and improve its contribution to food security.

2.4. Models for solar energy harnessing and drying process

2.4.1. Global solar radiation models

Several researchers have either developed or applied simulation models in the analysis of energy incident on a collector plate. Al–Ajlan *et al*. (2003) developed a simulation model for optimization of flat plate collector design in Riyadhi, Saudi Arabia, while Khoukhi and Murayama (2005) studied a theoretical approach of a flat plate solar collector with clear and low–iron glass covers taking into account the spectral absorption and emission within glass covers layer. In addition, Alfayo and Uiso (2002) studied models to predict the global solar radiation distribution and for evaluation of the available solar energy potential in Tanzania, whereas Chen *et al*. (2007) did a case study for an hourly solar radiation model under actual weather and terrain conditions in Heihe river basin. Further, De Souza *et al*. (2004) studied the variability of the global solar radiation over the area of Maceio (9^{o}40'S, 35^{o}42'W, 127 m), located in North Eastern state of Alagoas, Brazil, during the 1997–1999 period. Similarly, Bindi and Miglieta (1991) described a model for estimating daily global radiation from air temperature and rainfall measurements. On the other hand, Trabea (2000) did an analysis of solar radiation measurements at Al–Arish area, North Sinai, Egypt, whereas El–Adawi (2002) developed a new approach to modelling a flat plate collector, which uses the Fourier transform technique.

In addition to the above, Coops *et al.* (2000) developed a model for estimating the mean monthly solar radiation incident on horizontal and inclined slopes from mean monthly temperature extremes. Additionally, Ball *et al.* (2004) did an evaluation of solar radiation prediction models in North America, while, Spokas and Fercolla (2006) developed a mathematical model for estimating hourly incoming solar radiation from limited meteorological data . Similarly, Alam *et al.* (2005) developed a model for the simulation of solar radiation system. Jin *et al.* (2005) developed models which related the energy received at a certain locality to the latitude, altitude and the height above sea level of the position. Although the models developed were suitable for simulation of solar radiation for several places in China, they can be modified to suit different locations on the earth's surface. Further, these models have the advantage of taking altitude into consideration which was not captured by most of the earlier models.

2.4.2. Models for harnessing energy and fish drying by a solar dryers

Significant work has been carried out on the development of models for solar energy harnessing by solar dryers. Bolaji and Olalusi (2008) and Simate (2003) evaluated the performance of a mixed–mode solar dryer. Kalogirou (2003) described the working principles of the solar energy collector, and developed the equation for evaluating the energy of the working fluid along the collector plate length. Further, El–Adawi (2002) presented a new approach to modelling of a flat–plate collector which uses the Fourier transform technique. The study presents a method of evaluating solar radiation reaching a horizontal plate, the temperature gradient across

the collector plate, and the mean temperature of the fluid passing through the heating chamber with a uniform flow rate.

Ebuy (2007) studied the simulation of solar cereal dryer for deep bed dryers for drying of cereal grain. Joshi *et al*. (2005) studied the performance of solar drying systems, in which the study was grouped into two: direct and indirect solar air heaters, and was used to evaluate solar air heaters. In the study, solar tunnel dryers were evaluated under forced convection in the drying of *masyaura*, tomato, onions and radish, which cannot represent the drying of fish in the tunnel dryers. Bennamoun and Belhamri (2003) studied the design and simulation of a deep bed solar dryer evaluated it in the drying of onions. The analysis cannot therefore represent a solar tunnel dryer design or simulation for the drying of fish. In addition, Tiwari *et al*. (2006) did an experimental study of greenhouse prawn drying under natural convection and provided useful models in the analysis of solar drying, which may be useful in the analysis of drying of fish in the greenhouse solar dryer. However, though insightful, the study cannot simulate the drying of fish in a solar tunnel dryer.

2.5. Techniques and parameters in the optimization of solar dryers

A lot of research has been carried in the optimisation of solar dryers. Franke (1998) studied the modelling and optimal design of a central solar heating plant with heat storage in the ground using Modelica, while Senadeera and Kalugalage (2004)

studied the performance evaluation of an affordable solar dryer for drying crops. In addition, Ajam *et al*. (2005) developed an exergetic optimization of solar air heaters and did a performance comparison with energy analysis, whereas Smitabhindua *et al*. (2008) developed a mathematical model for optimal design of a solar–assisted drying system for drying bananas. Further, Charron and Athienitis (2006) studied the use of genetic algorithms for a net–zero energy solar home design optimisation tool, whilst Silvoso *et al*. (2003) undertook the optimization of dam construction costs using genetic algorithms. Furthermore, Sano and Kita (2002) used a Memory–based Fitness Evaluation GA (MFEGA) for optimization of noisy fitness function considering limitation of number of fitness evaluation in practical applications. Moreover, Sigurd (1994) studied the selection of equations for the calibration of strain gauges while Correia *et al*. (2004) studied the use of genetic algorithms in optimising of welding machine settings. Additionally, Montastruc *et al*. (2004) studied the use of genetic algorithm and gradient–based optimisation techniques for calcium precipitation. Finally, Ke and Ogura (2003) developed optimisation models for vowels and tones in sound systems. In spite of the studies undertaken in optimisation of the various systems using GA, none of the studies have been aimed at optimising the design a solar tunnel dryer using GA(s).

2.5. Literature review summary

Despite the significant amount of work done in the study of solar dryers, it is evident that worldwide acceptable simulation models for global solar energy reception and harnessing of the energy incident on a solar tunnel dryer, and the drying of fish in a

solar tunnel dryer have not been studied. In addition, notwithstanding the extensive research in the field of solar energy harnessing and the application of genetic algorithms in optimisation, the application of genetic algorithms in the optimisation of the design and performance of a solar tunnel dryer for the drying of fish has not been studied. Thus, based on these observations, this study aimed at optimising the design and performance of a solar tunnel dryer for fish drying.

CHAPTER THREE

MATERIALS AND METHODS

3.1. Relation between solar energy harnessing, fish dryer design parameters and drying of fish

3.1.1. Introduction

Development of the relationships between solar energy harnessing, dryer design parameters and drying of fish in the solar tunnel dryer requires that the environmental conditions, solar dryer design parameters and the characteristics of the drying fish are linked as shown by equation 3.1. In this equation, f, f_1, f_2, and f_3 are functions of the quality of the drying fish, the energy harnessed, the conditions of the drying air and the characteristics of the drying fish, respectively. On the other hand, q_i $x_{i,}$ y_i, z_i ($i=1,2,3,\ldots,n$) are the quality attributes of the drying fish, energy harnessing parameters, the conditions of the drying air, and the characteristics of the drying fish, respectively. The detailed analyses of the relationships in equation 3.1 are presented in the proceeding sections.

$$f(q_1, q_2, q_3, ..., q_n) = f_1(x_1, x_2, x_3, ..., x_n) f_2(y_1, y_2, y_3, ..., y_n) f_3(z_1, z_2, z_3, ..., z_n) \quad (3.1)$$

3.1.2. Model for global solar radiation

The daily global solar radiation, H_g, is defined as the amount of solar energy received on a horizontal surface at a particular place on the earth's surface (El–Sebaii and

Trabea, 2005). The determination of H_g is an important pre–requisite to the design and/or evaluation of the performance of any solar drying system. The computation of H_g requires that the daily extra–terrestrial solar energy, H_o (MJ/m^2), incident on a horizontal surface as given by equation 3.2, is determined (El–Sebaii and Trabea, 2005). In this equation, n is the day of the year (1 on January 1 and 365 on December 31), I_{sc} is the solar constant (W/m^2), φ is the latitude (degrees), ω_s is the sunset or sunrise hour angle (degrees), given by equation 3.3, and δ is the angle of declination for the location (degrees), evaluated using equation 3.4.

$$H_0 = \frac{24}{\pi}\left(1+0.033\cos\left(\frac{360n}{365}\right)\right) I_{sc}\left(\cos\varphi\cos\delta\sin\omega_s + \omega_s\sin\varphi\sin\delta\right) \qquad (3.2)$$

$$\omega_s = \pm cos^{-1}\left(-tan\varphi\, tan\delta\right) \qquad (3.3)$$

$$\delta = 23.45sin\left(360\left(\frac{284+n}{365}\right)\right) \qquad (3.4)$$

The models developed by Al–Ajlan *et al*. (2003), Jin *et al*. (2005) which give the relationship between H_g and H_o are of the form given in equation 3.5, in which $\overline{S}_a$ and $\overline{S}_p$ are the daily mean actual and possible sunshine hours, respectively, and a_i's are equation coefficients. The parameter $\overline{S}_p$ is determined from equation 3.6

$$H_g = H_o\left(\sum_{i=0}^{n} a_i\left(\frac{\overline{S}_a}{\overline{S}_p}\right)^i\right) \qquad (3.5)$$

$$\overline{S}_p = \frac{2}{15}\cos^{-1}\left(-\tan\varphi\tan\delta\right) \qquad (3.6)$$

In addition, the expression for determining the hourly global solar radiation on a horizontal surface, I_g (W/m^2), is given by equation 3.7 (Al–Ajlan *et al.*, 2003; Garg and Prakash, 2000), where ω is the hour angle (degrees), and a_j and b_j are coefficients, and are evaluated using equations 3.8, 3.9 and 3.10, respectively (Al–Ajlan *et al*., 2003), in which *Hr* is the hour of the day on 24 hour clock.

$$I_g = \left(\frac{\pi}{24} H_g^{'}\left(a_j + b_j \cos\omega\right)\right)\left(\frac{\left(\cos\omega - \cos\omega_s\right)}{\left(\sin\omega_s - \frac{\pi\omega_s}{180}\cos\omega_s\right)}\right) \qquad (3.7)$$

$$\omega = 15(12 - H_r) \qquad (3.8)$$

$$a_j = 0.409 + 0.5061\ Sin(\omega_s - 60) \qquad (3.9)$$

$$b_j = 0.6609 - 0.4767 Sin(\omega_s - 60) \qquad (3.10)$$

Equation 3.11 shows the relationship linking the global, direct (I_b) and diffuse (I_d) solar radiations. The determination of I_d requires computing the cloudiness ratio, k_t, as expressed in equation 3.12 (Al–Ajlan *et al.*, 2003). The computation of the daily diffuse solar radiation, H_d, is a requirement in determining I_d. The value of H_d depends on the ω_s and k_t, and is evaluated using either equation 3.13 or equation 3.14 (Garg and Prakash, 2000; Hasan, 2007).

$$I_b = I_g - I_d \tag{3.11}$$

$$k_t = \frac{H_g}{H_0} \tag{3.12}$$

For $\omega_s > 81.4^o$ and $k_t \geq 0.8$

$$H_d = H_g\left(1.311 - 3.022k_t + 3.427k_t^2 - 1.821k_t^3\right) \tag{3.13}$$

For $\omega_s \leq 81.4^o$ and $0.3 \leq k_t < 0.8$

$$H_d = H_g\left(1.311 - 3.560k_t + 4.189k_t^2 - 2.137k_t^3\right) \tag{3.14}$$

Once H_d has been evaluated, I_d is then computed using equation 3.15 (Garg and Prakash, 2000; Al–Ajlan *et al.*, 2003)

$$I_d = \left(\frac{\pi}{24}H_g\right)\left(\frac{\left(\cos\omega - \cos\omega_s\right)}{\left(\sin\omega_s - \frac{\pi\omega_s}{180}\cos\omega_s\right)}\right) \tag{3.15}$$

The values of I_b, I_d and I_g form important input parameters in the design of solar energy harnessing systems. In addition, the development of the models for predicting Ig considered the analysis of the models in existence, among them those developed by Al–Ajlan *et al.* (2003), Jin *et al.* (2005). The model developed by Jin *et al.* (2005) was selected to evaluate I_g since it incorporates several parameters, among them φ, δ, ω and the altitude, H_{asl} (m). The selected model was as presented in equation 3.16. In addition, the parameter I_g is evaluated from H_g using equation 3.17 (Jin *et al.*, 2005; Al–Ajlan *et al.*, 2003).

$$H_g = H_o \left\{ \begin{array}{l} \left(0.0218 + 0.0033\varphi + 0.0443\mathrm{H_{asl}}\right) + \left(0.9979 - 0.0092\varphi - 0.0852 H_{asl}\right)\dfrac{S_p}{S_a} \\ + \left(-0.5579 + 0.012\varphi - 0.1005 H_{asl}\right)\left(\dfrac{\overline{S}_p}{\overline{S}_a}\right)^2 \end{array} \right\} \tag{3.16}$$

$$I_g = 1.3\left(\frac{\pi}{24} H_g \left(a_j + b_j \cos\omega\right)\right)\left(\frac{\left(\cos\omega - \cos\omega_s\right)}{\left(\sin\omega_s - \dfrac{\pi\omega_s}{180}\cos\omega_s\right)}\right) \tag{3.17}$$

Prior to the evaluation of H_g, it was necessary to establish values of φ, H_{asl}, $\overline{S}_p$ and $\overline{S}_a$. The values of φ and H_{asl} were measured using a hand held global positioning system, GPS (Garmin Etrex Summit HC; Garmin, New South Wales, Australia) while $\overline{S}_a$ was evaluated as the daily mean of 5–year daily sunshine hours data available at the BEED, JKUAT. However the value I_g, generated by simulation of equation 3.17 did not agree with the ten–year mean satellite solar radiation data as obtained from NASA website (Kustever, 2010) for BEED, JKUAT, Juja, Kenya (*1.18^{o}S, 37^{o}E and 1460m altitude*). The discrepancy between the simulated and actual data sets was attributed to the localized nature of the global solar radiation model used. Thus, to enable simulation I_g for BEED, JKUAT, Juja, equation 3.17 was modified using curve fitting principles and trial and error, based on equations 3.16, using of graphical methods with trial and error, and and the day of the year, using curve fitting to yield the expressions in equations 3.18–3.20, such that:

For $n \leq 120$,

$$I_g = 1.2545\left(\frac{\pi}{24}H_g\left(a_j + b_j\cos\omega\right)\right)\left(\frac{\left(\cos\omega - \cos\omega_s\right)}{\left(\sin\omega_s - \frac{\pi\omega_s}{180}\cos\omega_s\right)}\right)\left(1 + 0.033\cos\left(\frac{360n}{365}\right)\right)^2\cos^2\delta \tag{3.18}$$

while for 120 <n<310

$$I_g = 1.0816\left(\frac{\pi}{24}H_g\left(a_j + b_j\cos\omega\right)\right)\left(\frac{\left(\cos\omega - \cos\omega_s\right)}{\left(\sin\omega_s - \frac{\pi\omega_s}{180}\cos\omega_s\right)}\right)\left(1 + 0.033\cos\left(\frac{360n}{365}\right)\right)\cos^2\delta \tag{3.19}$$

and for 310≤n≤365

$$I_g = 1.4235\left(\frac{\pi}{24}H_g\left(a_j + b_j\cos\omega\right)\right)\left(\frac{\left(\cos\omega - \cos\omega_s\right)}{\left(\sin\omega_s - \frac{\pi\omega_s}{180}\cos\omega_s\right)}\right)\left(1 + 0.033\cos\left(\frac{360n}{365}\right)\right)^2\cos^4\delta \tag{3.20}$$

3.1.3. Model for solar energy harnessing

Figure 3.1 exemplifies a schematic diagram of the solar energy harnessing system used in this study. The system is of length L, width w and depth d_t, and is made of a cover plate, a collector plate and an insulated air heating chamber. During energy harnessing, solar energy enters the system via the cover plate and heats the collector plate, which in turn heats the air in the heating chamber.

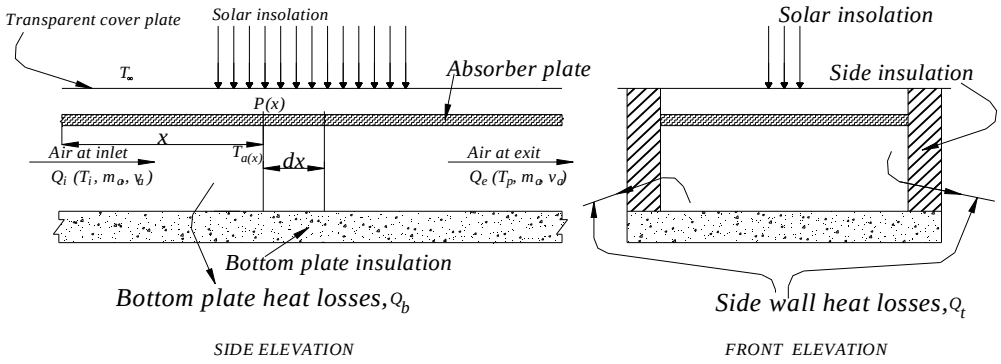

Figure 3.1: Side and front elevations of air heating chamber showing energy balance

The analysis of solar energy harnessing by the system assumes that the walls of the system are adiabatic and of negligible heat capacities, the energy harnessed is evaluated under steady state conditions (Ebuy, 2007) and the cover plate is opaque to solar energy re–radiated from the collector plate. The analysis also assumes that the properties of the heated air (viz., air flow rate, humidity, specific heat, viscosity, heat transfer coefficient and conductivity) other than temperature remain constant and the heating of air is a convective heat transfer process. Therefore, the temperature of air at any point in the heating chamber, which represents the energy harnessed, is given by equation 3.21 (Garg and Prakash, 2000; Sukhatme, 2003). In this equation, $T_{a(x)}$ is the temperature at distance x from the inlet (K), T_∞ is the ambient air temperature (K), I_c is the energy absorbed per unit area of the collector plate per unit time (MJ/m^2), U_L is the overall heat loss coefficient (W/m^2–K), A_c is the area of the collector plate (m^2), F is the collector efficiency factor, $\dot{m}_a$ is the air flow rate (kg/s) and C_p is the specific heat capacity of the humid air (J/kg–K). When

$x = L$ in equation 3.21, $T_{a(x)}$ becomes T_p, the temperature of the air at the exit of the solar energy harnessing system.

$$T_{a(x)} = T_\infty + \frac{I_c}{U_L} - \left(T_i - T_\infty + \frac{I_c}{U_L} \right) \left(- \frac{A_c F U_L}{\dot{m}_a C_p} \left(\frac{x}{L} \right) \right) \tag{3.21}$$

According to Garg and Prakash (2000), the parameter I_c is related to I_b, I_d and I_g as shown in equation 3.22. In this equation, R_b, R_d and R_r, are the conversion factors for direct, diffuse and reflected solar radiation, while A_b and $(\tau\alpha)_e$ are the albédo of the ground and the effective transmissivity–absorptivity product. The factors R_b, R_r, R_d and $(\tau\alpha)_e$ are evaluated using equations 3.23–3.26. In these equations, β is the tilt angle of the collector plate, τ is the transmissivity of the cover plate, α is the absorptivity of the collector plate and ρ_d is the diffuse reflectance of the cover plates at 60^o angle of incidence.

$$I_c = \{ I_b R_b + I_d R_d + (I_b + I_d) R_r A_b \} (\tau\alpha)_e \tag{3.22}$$

$$R_b = \frac{(\sin\delta \sin(\varphi - \beta) + \mathit{Cos}\delta \mathit{Cos}\omega \cos(\varphi - \beta))}{(\sin\delta \sin\varphi + \mathit{Cos}\delta \mathit{Cos}\omega \cos\varphi)} \tag{3.23}$$

$$R_d = \left(\frac{1 + \mathit{Cos}\beta}{2} \right) \tag{3.24}$$

$$R_r = \left(\frac{1 - \mathit{Cos}\beta}{2} \right) \tag{3.25}$$

$$(\tau\alpha)_e = \frac{\tau\alpha}{1 - (1 - \alpha)\rho_d} \tag{3.26}$$

Prior to the evaluation of $(\tau\alpha)_e$, the values of τ had to be determined based on equation 3.27, in which the parameters ρ_p and ρ_s are related to angles (degrees) of incidence, θ_i, and refraction, θ_2, as shown in Figure 3.2. The parameters ρ_s and ρ_p are computed using equations 3.28 and 3.29, respectively. In equations 3.27, k_c and t_c are the extinction coefficient of the cover glass (m^{-1}) and the collector plate thickness (m), respectively.

$$\tau = \frac{1}{2}\left(\frac{1-\rho_p}{1+\rho_p}+\frac{1-\rho_s}{1+\rho_s}\right)exp\left(\frac{-k_c t_c}{cos\theta_2}\right) \tag{3.27}$$

$$\rho_s = \frac{Sin^2(\theta_2-\theta_i)}{Sin^2(\theta_2+\theta_i)} \tag{3.28}$$

$$\rho_p = \frac{tan^2(\theta_2-\theta_i)}{tan^2(\theta_2+\theta_i)} \tag{3.29}$$

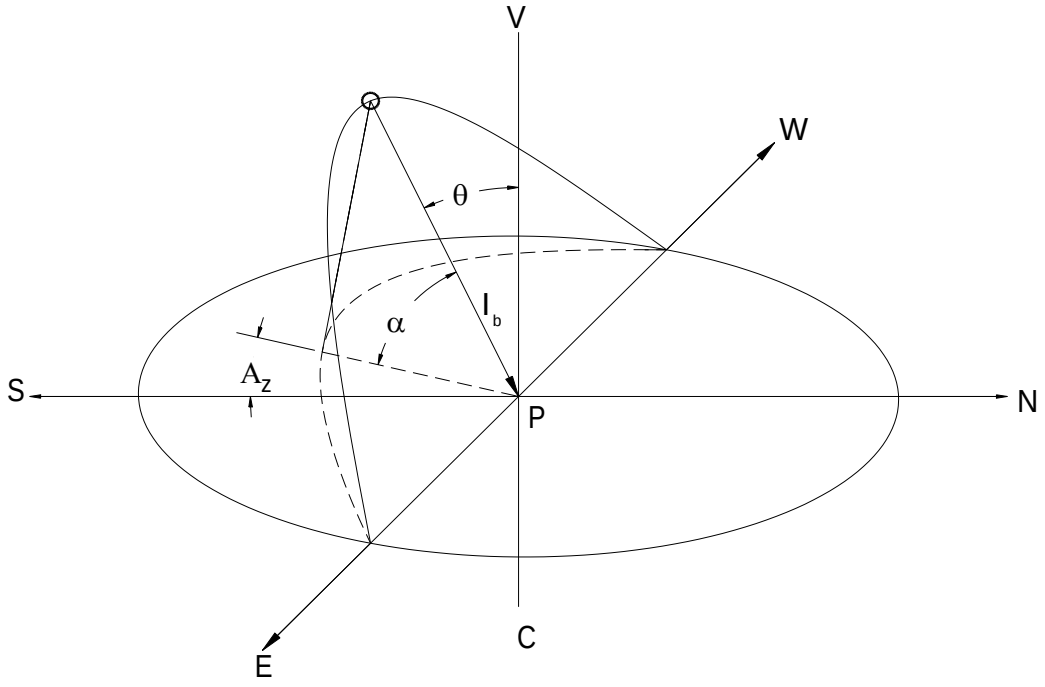

Figure 3.2: Solar angles in the apparent movement of the sun over the earth

The angle θ_i and θ_2 are determined by equation 3.30 and 3.31, respectively, in which η_a and η_c are the refractive indexes for air and the cover plate, respectively.

$$\theta_i = cos^{-1}\left\{Sin(\varphi - \beta)\sin\delta + \cos\delta\cos\omega\cos(\varphi - \beta)\right\} \quad (3.30)$$

$$\theta_2 = sin^{-1}\left(\frac{\eta_a \sin\theta_i}{\eta_c}\right) \quad (3.31)$$

The values of A_c, F and $\dot{m}_a$ in equation 3.21 are given by equations 3.32, 3.33 and 3.34, respectively, in which h_e is as expressed by equation 3.35. In this equation, h_b is the convective heat transfer coefficient between absorber plate and the air or the bottom plate of the heating chamber and the air ($WK^{-1}m^{-2}$), h_{eq} is the equivalent heat transfer coefficient ($WK^{-1}m^{-2}$) and ρ_a is the density of air (kg/m^3). The value of h_{eq} is evaluated from equation 3.36 as reported by Phoungchandang and Woods (2000), where σ, T_c, T_b, ε_p and ε_b are the Stefan–Boltzmann constant ($Wm^{-2}K^{-4}$), the collector plate temperature (K), the heating chamber bottom plate temperature (K), the emissivity of collector plate and the emissivity of heating chamber bottom plate, respectively.

$$A_c = L \times w \quad (3.32)$$

$$F = \left(1 + \frac{U_L}{h_e}\right)^{-1} \quad (3.33)$$

$$\dot{m}_a = v_s (W d_t)\rho_a \quad (3.34)$$

$$h_e = \left(h_b + \left(\frac{h_{eq} h_b}{h_{eq} + h_b}\right)\right) \quad (3.35)$$

$$h_{eq} = \frac{\sigma(T_c + T_b)\left(T_c^2 + T_b^2\right)}{\frac{1}{\varepsilon_p} + \frac{1}{\varepsilon_b} - 1} \tag{3.36}$$

The parameter h_b in equation 3.35 is determined using equation 3.37, while T_c and T_b are computed from equation 3.38 and 3.39, respectively (Al–Ajlan *et al*., 2003; Chemkhi *et al*., 2005; Ghiaus *et al*., 1997). In equation 3.37, N_u is the Nusselt number, K_v is the thermal conductivity of the drying air ($Wm^{-1}K^{-1}$) and d_e is the equivalent diameter of the air flow (m), which is evaluated from equation 3.40. For the flow to be in stable laminar flow, the parameter L_{cd}, which represents the ratio of the collector length–to–equivalent diameter and which is determined by equation 3.41, must be greater than 30.

$$h_b = \frac{N_u k_v}{d_e} \tag{3.37}$$

$$T_c = \frac{I_c + U_L T_\infty + h_e T_{a(x)}}{U_L + h_e} \tag{3.38}$$

$$T_b = \frac{h_{eq} T_c + h_b T_{a(x)}}{h_b + h_{eq}} \tag{3.39}$$

$$d_e = \frac{2Wd_t}{\left(W + d_t\right)} \tag{3.40}$$

$$L_{cd} = \frac{L}{d_e} \tag{3.41}$$

The values of Nusselt number, N_u, for turbulent and lamina flows are given by equations 3.42 and 3.43, respectively (Lienhard and Lienhard, 2006; Ghiaus *et al*., 1997), where R_e and P_r are Reynolds and Prandtl numbers, respectively. The

parameters R_e and P_r are determined from equations 3.44 and 3.45, respectively. In these equations, ν, α_a and μ are the kinetic viscosity (m^2s), thermal diffusivity (m^2s^{-1}) and dynamic viscosity ($kgm^{-1}s^{-1}$), respectively.

$$N_u = 0.0158(R_e)^{0.8} \tag{3.42}$$

$$N_u = 0.664R_e^{\frac{1}{2}}P_r^{\frac{1}{3}} \tag{3. 43}$$

$$R_e = \frac{\rho_a v_s d_e}{\mu} \tag{3.44}$$

$$P_r = \frac{\nu}{\alpha_a} = \frac{\mu C_p}{k_\nu} \tag{3.45}$$

Although the analysis of solar energy harnessing in the air heating chamber assumes adequate lagging which implies that the heating chamber walls are adiabatic, the overall heat loss coefficient used in equations 3.21, 3.33 and 3.38 is employed to establish the extent of heat losses through the walls and is given by equation 3.46 (Kaushika and Sumathy, 2003; Al–Ajlan *et al.*, 2003). In this equation, U_t, is the heat loss coefficient for both the collector and cover plates (also termed top heat loss coefficient), while k_b and t_b, are the conductivity and the thickness of the insulating material at the bottom of the heating chamber, respectively. On the other hand, L_1, k_e and t_e are the depth, conductivity and thickness of the insulating material of the heating chamber walls, respectively.

$$U_L = U_t + \left\{\frac{k_b}{t_b}\right\} + \frac{(L+w)L_1k_e}{t_e} \tag{3.46}$$

Al–Ajlan *et al*. (2003) and Khoukhi and Maruyama (2004) reported that the parameter U_t, can be evaluated using the expression in equation 3.47, where f_u and C are determined using equations 3.48 and 3.49, respectively, and h_w is the wind heat transfer coefficient. The coefficient h_w is obtained from equation 3.50 (Hassan, 2000).

$$U_t = \left(\frac{N}{\frac{C}{T_c}\left(\frac{T_c - T_\infty}{1+f_u}\right)^{0.33}} + \frac{1}{h_w} \right)^{-1} + \left(\frac{\sigma(T_c^2 + T_\infty^2)(T_c + T_\infty)}{\frac{1}{\varepsilon_p + 0.0425(1-\varepsilon_p)} + \frac{1+f_u}{\varepsilon_g} - 1} \right) \tag{3.47}$$

$$f_u = (1 + 0.091N)\left(1 - 0.04h_w + 0.0005h_w^2\right) \tag{3.48}$$

$$C = 365.9(1 - 0.00883\beta + 0.0001298\beta^2) \tag{3.49}$$

$$h_w = \frac{8.6V^{0.6}}{L^{0.4}} \tag{3.50}$$

The computation of U_t requires that an initial assumed value for T_c that is slightly higher than T_∞ is used (Al–Ajlan *et al*., 2003; Khoukhi and Murayama, 2004). Using Equation 3.38, T_c is then recalculated and the new value is used to evaluate U_t. The process is repeated until the change in T_c is not significant. The value of U_t obtained is applied in equation 3.46 to determine the overall heat loss coefficient.

The sensible heating of the drying air in the heating chamber results in temperature gradient along the heating chamber. Assuming that the inlet air temperature is equal to the ambient air temperature, the plenum temperature which is obtained when $x=L$

(equation 3.21) is given by equation 3.51. The temperature T_p is taken as the temperature of the drying air just before it enters the fish drying chamber of the solar tunnel dryer, and is an indicator of the energy harnessed by the drying air.

$$T_p = T_\infty + \frac{I_c}{U_L}\left(1 - \exp\left(-\frac{A_c F U_L}{\dot{m}_a C_p}\right)\right) \tag{3.51}$$

3.1.4. Development of the fish drying model

To develop the fish drying relationships, the drying of fish is assumed to take place in a chamber of length L_2, width w_2 and depth d_d. The drying chamber is considered as control volume with a unit depth and is represented by Figure 3.3. In order to analyse the drying process, it was assumed that the drying system is adiabatic (Ebuy, 2007) due to proper lagging using highly polished and reflective internal surfaces which reduce heat losses by reflecting incident energy. It was also assumed that that the thermal properties of the drying fish are homogeneous at any given time throughout the drying bed (Sablani *et al*., 2003) and that heat and moisture transfer exist only in the direction of air flow (Fudholi *et al*., 2010). Also, the heat transfer through the fish was assumed to be by conduction with boundary convection (Perumal, 2007) and the drying process to be purely diffusion (Sablani *et al*., 2002). Further, the influence of air velocity to the drying process was assumed to be trivial as observed by Hansen and Keener (1993). Furthermore, it was assumed that there was no constant rate drying period and therefore, all drying took place in the falling rate drying period. The mass flow rate of air therefore remains constant throughout

the drying process (Ebuy, 2007). Hence, the drying rate of the fish is given by equation 3.52 (Joshi *et al*., 2005; Phoungchandang and Woods, 2000), where *M* is the moisture content (kg/kg, dry basis), *t* is the drying time (s), *k* is the drying rate constant (s^{-1}) and M_e is the equilibrium moisture content (kg/kg, dry basis).

$$\frac{\partial \mathrm{M}}{\partial \mathrm{t}} = -k(M - M_e) \tag{3.52}$$

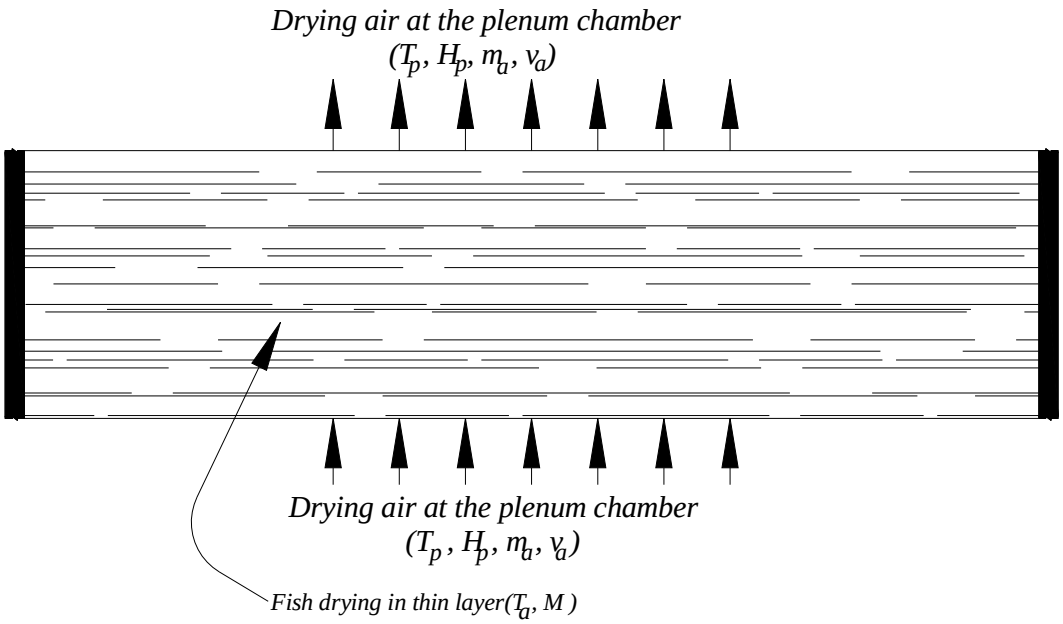

Figure 3.3: Thin layer drying control volume (assuming unit depth)

The solution to equation 3.52 is evaluated using equation 3.53 (Kadam and Samuel, 2006; Jian and Pathare, 2007), in which *MR* is the moisture ratio and M_o is the initial moisture content (kg/kg, dry basis). Equation 3.52 can also be expressed as the Fickian diffusion model as presented in equation 3.54, where D_f is the effective diffusivity of the drying fish (ms^{-2}). The drying of the fish takes place in trays in

thin layers in the drying chamber, which are considered to be of planar geometry. Therefore, the solution to equation 3.54, under the boundary conditions in equation 3.55, is represented by equation 3.56 (Trujillo *et al.*, 2007). In equation 3.56, *d* is half thickness of the drying material.

$$MR = \frac{M - M_e}{M_o - M_e} = Exp(-kt) \tag{3.53}$$

$$\frac{\partial M}{\partial t} = D_f \frac{\partial^2 M}{\partial y^2} \tag{3.54}$$

$$M\left(t = 0,\ \mathrm{y}\right) = M_0;\ M(t = t_\infty, y) = M_e;\ \frac{\partial M}{\partial y}(y = 0) = 0 \tag{3.55}$$

$$MR = \frac{M - M_e}{M_o - M_e} = \frac{8}{\pi^2}\sum_{n=0}^{\infty}\left(\frac{1}{2n-1}\right)^2 \exp\left(-(2n-1)^2\left(\frac{\pi}{d}\right)^2 D_f t\right) \tag{3.56}$$

For large values of *t* typical of drying processes (Sacilik and Unal, 2005; Horner, 1992), the first term of the series shown in equation 3.56, obtained by considering only first term of the series n = 1 and neglecting the higher term (Mudgal and Pande, 2007) is used to evaluate moisture ratio as in equation 3.57. Since equilibrium moisture content is a function of relative humidity of the drying air (Mujumdar and Devahastin, 2000; Ng *et al*., 2006), and because under solar drying the relative humidity is difficult to hold constant, the equilibrium moisture content of the drying fish changes with varying relative humidity. This change complicates the application of equations 3.53 and 3.57 in the analysis of the drying. Kingsly *et al*. (2007) and Sacilic *et al*. (2006) suggested that for varying relative humidity, the equilibrium

moisture content in equation 3.53 is omitted in analysis, and therefore, the moisture ratio is given by equation 3.58.

$$MR = \frac{M - M_e}{M_o - M_e} = \frac{8}{\pi^2} exp\left(\frac{-\pi^2}{d^2} D_f t\right) \tag{3.57}$$

$$MR = \frac{M}{M_o} = Exp(-kt) \tag{3.58}$$

The finite difference form of equation 3.57 can be represented by equation 3.59 (Bala, 1997). In this equation, M_t is the moisture content (kg/kg, dry basis) of fish at time *t (s)* and M_{t+1} is the moisture content at time *t+1(s)*.

$$M_{t+1} = M_t e^{-k\Delta t} + M_e(1 - e^{-k\Delta t}) \tag{3.59}$$

According to Hamdami *et al.* (2006) and Corzo *et al.* (2008), the effect of temperature on the drying of fish in a drying chamber, taking into account the effective diffusion coefficient, is expressed in an Arrhenius form (equation 3.60). In this equation, D_o, E, R and T represent the pre–exponential factor (ms^{-2}), the activation energy (J/mol), the universal gas constant (J/K–mol) and the temperature of the drying air (K), respectively.

$$D_f = D_o \exp\left(-\frac{E}{RT}\right) \tag{3.60}$$

Shrinkage has a direct influence on the drying of fish since it reduces its dimensions and consequently alters the drying kinetics (Talla *et al.*, 2004; Senadeera *et al.*, 2005;

Pinto and Tobinaga, 2006). In turn, shrinkage affects the effective diffusivity, D_{sf} (m/s^2), of fish during drying. Therefore, the values of D_{sf} for fish during drying must be evaluated as shown in equation 3.61 (Batista *et al*., 2007), where, $\beta_s^{'}$ is the linear shrinkage coefficient. Using the analysis of volumetric shrinkage by Talla *et al*. (2004) and Krokida and Maroulis (2001), the value of β', can be expressed as in equation 3.62 (Dissa *et al*., 2008), where ρ_{sd} and ρ_w are the solid density of fish and the density of water (kg/m^3), respectively.

$$D_{sf} = D_f \left(\frac{1}{1+\beta_s^{'} M} \right)^2 \tag{3.61}$$

$$\beta_s^{'} = \left(\frac{\rho_{sw}}{\rho_{sw} + \rho_w M_o} \right)^{\frac{1}{3}} \tag{3.62}$$

Furthermore, an analogy can be drawn between equations 3.53 and 3.57 which give the relation between the drying rate constant *k* and the effective diffusivity D_{sf} for the drying fish as in equation 3.59 (Hassini, 2006; Mujaffar and Sankat, 2005). Based on equation 3.63, the effective diffusivity has a direct proportionality with the square of the material thickness. Besides, the relationship between the thickness of a drying fish, shrinkage coefficient, and moisture content at any time in the drying process is given by equation 3.64 (Waje *et al*., 2005; Batista *et al*., 2007), in which d_s and d_o represent shrinkage dependent material thickness (m) and the initial thickness of the drying fish (m), respectively.

$$k = \frac{\pi^2 D_{sf}}{d^2} \tag{3.63}$$

$$d_s = d_o\left(1 - \beta' \frac{M}{M_o}\right) \tag{3.64}$$

Hadrich *et al*. (2008) stated that the dependence of E, and D_o on the drying temperature is represented as in equations 3.65–3.66, in which a_x and b_x are coefficients.

$$E = exp\left(-1308.795 + \frac{60723.17}{\left(T_p - 273\right)} + 195.799ln\left(T_p - 273\right)\right) \tag{3.65}$$

$$D_o = \left(1554.946 - 0.059 \times \left(T_p - 273\right) + 0.29271\left(T_p - 273\right)^2\right)\left(a_x + b_x \mathrm{M}\right) \tag{3.66}$$

By combining the analysis of structural properties of shrinkage dependent drying as analysed by Talla *et al*. (2004), Trujillo *et al.* (2007) and Hadrich *et al.* (2008) equations 3.61–3.62 and 3.64 can be combined to yield the parameter D_{sf} as expressed in equation 3.67. In addition, merging 3.63 and 3.67 yields the shrinkage–dependent drying rate constant, k_s, given by equation 3.68.

$$D_{sf} = D_o\left(\frac{\rho_s + \rho_w M_0}{\rho_w M_0 + \rho_s\left(1 + \rho_s\right)}\right)^2 \exp\left(-\frac{E}{RT_p}\right) \tag{3.67}$$

$$k_s = D_o\left(\frac{\pi M_o}{d_o\left(1 + \beta_s' M\right)\left(M_o - \beta_s' M\right)}\right)^2 exp\left(-\frac{E}{RT_p}\right) \tag{3.68}$$

In the analysis of shrinkage–drying of fish in a solar tunnel dryer, the finite difference form of moisture content of the drying fish is obtained by replacing k in equations 3.58 with k_s as given in equation 3.68, and manipulated to yield a finite difference moisture content equation in equation 3.69.

$$M_{t+\Delta t} = M_t \exp\left(-D_o \left(\frac{\pi M_o}{d_o \left(1+\beta_s^{'} M_t\right)\left(M_o - \beta_s^{'} M_t\right)} \right)^2 exp\left(-\frac{E}{RT_p} \right) \Delta t \right) \qquad (3.69)$$

3.2. Computer simulation models for energy harnessing and fish drying

3.2.1. Model for energy harnessing

A visual basic program (Microsoft Visual Basic 6.0^{TM}) was developed to simulate the global solar radiation, I_g, (equations 3.18–3.20) incident on the solar tunnel dryer and the solar energy harnessed as represented by T_p (equation 3.51). The important input variables in the simulation of I_g are φ, H_{asl}, which were determined using a hand held GPS (Garmin Etrex Summit HC; Garmin, New South Wales, Australia), $\overline{S}_a$ and T_∞. Three year (i.e., 2000–2002) daily sunshine data were obtained from field station weather records at BEED in JKUAT, and used to evaluate $\overline{S}_a$. The parameter $\delta, \overline{S}_p$, a_j and b_j were determined using equations 3.4, 3.6, 3.9 and 3.10, respectively.

In order to simulate T_p, the mean hourly ambient air temperature (T_∞) was evaluated from a 3–year hourly temperature data obtained from weather data records at BEED, JKUAT, while I_c was determined using equation 3.22. In this equation the values of R_b, R_d and R_r were calculated from equations 3.23–3.25, respectively, in which the value of β was assumed to be zero, which is the tilt angle for a horizontally laid collector–plate. In addition, the albedo of the surrounding area was based on the nature of the surface, where areas such as grasslands, concrete surfaces, near buildings, have a low value of 0.2 (Al–Ajlan *et al*., 2003) as opposed to snowy and shiny surfaces which have an albedo of between 0.7–0.9 (Castro *et al*., 2001). Further, it was necessary to evaluate the values of $(\tau\alpha)_e$ as in equation 3.26, in which τ was determined using equations 3.25–3.29, whereas the values of α were selected from Table 3.1.

It is desirable that a high value of α (0.9–0.99) is used in the design of solar energy harnessing systems (Garg and Prakash, 2000), for better absorption of solar radiation. This is because use of low values would mean using collector plate with low absorptivity, and therefore reducing the energy harnessing potential of the collector dryer. Based on equation 3.25, an increase in the value of α results in increased value of $(\tau\alpha)_e$, and consequently, the value of I_c, in equation 3.22. Further, the cover plate thickness and refractive index were selected from Table 3.2. The diffuse reflectance ρ_d was taken as 0.15 (Sukhatme, 2003), while k_c was set at 5. Normally k_c varies between 5 and 25 m^{-1}, however, design requires that a low value of k_c is used (Sukhatme, 2003, Al–Ajlan *et al*., 2003). This is because an increase in

the value of k_c woukd result in reduction in τ (equation 3.27) and this would result in reduction of the value of $(\tau\alpha)_e$ (equation 3.25) and subsequently reduce the value of I_c. The physical implication of increased value of k_c is that the cover plate in use is of poor transmittance, which would reduce the quantity of solar energy transmitted through the cover plate.

Table 3.1: Properties of selective surface coatings

Coating (Selective electroplated deposits)	Substrate	Absorptivity	Emissivity	T_{max}(^oC)
lack Nickel on Bright Nickel	Fe, Cu	0.96	0.07	>288
Black Nickel on Bright Nickel	Zn/Al	0.96	0.07	>288
Black Nickel	Zn/Fe	0.94	0.09	
Black Nickel	Fe	0.9	Low	
N_iS/Z_nS	Al	0.94	0.15	
Black Chrome on Bright Ni	Fe, Cu	0.95	0.09	427
Black Chrome on Bright Ni	Zn/Al	0.95	0.12	427
Black Chrome on Bright Ni	Any	0.96	0.1	
Black Chrome on Bright Ni	Ni/Al	0.95	0.5	
Black Chrome on Bright Ni	Cu	0.95	0.08	316
Black Chrome on Bright Ni	Zn/Fe	0.95	0.16	427
Black Chrome on Bright Ni	Fe	0.91	0.07	427
Black Chrome on Bright Ni	Fe	0.94	0.2	150

Source: Garg and Prakash (2000)

Table 3.2: Refractive indexes and thicknesses for various cover material

Material	Refractive Index	Thickness (m) $\times 10^{-3}$
Glass	1.518	3.175
FibreGlass Reinforced Polyester (sunlight)	1.540	6.350
Acrylic (Plexiglass)	1.490	3.175
Polycarbonate (lexan)	1.586	3.175
Polytetraflouroethylene (Teflon)	1.343	5.080
Polyvinyl Fluoride (Tedlar)	1.460	1.016
Polyester (Mylar)	1.640	1.270
Polyvinylidene Fluoride (Kynar)	1.413	1.016
Polyethylene	1.500	1.016

Source: Sukhatme (2003)

Other parameters that were used in the simulation of T_p are A_c, F', U_L, $\dot{m}_a$ and C_p. The length and width of the collector plate which define A_c as used in equation 3.32 were measured manually. The value of U_L used in determining F in equation 3.33 was evaluated using equation 3.46, in which the values of k_b as tabulated in Appendix 3 were used, while t_b considered the range of different thicknesses of insulating soft–board material available material in the market, ranging from 5 mm to 12.5 mm. Other thicknesses of the same material vailable in the market were also tried. In addition, L_1 as used in equation 3.46 was measured manually, whereas the values of k_e and t_e were equal to k_b and t_b, respectively, as the same material with the same thickness was used for insulating the sides and bottom of the dryer. The evaluation of U_t (equations 3.46) requires that an initial assumed value for T_c that is slightly higher than T_i is used (Al–Ajlan *et al.*, 2003; Khoukhi and Murayama, 2004). In this study, an initial value of T_c which was 10^oC above T_i was utilised. Using equation 3.38, T_c is then recalculated and the new value is used to evaluate U_t. The process is repeated until the change in T_c is not significant. The value of U_t obtained is then applied in equation 3.46 to determine U_L.

Table 3.3: Thermodynamic and transport properties of air–water system

Property	Value or expression
K_v	$2.4525\times10^{-2}-7.889\times10^{-5}T-1.790\times10^{-8}T^2-8.570\times10^{-12}T^3$
M	$1.691\times10^{-5}+4.984\times10^{-5}T-3.187\times10^{-11}T^2+1.391\times10^{-14}T^3$
ρ_a	$353.44/T_a$
C_p	$1.00926\times10^{3}-4.0403\times10^{-2}T+6.1759\times10^{-4}T^2-4.097\times10^{-7}T^3$
$P_{(T)}$	$exp(25.317)-5144/T_a$
C_{pv}	$1.883-1.6737\times10^{-4}T+8.3486\times10^{-7}T^2-2.6922\times10^{-10}T^3$
C_{pw}	$2.8223+1.1828\times10^{-2}T-3.5043\times10^{-5}T^2+3.601\times10^{-8}T^3$

Source: Tiwari *et al.* (2006), Mujumdar and Devahastin (2000)

Additionally, the parameter h_e as used in equation 3.33 was determined based on equation 3.35, in which h_b was evaluated from equation 3.37. In equation 3.37, the value of N_u was evaluated either using equation 3.42 or 3.43, depending on the value of L_{cd} and R_e as calculated by equations 3.41 and 3.44, respectively. The computation of R_e required that the velocity of air, v_a (m/s), air density, ρ_a (kgm^{-3}), the dynamic viscosity of air μ(kg/m–s), and d_e (also used in determining h_b in equation 3.37) are determined. Conversely, the evaluation of P_r required that μ, C_p and the thermal conductivity of air and k_v (W/m–K) be established. The data for the parameter v_a were obtained from weather data available at BEED, JKUAT and were used in the evaluation of ρ_a, μ, K_v, while values of C_p were determined from expressions presented in Table 3.3, based on the temperature of the drying air. In addition, d_e was evaluated using equation 3.40. Finally, the determination of h_{eq} was a prerequisite to the computation of h_e, and this required values for σ (i.e., $\sigma = 5.67\times10^{-8}$ Wm^{-2}K^{-4}), T_c, T_b, ε_p and ε_b. Equations 3.38 and 3.39 were utilized to calculate the values of T_c and T_b, while the values of ε_p and ε_b used were obtained from Appendix B. The parameter T_p is an important input parameter, among others, in the drying process. A flow chart of the energy reception and harnessing algorithm during the simulation process is presented in Figure 3.4, and the corresponding computer program is given in Appendix 1.

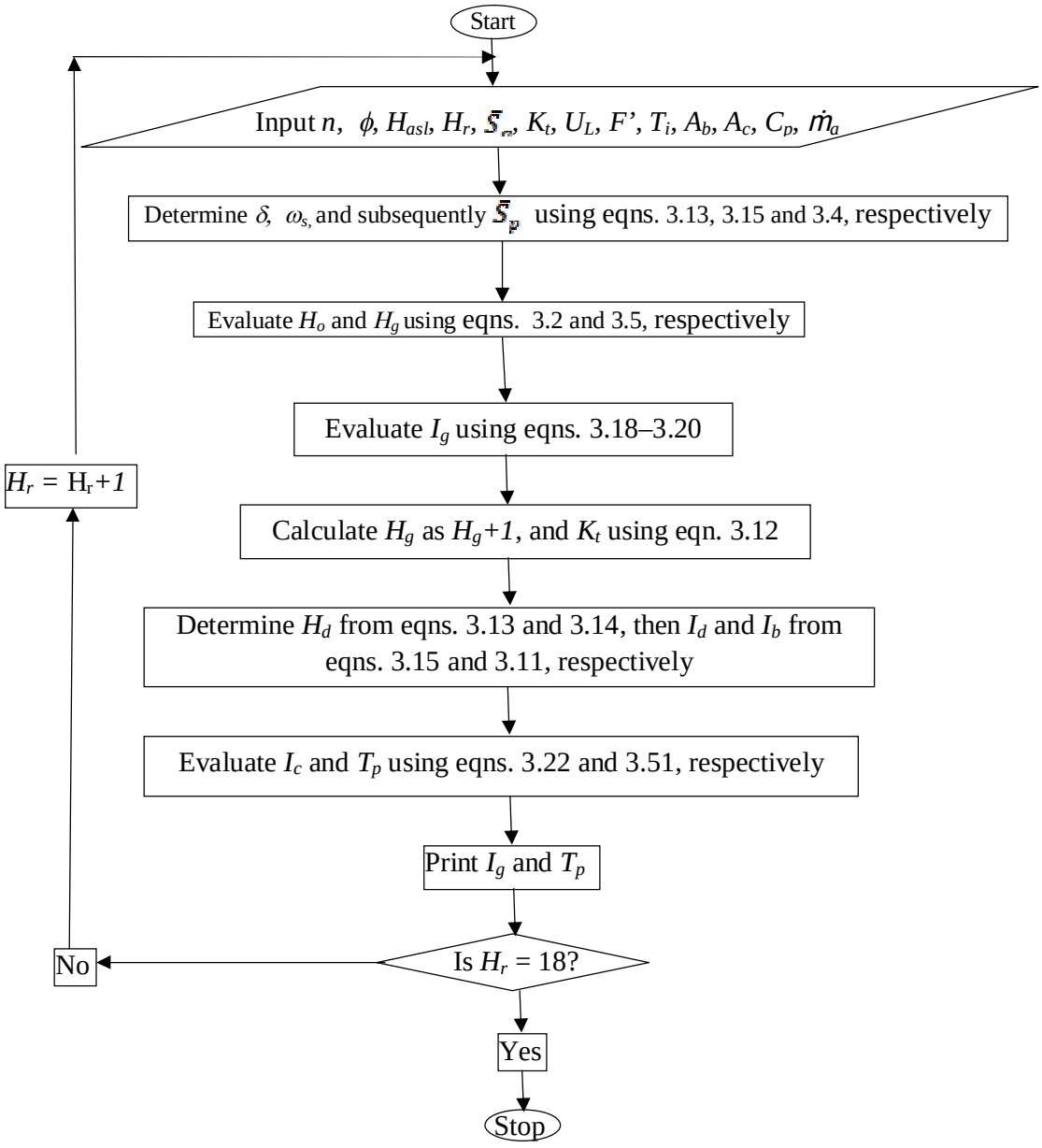

Figure 3.4: A flow chart for simulating energy reception and harnessing.

3.2.2. Model for fish drying

The simulation of the drying of fish in the solar tunnel dryer was also executed in Visual Basic 6 (Microsoft Visual Basic 6.0^{TM}). The input parameters in the simulation process (equation 3.69) include T_p, as computed in Section 3.2.1, H_r, M_t, M_o, d_o, E, D_o, $\beta_s^{'}$, R, and t, while the output is the moisture content of the fish at time $t+\Delta t$, $M_{t+\Delta t}$. In order to simulate the drying process, the values of parameters $\beta_s^{'}$, E and D_o were evaluated using equations 3.62, 3.65 and 3.66, respectively. The values of the other input variables are as tabulated in Table 3.4. In the simulation process a_x and b_x were initially assigned values given by Hadrich *et al*. (2008). These values were further refined during the simulation process, using trial and error, to improve the performance of the model. The final values obtained are presented in Table 3.4. A flow chart of the fish drying algorithm used during the simulation process is presented in Figure 3.5, whereas the corresponding computer program is also given in Appendix 1A.1. The overall computer Graphics User Interface used for the simulation process during the energy harnessing and the drying process is shown in Appendix 1A.2.

Table 3.4: Parameters used in simulating in drying of fish in a solar tunnel dryer

Parameter	Value	Source
Thickness of fish, d_o (mm)	12.5	Measured
Dry density of fish, ρ_s (kg/m^3)	1356	Rahman *et al.* (1996)
Density of water, ρ_w (kg/m^3)	1000	Rahman *et al.* (1996)
Initial moisture content of fish, M_o (kg/kg, d.b)	6.10	Measured
Universal gas constant, R (J/mol^{-}K)	8.3145	Sacilik and Unal, 2005
$b_x(\times 10^{-7})$	4.8	Hadrich *et al.* (2008)
$a_x(\times 10^{-7})$	3	Hadrich *et al.* (2008)

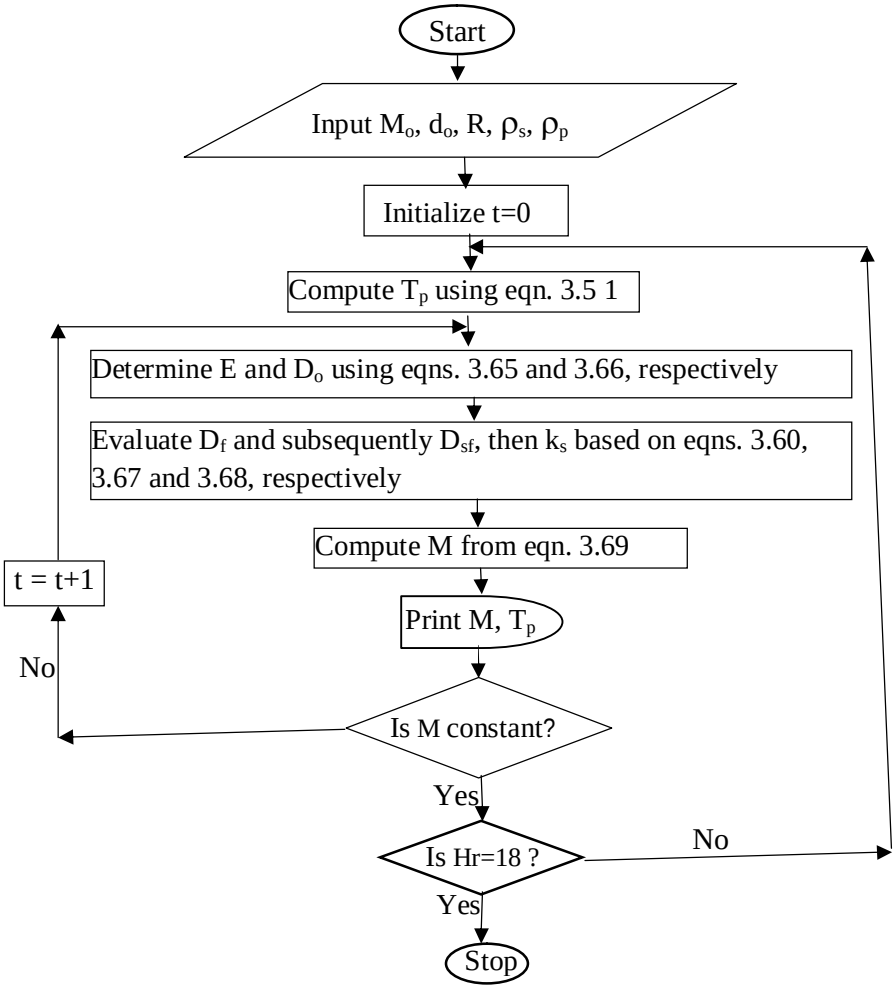

Figure 3.5: A flow chart for simulating fish drying.

3.3. Validating the performance of the developed simulation models

3.3.1. Description of the solar tunnel dryer used in the validation process

Figure 3.6 shows a schematic diagram of the solar tunnel dryer used in this study. The actual solar tunnel dryer is presented in Plate 3.1. The dryer has a solar energy

harnessing section, which is the air heating chamber, and a drying chamber. Both chambers are completely sealed from light to preserve light sensitive nutrients in fish during drying. In the course of energy harnessing, solar radiation enters through the cover plate and heats the collector plate. Since the cover plate is opaque to solar energy reradiated from the collector plate, it concentrates most of the incident energy in the heating chamber (Garg and Prakash, 2000). In addition, air enters the heating chamber through an inlet (Point A) and exits at point B as it enters the drying chamber. As the air moves from point A to point B, heat energy is transferred from the collector plate to the air, through convective heat transfer mechanism. A temperature gradient exists within the heating chamber, with the temperature at point A being lower than that at point B (the plenum chamber temperature). Thus, the rise in air temperature depicts solar energy harnessing at the tunnel section of the solar dryer.

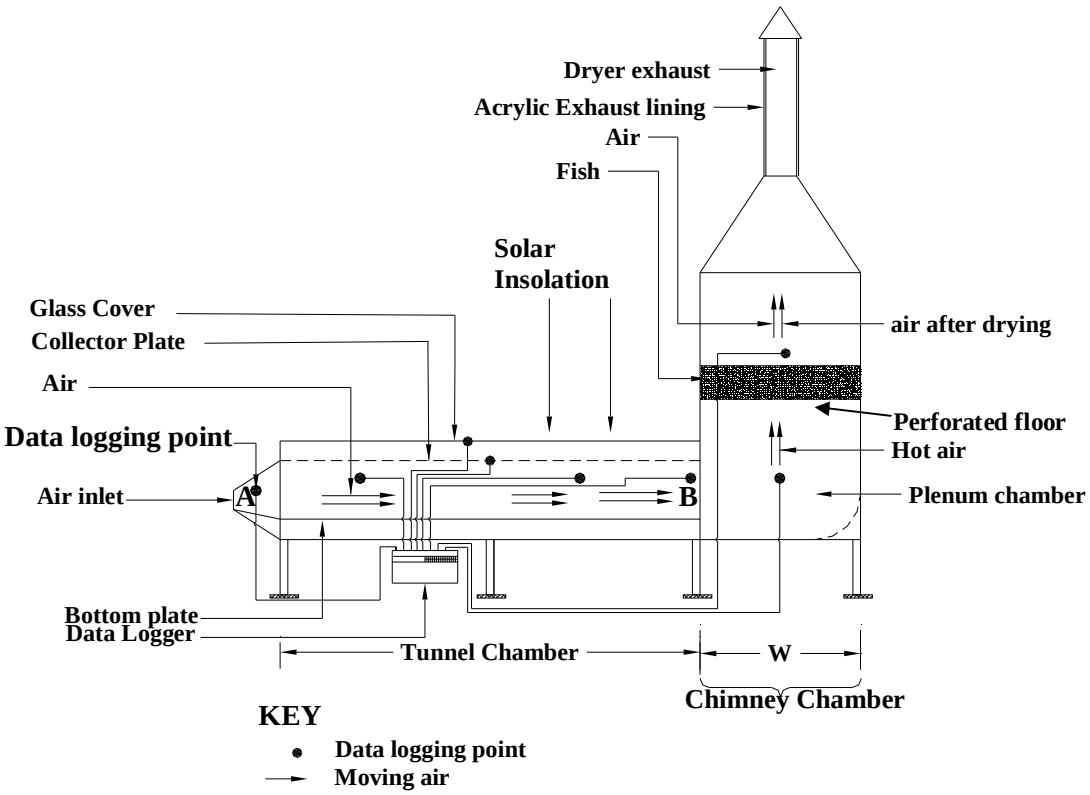

Figure 3.6: A schematic diagram of the solar tunnel dryer

The tunnel section of the dryer measures 2.44m long, 1.22m wide and 0.54m high, and has a 19mm thick rectangular galvanised iron (GI) collector plate, which is painted black for enhanced absorption and emission of solar energy, and a glass cover–plate. The bottom plate of the tunnel section was made of aluminium painted GI sheet, to reflect energy incident on the surface. The rear side wall of the tunnel chamber was made of aluminium coated GI sheet. In addition, the front wall of the tunnel chamber had two sets of overlapping doors through which fish was placed in the chamber, and thermocouples from various data logger channels were inserted inside the dryer. Further, the inner walls of the doors were made of aluminium coated GI sheets, while the bottom

and the side walls of the sheets were insulated with soft-board which was sandwiched between the inner and outer GI sheets to minimise energy losses.

The dimensions of the drying chamber, on the other hand, were 1.22m long, 0.9m wide and 0.7m high for the rectangular cross–section. Those for the tapered section of the chamber were 1.22m x 0.7m at the bottom, and 0.2m by 0.2m at the narrow end. The chamber was made of GI sheets, with the inner walls coated with aluminium while the outer walls were painted black. An exhaust system secured above the chamber was lined with acrylic glass to trap solar energy for heating the exhaust air, in order to enhance natural convection. At the base of the exhaust pipe was a solar–driven 12V, 0.16A 1.92W d.c. suction fan, capable of delivering $1.2m^3/s$ of air, and could induce forced convection in the dryer whenever necessary.

Plate 3.1: The solar tunnel dryer

3.3.2. Validating the energy harnessing model

a) Data acquisition

The validation of the energy harnessing model was composed of two components, namely the global solar radiation and the energy harnessing models. Thus, it was necessary to acquire the appropriate data for the validation of the two models. Further, the simulation global solar energy reception model was validated using Satellite solar radiation data for the experimental station. The experimental site was located at the Biomechanical and Environmental Engineering Department of the

Jomo Kenyatta University of Agriculture and Technology, in Juja township, 10 km West of Thika town and 45km East of Nairobi, Kenya. The latitude, longitude and altitude of the location are 1.18^{o}S, 37^{o}E and 1460m above sea level, respectively. Ten year daily satellite global solar radiation data (viz: 1996–2005) for the experimental site was downloaded from the free–source NASA website (Kustever, 2010). The mean daily solar radiation was computed from the downloaded data using excel spreadsheet (MS Excel 2007^{TM}), and compared with simulated data.

Using the solar tunnel dryer exemplified by Figure 3.6, inlet air and plenum chamber temperatures were measured at points A and B, respectively. The measurement was carried out using electronic thermocouples which relayed the temperature readings to an automatic electronic data logger (Thermodac Eto Denki E, Shimadzu, Japan). The data was measured between 7 O'clock and 18 O'clock, each day at one hour interval, giving 12 data per day, and a total of 60 data for the five data acquisition days. The data obtained was compared to the simulated plenum chamber temperature data. In addition, the relative humidity of air at the same points was measured using RS–10 Thermo Recorder (Tabai Espec Corporation, Tokyo, Japan).

b) Evaluating the performance of the model

To validate the developed models, comparison was made between simulated and actual data for both the global solar radiation and energy, using graphical methods, residual analysis, regression analysis and Student's t–test. In order to establish the

repeatability of experimental data, the mean and standard deviations of the data were also established. The absolute residual error ε_r was determined as shown in equation 3.70 (Uluko *et al*., 2006; Kanali, 1997), in which ψ_p and ψ_m are the predicted and actual values, respectively. The prediction performance ($\eta_{\mu m}$) of the model at μ_m% residual error interval was determined by equation 3.71, where ς_c and ς_t represent the number of data within the interval and the total trial data, respectively. In addition, regression analysis and the two tail Student's t–test were carried out in excel spreadsheet (MS Excel 2007^{TM}) to relate the predicted and actual data

$$\varepsilon_r = \left| \frac{\psi_p - \psi_m}{\psi_m} \times 100 \right| \tag{3.70}$$

$$\eta_{\mu m} = 100 \times \frac{\varsigma_c}{\varsigma_t} \tag{3.71}$$

3.3.3. Validating the fish drying model

Tilapia fish (*Oreochromis niloticus*) were procured from the fish landing sites along Chania River near Thika Town, Kenya, and placed in ice boxes immediately, before being transported to a Food Science laboratory at JKUAT. In the laboratory, the fish were beheaded, de–scaled, eviscerated and thoroughly washed, before being split open longitudinally and cut into 200 pieces of approximately 5cm by 5cm by 1.25cm as recommended by Oduor-Odote *et al.*(2008). Three pieces of fish were selected at random from the sample, and used to evaluate the initial moisture content. The remaining pieces were spread in a drying tray as Plate 3.2, and placed in the drying

chamber of the solar tunnel dryer to dry shown in Figure 3.5. The dryer was exposed to sun under prevailing atmospheric conditions. The moisture content of the drying fish was determined using standard Association of Analytical Communities (AOAC) proximate analysis method (Kiaye, 2004; Ogunjobi *et al.*, 2005). The performance of the simulated model was evaluated by comparing actual and simulated data, as detailed below Section 3.3.2(b).

Plate 3.2: Fish in a drying tray

3.4. Optimizing solar tunnel dryer design using genetic algorithms

3.4.1. The Goal genetic algorithm

The GOAL genetic algorithm used in this study was downloaded from the internet (downloadable at www.oocities.com/geneticoptimisation, 2008). It is a free source GA and is able to solve complex problems using real and binary coding, for multiple variate functions which have several constraints and present complex objective functions. The algorithm was encoded in Visual Basic Script; which facilitates the formulation of optimisation problems. In the formulation of the problem, a Graphics User Interface (GIU) is available where variables are input before the process of selection, coding, reproduction, mutation, decoding, evaluation of fitness, replacement of the parents with off–springs and further iteration processes take place. The algorithm loops the process until a set of pre–established conditions is met, when it generates an array of optimal decision variables, which give the desired output, in this case plenum chamber temperatures. The generation of the solutions using the Goal followed the process shown in Figure 3.7. The GIU of the GA used in this study is presented in Figure 3.8.

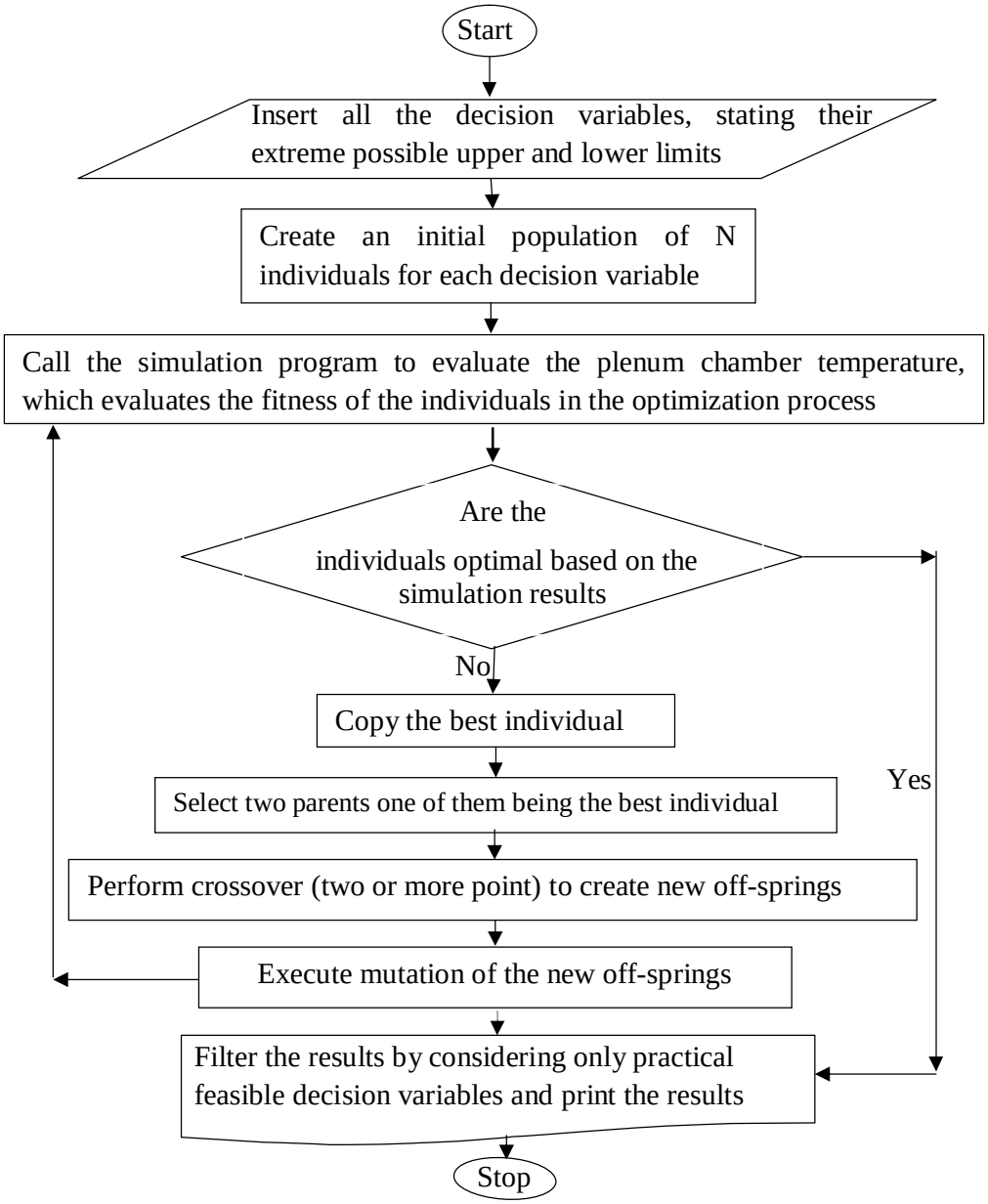

Figure 3.7: A flow chart for solar dryer optimization using genetic algorithm.

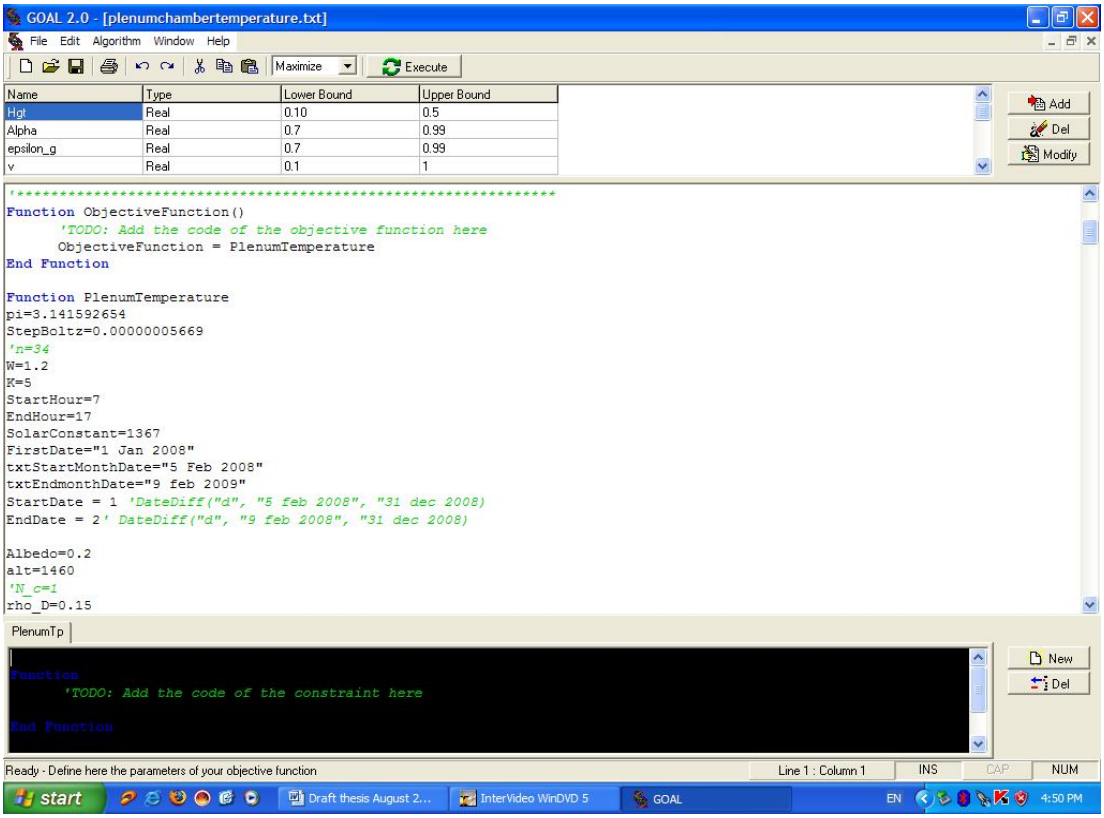

Figure 3.8: The graphics user interface for Goal genetic algorithm.

3.4.2. The optimisation problem

The optimisation of the solar tunnel dryer involves executing the Goal GA in order to generate a combination of input parameters that would yield the maximum plenum chamber temperature, subject to a set limit of the maximum plenum chamber temperature, and dimensions of the solar tunnel dryer. The limiting temperature was guided by the minimum temperature for development of micro–organisms as stated earlier, while the upper limit of the temperature was set as that which must avoid the effects of overheating (see section 2.3.3). The cross–sectional area of the cover plate is guided by the length and width of the cover plate. These two parameters are

further limited by ergonomics and transportability of the dryer. In this study, the length and the width of the solar tunnel dryer were set at 10m and 1.5m, respectively. Based on the preceding information, the objective function of the optimisation problem is expressed as shown in equation 3.72.

$$\begin{aligned} &\textit{Maximize } T_p = T_\infty + \frac{I_c}{U_L}\left(1 - \exp\left\{-\frac{A_c F U_L}{\dot{m}_a C_p}\right\}\right) \\ &\textit{subject to} \begin{pmatrix} 50 \le T_p \le 60 \\ 0 < A_c \le 15 \\ 0 < b_d \le 1 \\ 0 < V \le 15 \end{pmatrix} \end{aligned} \qquad (3.72)$$

The input parameters in the optimisation process were classified as environmental parameters, material parameters and parameters defining airflow properties. The environmental input variables include φ, H_{asl}, $\overline{S_a}$ and T_∞, which were determined as described in section 3.2.1. In addition, the material variables used in the optimisation comprise β, A_b, α, ρ_d, k_c, η, θ_i, θ_2, L, w, k_b, t_b, L_1, k_e, and t_e. Other material parameters were σ (i.e., $\sigma = 5.67\times10^{-8}$ $Wm^{-2}K^{-4}$), T_c, T_b, ε_p and ε_b, while the parameters defining the air flow properties are V_a, μ, C_p, *humidity*, T_a, K_v, ρ_a, and the partial vapour pressure, $P_{(T)}$. On the other hand, the output parameters were plenum chamber temperature and the moisture content of the dried fish.

In the simulation, the input parameters were declared in the graphic–user interface (Figure 3.9). By selecting "add" button located close to top right hand corner, a

parameters window in the graphic user interface opens (Figure 3.10). Through this window, the parameter name was entered, the type of coding of the parameter selected between real and binary, its lower and upper bounds declared, and the input parameter accepted. Once the input parameters were declared, they were displayed in the graphic user interface under the name, type of coding, upper and lower bounds as shown in Figure 3.12. This process was used to declare all the variables used in the optimisation process.

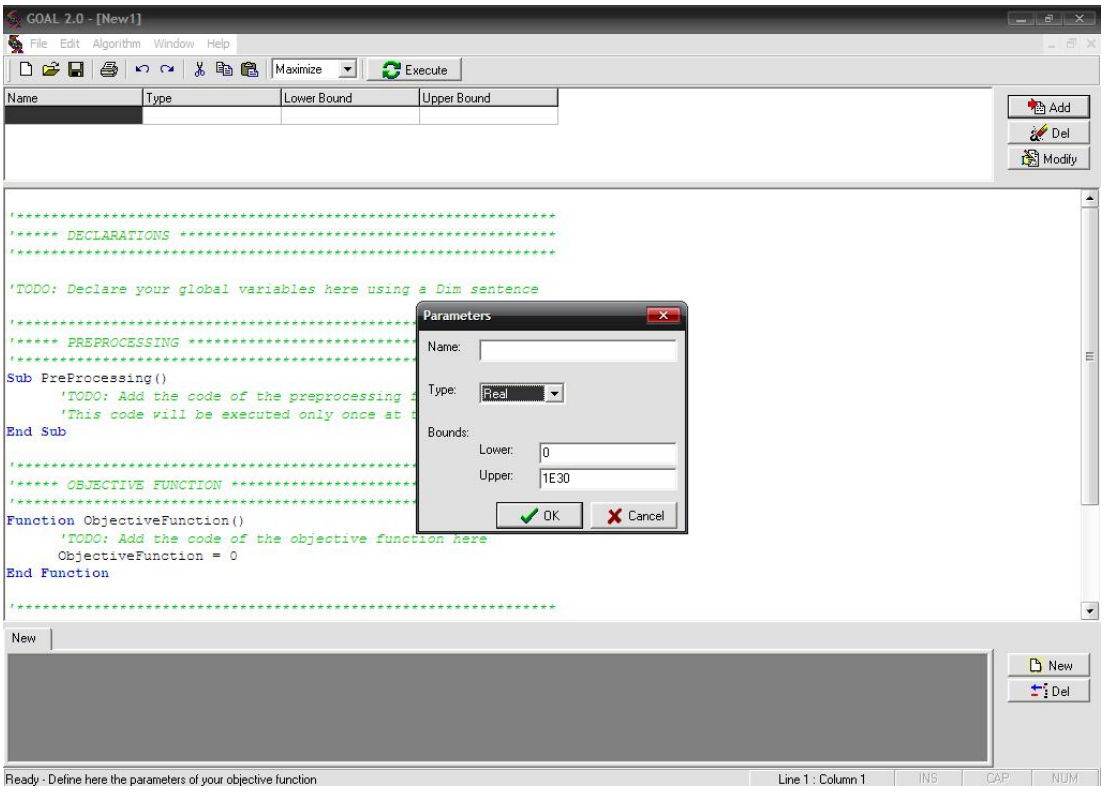

Figure 3.9: Goal genetic algorithm graphic user interphase with parameter input window.

The visual basic simulation model code which was used in Section 3.2 was modified to evaluate the objective function in the Goal genetic algorithm (Figure 3.9) coded in Visual Basic Script. In addition, by clicking the "new" command button at the bottom right corner of the graphic–user–interface (Figure 3.9), a window emerges which is used in the declaration of the constraints (Figure 3.10). Once the name of the constraint is entered and accepted by clicking "ok" in the constraints window, the name of the constraint appears in the lower left hand corner of the graphic user interphase (Figure 3.11). The code for evaluating the constraint is written in the window below the constraint (Figure 3.11). After the code development, by selecting the "options" under the "algorithm" in the pull–down menu (Figure 3.12), a combination of various genetic algorithm parameters options (Figure 3.13) were chosen. Among these options were population size, number of generations, type of reproduction which is either two–point, three–point or four–point crossover, type of selection (viz., tournament, rank or sigma), reproductive probability, mutation probability, number of elitism preservation individuals, population refreshing period and the percentage of the population refreshed.

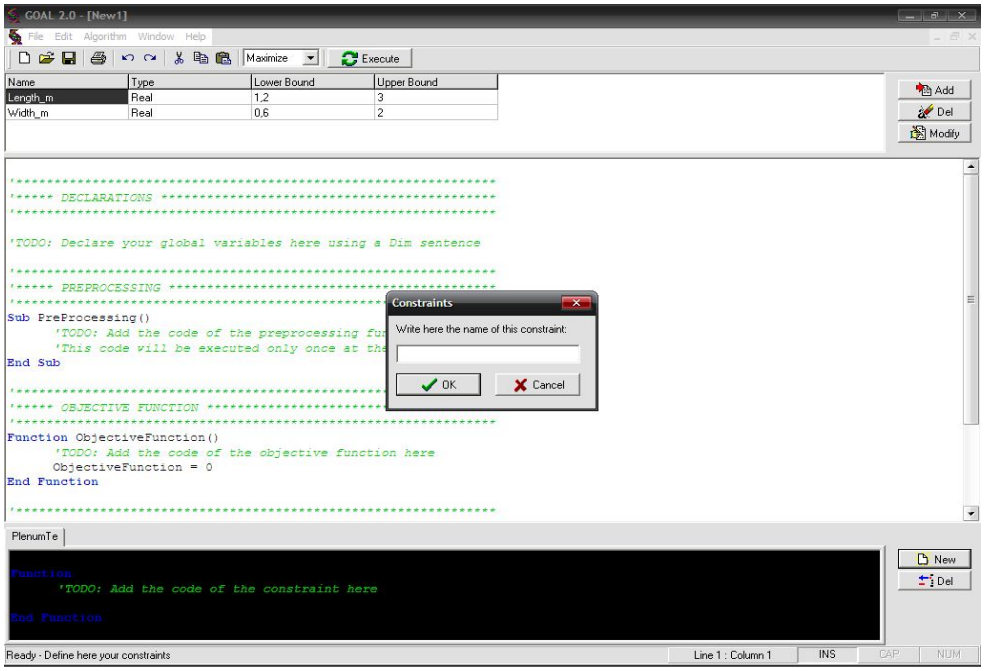

Figure 3.10: The graphic user interphase with the constraints declaration window.

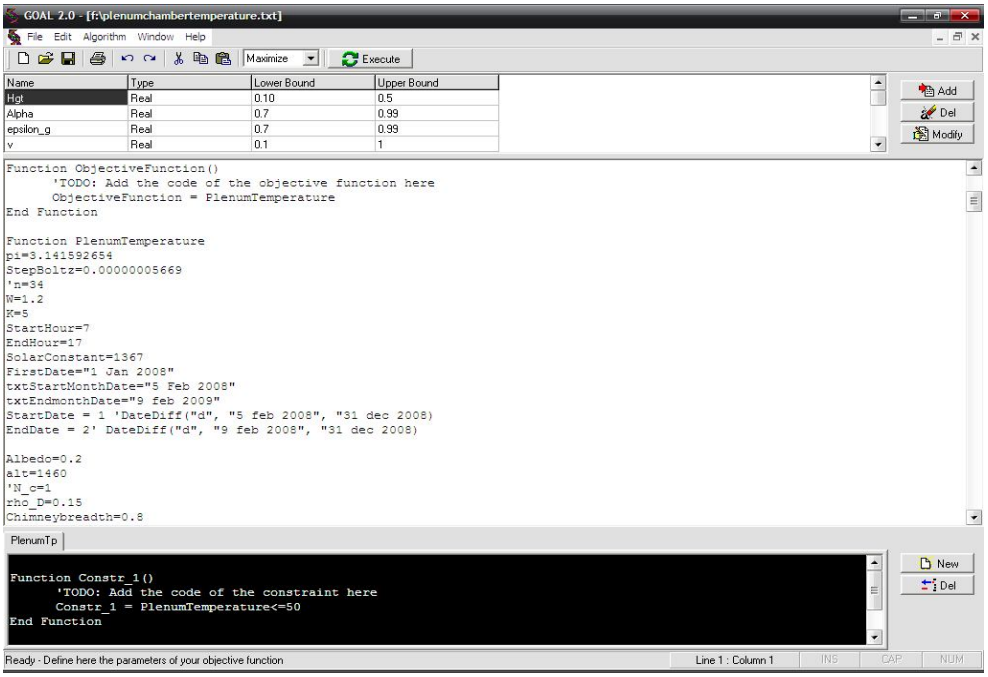

Figure 3.11: Goal genetic algorithm graphic user interface showing the constraint code.

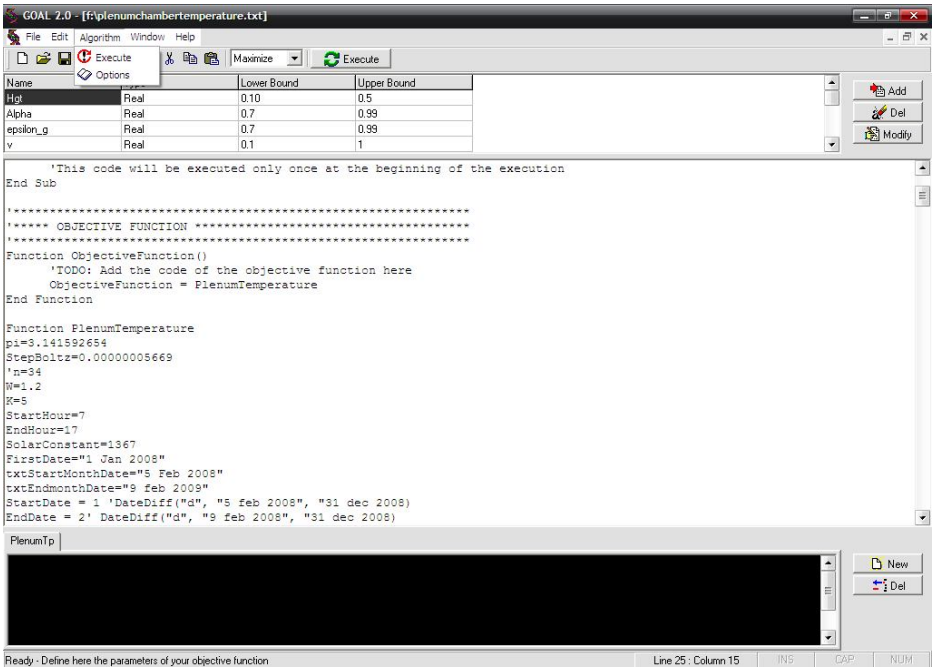

Figure 3.12: The Goal genetic algorithm options

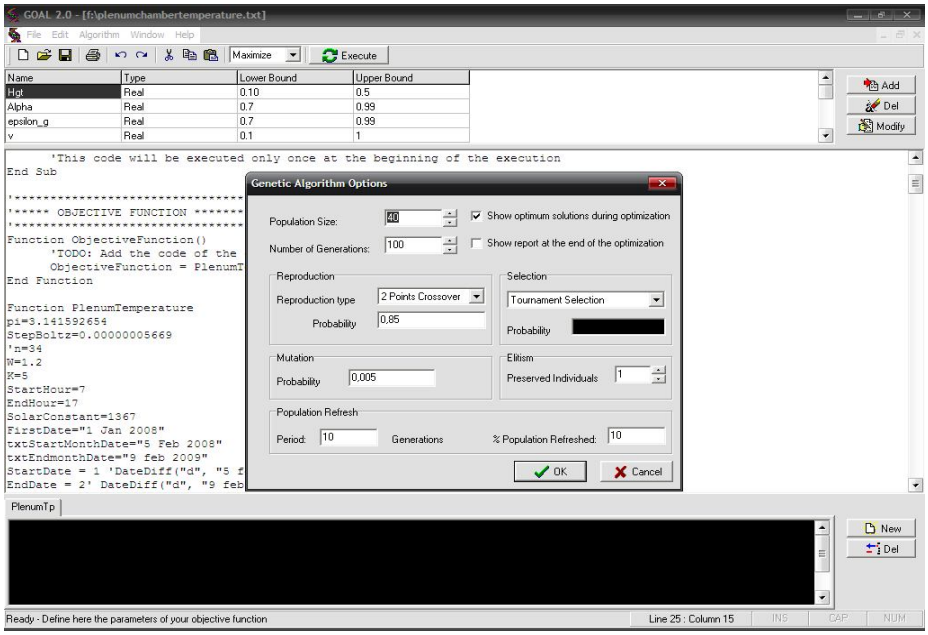

Figure 3.13: The Goal genetic algorithm graphic user interface options window.

The default parameters of the GA options are presented in Table 3.5. The table further presents the parameters used in the optimisation process in this study. The values of the GA parameters could be altered as shown in the Genetic Algorithm options provided in Figure 3.13, to improve the performance of the GA by altering the convergence rate. However, although convergence could be improved by altering of the GA parameters, the speed of convergence could be greatly reduced based on the combination of parameters altered. After more than 80 trials in this study, the set of parameters in the second column of Table 3.5 were found to converge within a one hour period, in a 3.06GHz, 512MB RAM computer. Any further alteration aimed at improving the convergence increased the convergence time to between 1 hour and 18 hours. Thus these parameters were considered as the most adequate combination for the execution of the Goal genetic algorithm. Once the most suitable parameters were selected (inset in Figure 3.13), and the algorithm debugged, the genetic algorithm was executed by clicking on the "execute" command on the GIU (Figure 3.13).

Table 3.5: The Goal genetic algorithm parameters

Parameter	Value
Population N,	60
Generations	100
Reproduction cross–over points	3
Reproduction probability	0.99
Selection type	Elitism tournament
Mutation probability	0.001
Reproduction probability	0.99
Selection probability	0.99
Elitism preserved individuals	2
Population refresh period (generations)	60
% population refreshed	10

Once executed, the GA automatically generated a report with the results of the optimization, and the evolution of several statistical parameters which include the mean value, the standard deviation, the number of mutations and reproductions in each generation. The output of the optimisation process is a set of design and material variables, which yielded different values of the plenum chamber temperature. A combination of a set of decision variables that yielded the expected plenum chamber temperature was selected after 80 iterations (Balsa–Canto *et al.*, 2002).

3.5. Performance of the optimised solar tunnel dryer

3.5.1. Development of the optimised solar tunnel dryer

Based on the optimisation results obtained in this study, the solar tunnel dryer that was used in the validation of the simulation models (Plate 3.1) required modification. The modifications made on it included a reduction of the depth of heating chamber and the drying chamber from 0.54m to 0.11m and 0.7 to 0.27m, respectively.

Although the value of the optimised collector plate tilt angle was 0.97^{o}, the angle was of the modified solar tunnel dryer was maintained at the original value of 0^{o}. The initial refractive index of the cover plate was 1.45, but based on the optimisation, a different material with refractive index of 1.31 was used. The other parameters (viz., heating chamber and drying chamber lengths and widths, bottom plate and side wall material, thickness of insulation) remained as in the solar tunnel dryer in Figure 3.6.

3.5.2. Evaluating the performance of the optimised solar tunnel dryer

The evaluation of the performance of the optimised solar tunnel dryer was based on the energy harnessed and the quality of the dried fish.

a) Performance in energy harnessing and drying of fish

In order to evaluate the performance of the optimised solar tunnel dryer, it was necessary to collect and compare data under four different treatments. Treatments 1 corresponds to the drying of fish in the non-optimised solar tunnel dryer (*NOSTD*) while Treatment 2 corresponds to that for the optimised solar tunnel dryer (*OSTD*). On the other hand, Treatments 3(a) and 3(b) correspond to drying of fish in the open sun *(OS)*.

Treatment 3(a), *OS(a),* was carried out simultaneously with *NOSTD* whereas Treatment 3(b), *OS(b),* was conducted simultaneously *OSTD*. Data for *NOSTD* and *OS(a)* were initially acquired simultaneously for three consecutive days. Thereafter,

the data for *OSTD* and *OS(b),* were acquired simultaneously for another three consecutive days. The reason why the data for *NOSTD* and *OSTD* could not be carried out simultaneously was because of the high costs involved in construction of the two drying systems. In the acquisition of the data, experiments under *NOSTD* and *OS(a)* were carried out with the for three consecutive days. The dryer was then modified to the optimal conditions within one day, and then tests under *OSTD* and *OS(b)* were performed immediately for another three consecutive days. The data acquired included the plenum chamber temperature, the ambient temperature, moisture content of the fish during drying, the humidity of the ambient and drying air, and the air flow rate. The plenum chamber and ambient air temperature data were obtained as described in Section 3.3.2. Similarly, the moisture content of the fish was obtained as described in Section 3.3.3.

A comparison was made between data under the four treatments, using graphical methods, student's *t–test*, analysis of variance and MS excel spreadsheet (MS excel 2007^{TM}). The parameters utilized in the comparison were the energy harnessed and moisture content of the drying fish. In order to establish the performance of the dryers, it was also necessary to determine the relative humidity in the drying process. To establish the repeatability of the study, the mean and standard deviation values of the mean plenum chamber temperatures and moisture ratio for the actual data points were determined.

b). Quality attributes of dried fish

i) Colour

The colour of fish under the four Treatments (*NOSTD, OSTD, OS(a), and OS(b)*) during drying was measured using a Minolta colour and colour difference meter (Minolta camera, CR 300, Osaka, Japan), which had been standardized on a white paper No. 11933069. This system uses three standard colour values: L^*, a^* and b^* to describe the precise location of a particular colour on a standard colour chart (Mohammadi *et al.*, 2008; Kiaye, 2004). The hue angle (H^*) was calculated using equations 3.73 (Mohammadi *et al.*, 2008). Using the L^*– and the H^*– values as represented on standard colour charts the colour and colour changes on ythe drying fish were determined.

$$\begin{aligned} H^* &= \tan^{-1}\left\{\frac{b^*}{a^*}\right\} \text{ for } a>0,\ b>0, \\ &= \left(180 + \tan^{-1}\left\{\frac{b^*}{a^*}\right\}\right), \text{ for } a<0,\ b>0; \text{ and for } a<0,\ b<0, \\ &= \left(360 + \tan^{-1}\left\{\frac{b^*}{a^*}\right\}\right), \text{ for } a>0,\ b<0, \end{aligned} \qquad (3.\ 73)$$

ii) Proximate analysis

The analysis of crude proteins for the fish dried under the four Treatments (*NOSTD, OSTD, OS(a) and OS(b)*) was carried out based on the standard Micro–Kjedahl's procedure as described by Kiaye (2004) and Miguel *et al*. (1994). Crude lipids were determined by proximate analysis using standard AOAC methods (Miguel et al.,

1994). In determination of rancidity, lipid peroxidation products were determined using the standard thiobarbituric acid reactive substances (TBARS) in fish flesh according to the procedure described by Menoyo *et al.* (2002) and Ke *et al.* (1984). Putrefaction in the fish, which is an indication of spoilage of proteins, was measured using the standard Total Volatile Base Nitrogen (TVB–N) procedure described by Mohan *et al.* (2008), Antoine *et al.* (2002) and Özoğul and Özoğul (2000). The rancidity and putrefaction of the fish were established by comparing the obtained TVB–N and TBARS values with the threshold values in Tables 3.6 and 3.7.

Table 3.6: TVB-N quality categorization criteria for fish and fishery

TVB–Value (mg/100g)	Quality Classification
<25	Very good
25–30	Good
30–35	Marketable
>35	Spoilt

Source: Duyar *et al.* (2008) and Robles–Martinez *et al.* (1982).

Table 3.7: Recommended guidelines on rancidity quality assessment in fish

Degree of rancidity	TBARS value (µg(MA)/kg	Overall quality
Not rancid	0–8	Excellent
Slightly rancid	9–20	Good
Moderately rancid	>21	Unacceptable

CHAPTER FOUR

RESULTS AND DISCUSSION

4.1. Relationships between incident solar energy, dryer design parameters and drying characteristics of fish

The relationships between the incident solar energy, solar tunnel dryer design parameters and the drying characteristics of fish were developed as detailed in Section 3.1. The development was based on the energy radiated by the sun on a horizontal surface, the harnessing of solar energy by air flowing through the heating chamber of the solar tunnel dryer and thin layer drying of fish in the dryer.

4.2. Simulation of the harnessed solar energy and the drying process

A computer model for the simulation of the established relationships in Section 4.1 above was developed as presented in Figure 3.4 and Figure 3.5. The corresponding computer model for simulating the energy harnessed and the drying process is presented in Appendix A1, while the Graphic User Interface is presented in Appendix A2.

4.3. Performance of the developed computer simulation models

The validation of the performance of the developed computer models was carried out by comparing simulated and actual data, using graphical methods, residual error analysis and either analysis of variance (ANOVA) or student's t–test. The models considered were global solar energy, energy harnessing and fish drying.

4.3.1. Global solar energy model

Figure 4.1 compares simulated daily annual global solar radiation with the 10–year (1996–2005) mean satellite solar radiation. The figure shows similar trend between the simulated and actual data for global solar radiation. In addition, the data agrees well with observations by Jin *et al.* (2005). The figure further shows that there were fluctuations of solar radiation, with global maxima and local maxima corresponding to 50^{th} and 275^{th} day of the year, respectively, over the 10 year period. These days are on the 19^{th} February and 1^{st} October of the year, respectively. Furthermore, Figure 4.1 shows that the global and local minima occur on the 175^{th} and 325^{th} day of the year, respectively which are on 24^{th} June and 21^{st} November of the year, respectively. The maxima and minima coincide with the hot and cold seasons in the region as reported by (Watako *et al.*, 2001).

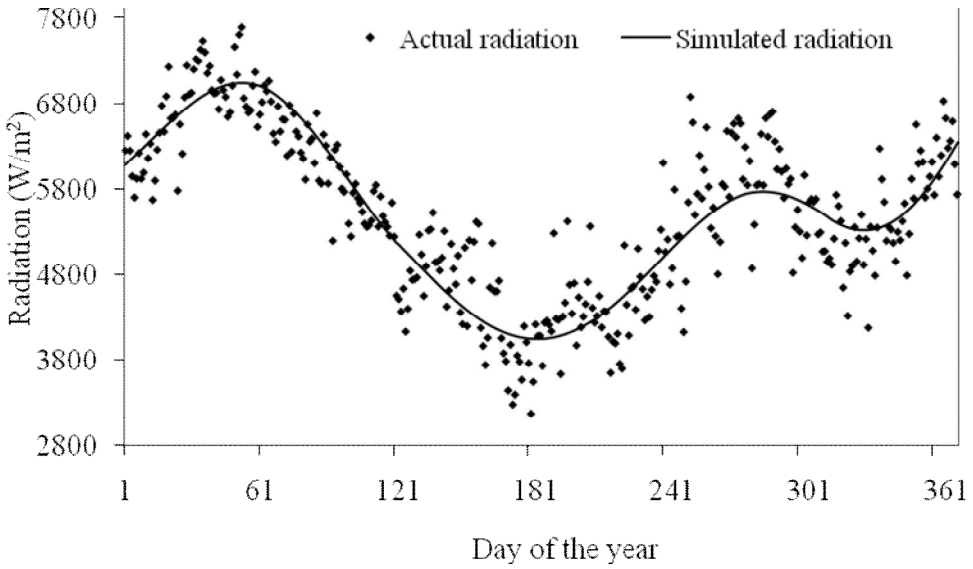

Figure 4.1: Annual variation of daily simulated and mean (10–year) of daily global solar radiation

The mean and standard deviation for the actual data were 5606.6(W/m^2/day) and 974.09, respectively, while those for simulated data were 5494.85 (W/m^2/day) and 901.6, respectively. Although the expected deviation from the mean is zero, both simulated and actual data showed significant deviation from mean. This could be attributed to the oscillatory nature of annual variation of the global solar radiation. In addition, the standard deviation for the actual data was higher than that for simulated data. This implies that the actual data is more spread from the mean than the simulated data, which could be attributed to erratic behaviour of weather, resulting from erratic wind bursts which cause cooling effects on surfaces (Dai and Trenberth, 2003; Seiki *et al.*, 2011).

The results of the absolute residual error analysis (Kanali, 1997) between the simulated and the mean of 10–year satellite solar radiation for the 4380 data ranged from 0.04–27.7%, with a mean value of 6.96%. This implies that there were discrepancies between the simulated and actual which on several days of the year rose to about 30%, but which were slightly above 5% residual error interval, and which on average were within 10% residual error interval. The discrepancy between the actual and the simulated data could be associated with hourly weather variations attributed to wind bursts (Dai and Trenberth, 2003; Seiki *et al.*, 2011), which cause abrupt cooling effect on surfaces.

Based on 5 and 10% residual error intervals the performance of the model was 51.4 and 78.4%, respectively. In addition, linear regression analysis on the data yielded a strong correlation between the simulated and actual solar radiation since the coefficient of determination (R^2), which had a value of 0.788 as shown in Equation 4.1, was high. This observation is consistent with results obtained by Mechlouch and Brahim (2008) when they developed a global solar radiation model for the design of solar energy systems. Further, a two tailed Student's *t*–test at 5% level of significance showed no statistical difference between simulated and actual global solar radiation ($t_{stat} = 0.17$, $t_{crit} = 1.65$). Therefore, the developed model can be used to simulate global solar radiation incident on a horizontal surface.

$$H_{sim} = 0.8215H_{act} + 970.90, \qquad R^2 = 0.788. \tag{4.1}$$

4.3.2. Model for harnessed solar energy

The energy harnessed by the solar tunnel dryer was represented by the plenum chamber temperatures. Figure 4.2 compares the simulated, and the means of 5–day actual plenum chamber and inlet air temperatures. The figure shows that although the simulated and actual plenum chamber temperatures had similar trends between 07.00 hours and 18.00 hours (24 hour clock), the former temperatures were always slightly higher than the latter. The developed model assumed that heat losses were only those that can be calculated using overall heat loss coefficient. However, condensation on the collector plate was prevalent in the early hours of the day and its evaporation must have consumed some energy, resulting in lower plenum chamber temperatures. Future studies should establish the possibility of incorporating adverse weather effects such as condensation in the simulation models. This would probably narrow the gap between the simulated and actual data for energy harnessing.

The fact that the actual plenum chamber temperatures were always higher than the inlet temperature demonstrates the ability of the dryer to harness solar energy and convert it to heat energy. However, the simulated and actual plenum chamber temperatures were almost the same at the 13^{th} hour of the day. This `corresponds to the time of the day when the temperatures are highest (Kaplanis,2006; Trabea, 2000; and Pidwimy, 2006). Unlike in the morning hours, there was no condensation in the system at this hour. Thus, there was no energy expended in vapourising a condensate and as a result, all the energy harnessed is manifested in temperature rise,

hence the tendency for the simulation temperature to be superimposed on the actual temperature points at that hour.

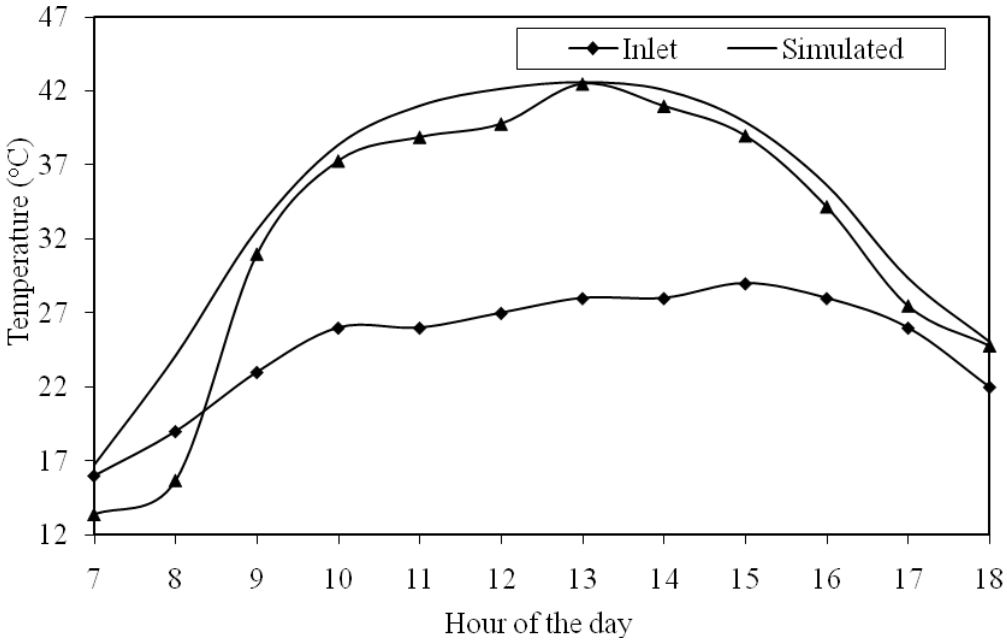

Figure 4.2: Mean of actual and simulated temperatures and inlet air temperatures

Based on residual error analysis between the simulated and the actual plenum chamber temperatures for 60 data in each category of temperatures, ε ranged between 0.28 and 53.9%. In addition, the performance of the model at 5 and 10% residual error intervals was 50 and 83.3%, respectively. The low performance of the model at 5% residual error interval could be attributed to the low heating chamber temperatures in the early hours of the day which resulting in values of ε ranging between 25 and 53.9%. Further, with the exclusion of these data with the values of ε ranging between 25 and 53.9%, the performance of the model at 5% residual error

interval was 60%. Furthermore, regression analysis demonstrated the existence of a strong linear correlation between the simulated and actual plenum chamber temperatures, since R^2 had a high value (0.9621). Additionally, a two tailed Student's *t–test* at 5% level of significance showed that there was no statistical difference between the simulated and plenum chamber temperatures ($t_{stat} = 0.55$, $t_{crit} = 1.72$). Hence, the model developed for simulation of harnessed energy can be used to predict the harnessing of solar energy by the solar tunnel dryer.

4.3.3. Fish drying model

Figure 4.3 shows how the simulated and actual moisture ratio of Tilapia fish (*Oreochromis niloticus*) during drying. The figure also shows how day–time ambient and plenum chamber temperatures changed during drying. The figure further shows that moisture ratio of the fish reduced as the drying time increased. In addition, it indicates that the reduction in moisture ratio with time was exponential. The exponential reduction of moisture content against time was further reinforced by Figure 4.4, in which the best curve of fit for moisture ratio against time was presented on a semi–log scale. This behaviour is consistent with the drying of most biological material, as observed by Konishi and Kobayashi (2003) when they studied the characteristic innovation of a food drying process revealed by the physicochemical analysis of dehydration dynamics. As illustrated in Figure 4.3, the actual and simulated moisture ratio show similar trends, and are fairly indistinct. This shows that the model can be used to predict the drying process.

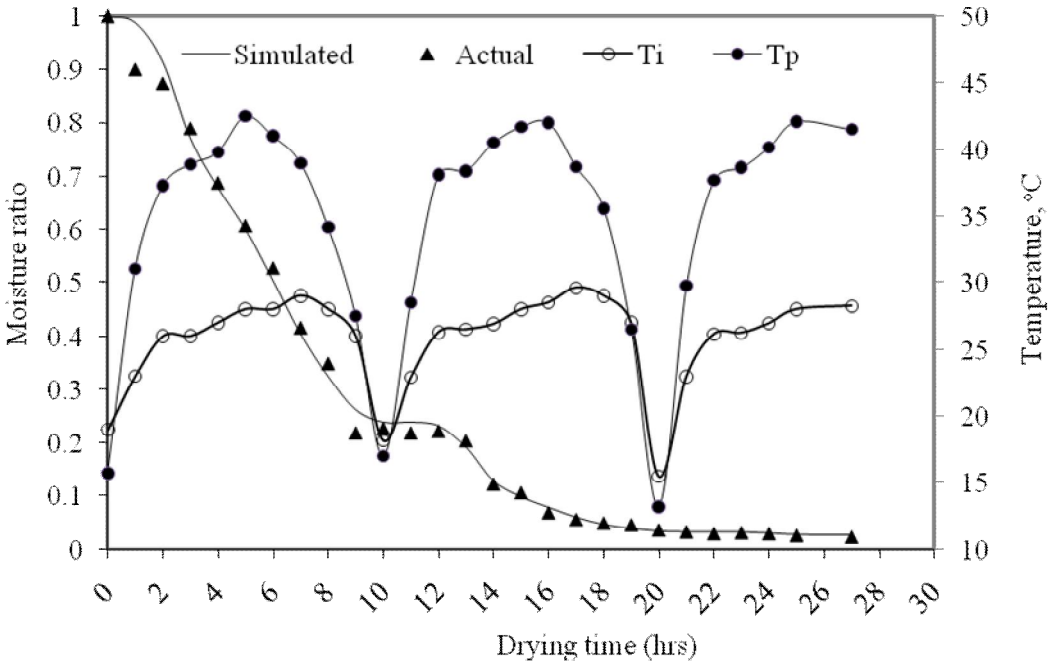

Figure 4.3: Variation of moisture ratio with drying time. In the figure, Ti and Tp are inlet and plenum chamber temperatures, respectively.

In Figure 4.3, the simulated and actual moisture ratio remained fairly constant in the first two hours of drying, and between the 9th and the 12th drying hours. This period coincided with the early hours of the first and the second drying days, when temperatures were extremely low due to condensation of moisture on the collector plate and the cover glass, and low ambient air temperatures. As the drying air temperature decreases, the vaporisation potential of moisture at the surface of the fish, and the rate of transfer of moisture from the body of the drying fish to its surface are reduced, and this reduces the drying rate (Mujumdar and Devahastin, 2000), as evident in the early hours of each day during drying.

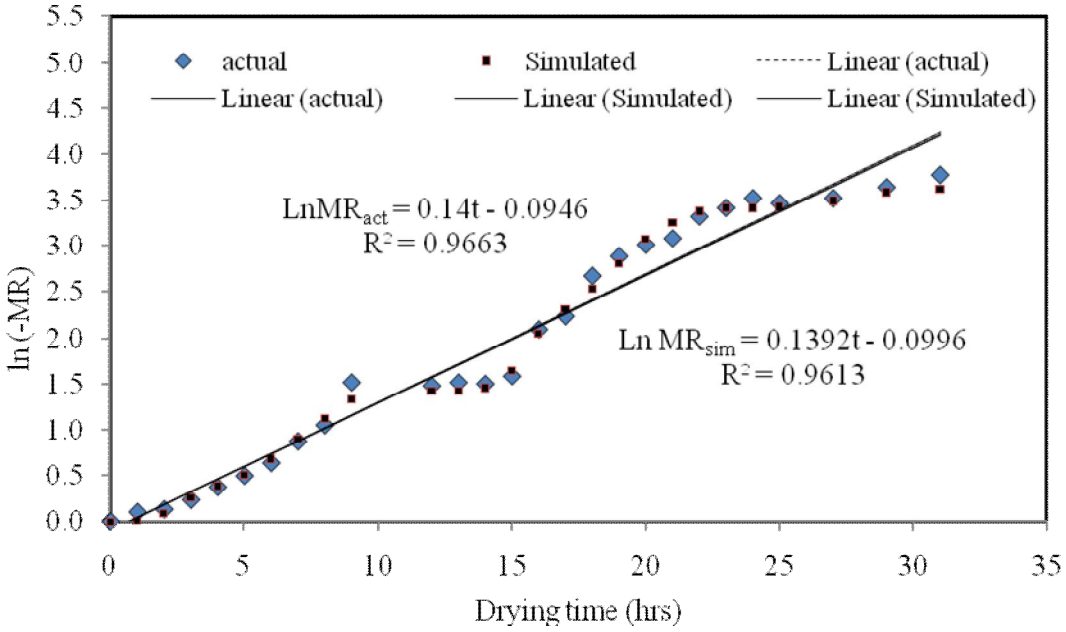

Figure 4.4: Variation of natural logarithm of moisture content over drying time.

The variation of plenum relative humidity, ambient and plenum chamber temperatures are presented in Figure 4.5. The figure shows that as the temperature increased, the relative humidity decreased. Reduction in humidity of the air implies that the drying air is capable of absorbing more moisture (Mujumdar and Devahastin, 2000). This could explain the fast drying rate at day time, when temperatures were high, compared to the morning hours, and subsequently the slow drying during the morning hours as explained earlier.

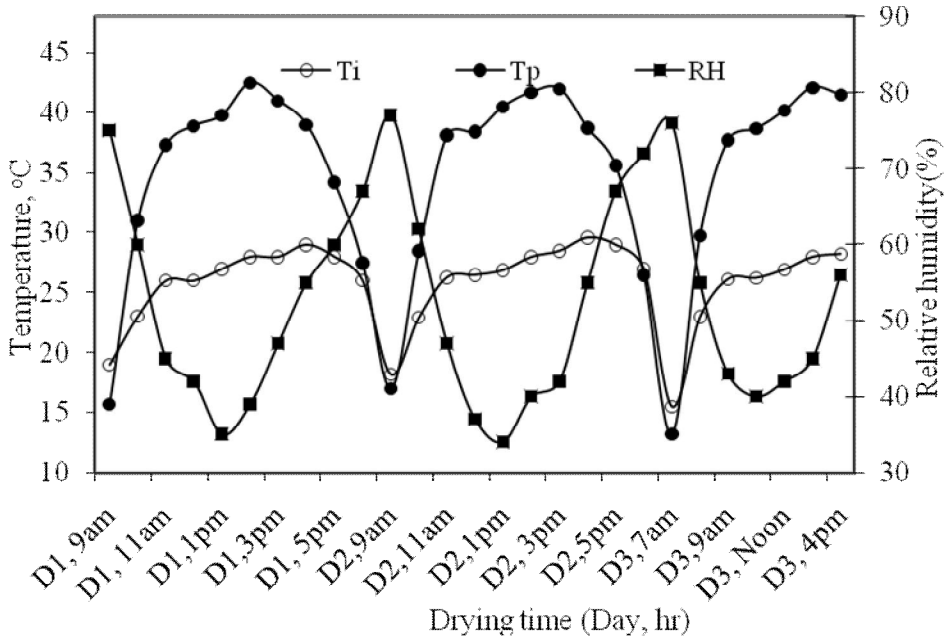

Figure 4.5: Variation of inlet and plenum temperature, and relative humidity with drying time. In the figure, *RH* and *D* correspond to the air relative humidity and the day of drying, respectively.

The performance of the model was established by determining the residual errors between simulated and actual moisture ratios. Twenty–seven (27) data sets, and 5 and 10% residual error intervals were used. Table 4.1 presents the results of the residual error analysis and the corresponding model performance. The table further presents the mean residual error, the standard deviation of the residual error, and the model performance at 5 and 10% residual error intervals. From the table, the absolute residual error varied from 0–19.4%, while the performances of the model at 5 and 10% residual error intervals were 44.4 and 81.5%, respectively. The low performance of the model at 5% could be attributed to low heating chamber temperatures experienced before 11.00 hours which had the effect of condensation on the collector plate. In order to vapourize the condensate, latent heat of

vapourisation must have been utilised from the system, consequently reducing the temperatures in the air drying chamber, whose effect must have been reduced drying rate.

Table 4.1: Residual error analysis between simulated and actual moisture ratio

t (hrs)	[b]MR_{Mean} (s.d)	MR_{Sim}	ε(%)	t(hrs)	[b]MR_{Mean} (s.d)	MR_{Sim}	ε(%)
0	1.00(0.00)	1.00	0.0	14	0.12(0.02)	0.13	4.0
1	0.90(0.02)	0.99	9.6	15	0.11(0.02)	0.10	7.7
2	0.88(0.01)	0.92	4.7	16	0.07(0.02)	0.08	14.3
3	0.79(0.02)	0.77	2.3	17	0.06(0.01)	0.06	5.9
4	0.69(0.02)	0.68	1.2	18	0.05(0.01)	0.05	6.7
5	0.61(0.02)	0.60	1.1	19	0.05(0.01)	0.04	17.9
6	0.53(0.02)	0.50	4.4	20	0.04(0.01)	0.03	4.6
7	0.42(0.01)	0.40	2.8	21	0.03(0.02)	0.03	0.0
8	0.35(0.02)	0.32	7.0	22	0.03(0.01)	0.03	11.1
9	0.22(0.02)	0.26	19.4	23	0.03(0.01)	0.03	5.3
10	0.23(0.01)	0.24	5.0	24	0.03(0.01)	0.03	0.0
11	0.22(0.01)	0.24	9.0	25	0.03(0.01)	0.03	6.3
12	0.22(0.01)	0.23	4.4	26	0.02(0.01)	0.03	14.3
13	0.20(0.02)	0.19	6.4				
Mean ε(%)		6.48		Performance at 5% ε(%)		44.4	
Mean standard deviation		5.18		Performance at 10 ε(%)		81.5	

[b]The values in parenthesis are standard deviations for the mean moisture ratios; ε, percentage residual error; t, time.

Further, the mean residual error and the standard deviations were 6.48% and 5.18%, respectively. The mean and the standard deviation were within the 10% residual error interval. A well performing model is expected to have simulated points superimposed on the actual points of the moisture content. The ε(%), the mean ε(%) and the standard deviation of the residual error for such a model would all be zero. However, the standard deviation value of 5.18%, which is a measure of the deviation

from the mean shows the data were scattered slightly from the mean. This could be attributed to moisture condensation on the collector plate, which was experienced during drying as stated earlier, which must have interfered with drying progress, and which was not considered in the model development. During sampling, the doors to the drying chamber were opened in order to access the drying samples, and this allowed fresh air into the drying chamber. In addition, this must have interfered with the drying process, contributing to the residual error in the drying process.

Regression analysis on the data yielded a strong linear correlation between simulated and actual moisture ratio since a high coefficient of determination ($R^2 = 0.995$) was attained. Additionally, based on a two–tailed *Student's t–test* there was no significant difference between the simulated and actual moisture ratio of the fish during drying at 5% level of significance($t_{stat} = -0.960$; $t_{crit,\ 5\%} = 2.059$). These observations demonstrate the ability of the model to predict the drying of Tilapia fish in a solar tunnel dryer. The final moisture content attained was 12.5%, dry basis, after 22 drying hours, which is consistent with the observations by Chavan *et al*. (2008) who studied the development of edible texturised dried fish granules from low–value fish Croaker (*Otolithus argenteus*) and its storage characteristics.

4.4. Optimisation of the design parameters of the solar tunnel dryer

The optimisation process carried out using Goal Genetic Algorithm generated a set of optimal design variables by the Goal Genetic Algorithm whose "fitness"value would be the desired plenum chamber temperatures. The results of the operation of the Genetic Algorithm are presented in Table 4.2. In the table, L, b_d, A, w, V, v, β, η and T_p represent the collector plate length, air heating chamber depth, collector plate surface area, collector plate width, air heating chamber volume, air flow velocity, tilt angle, cover glass refractive index and plenum chamber temperature, respectively.

The criterion for selection of the most optimal set of design parameters was set as the plenum chamber temperature. The other criteria were as indicated in equation 3.72. The set of design variables which met the set criteria was selected. The design variables parentheses, as shown in the ninth row of the table, were considered to be the most optimal design variables. These values met the criteria set for the optimisation, and yielded a plenum chamber temperature of 60^{o}C.

Table 4.2: Optimal design variables generated by Goal genetic algorithm

L (m)	b_d (m)	A (m^2)	w (m)	V (m^3)	v (m/s)	β(^{o})	η	T_p (^{o}C)
2.45	0.11	0.2695	1.15	0.30992	0.05	0.89	1.31	59.6
2.45	0.11	0.2695	1.16	0.31262	0.05	0.97	1.31	59.2
2.40	0.10	0.2400	1.24	0.29760	0.05	0.58	1.40	56.8
2.43	0.11	0.2673	1.16	0.31006	0.05	0.59	1.44	58.8
2.45	0.11	0.2695	1.17	0.31531	0.05	0.42	1.31	57.9
2.45	0.10	0.2450	1.16	0.28420	0.05	0.71	1.31	58.2
2.35	0.11	0.2585	1.22	0.31537	0.05	0.58	1.35	59.6
(2.44)	**(0.11)**	**(0.2684)**	**(1.22)**	**(0.32745)**	**(0.05)**	**(0.07)**	**(1.31)**	**(60.0)**
2.40	0.10	0.2400	1.17	0.28080	0.05	0.87	1.37	56.5
2.43	0.10	0.2430	1.20	0.29160	0.05	0.42	1.31	57.2
2.45	0.11	0.2695	1.16	0.31262	0.05	0.90	1.31	55.3
2.42	0.11	0.2662	1.15	0.30613	0.05	0.12	1.42	58.9
2.45	0.11	0.2695	1.15	0.30992	0.05	0.99	1.34	59.4
2.42	0.10	0.2420	1.21	0.29282	0.06	1.00	1.33	57.6
2.45	0.10	0.2450	1.18	0.28910	0.05	0.80	1.32	57.2
2.38	0.10	0.2380	1.18	0.28084	0.05	0.98	1.44	55.8
2.41	0.10	0.2410	1.16	0.27956	0.06	0.88	1.30	55.8
2.41	0.10	0.2410	1.23	0.29643	0.05	0.79	1.46	57.6
2.42	0.10	0.2420	1.15	0.27830	0.05	0.61	1.55	58.2

The parameters in parenthesis represent the optimal values.

The values in Table 4.2 give the optimised length of the solar tunnel dryer as 2.44m, and the width as 1.22m. In addition, the depth of the air heating chamber was generated as 0.11m. The above dimensions show that the depth of the heating chamber had been overdesigned. In addition, airflow cross–section was $0.27m^2$, and the air flow volume was $0.33m^3$, which agreed well with the conditions set in equation 3.72. Further, the optimal value of the tilt angle for the collector plate was evaluated as 0.07. According to Garg and Prakash (2000), the solar insolation incidence is at a maximum when the tilt angle is zero. Subsequently, the optimal value for the tilt angle can be approximated to zero.

4.5. Performance evaluation of the optimised solar tunnel dryer

4.5.1. Development of the optimised solar tunnel dryer

The optimised solar tunnel dryer that was developed in this study is exemplified schematically in Figure 4.6. It consisted of two chambers: the tunnel and the chimney sections. The tunnel is used for heating the drying air before it enters the chimney. The two chambers are completely sealed from light to preserve light sensitive nutrients in fish. The tunnel section of the dryer measures 2.44m long, 1.22m wide and 0.11m high, and has a 19mm thick rectangular galvanised iron (GI) collector plate, which is painted black for enhanced absorption and emission of solar energy, and a glass cover–plate. In addition, the bottom plate of the tunnel section was made of aluminium painted GI sheet, to reflect energy incident on the surface. The side walls of the tunnel chamber were made of aluminium coated GI sheet. The bottom and the side walls of the sheets were insulated with softboard which was sandwiched between the inner and outer GI sheets to minimise energy losses. Other aspects of the optimised dryer were similar to those of the solar tunnel dryer described in section 3.3.1.

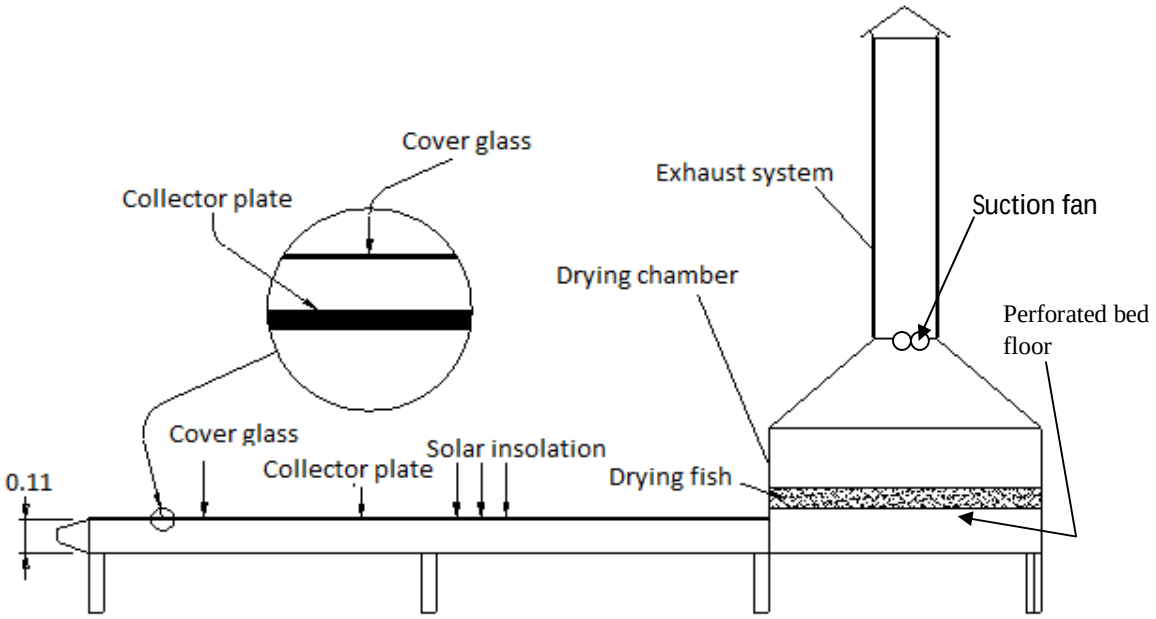

Figure 4.6: Schematic diagram of the optimised solar tunnel dryer.

4.5.2. Performance of the optimised solar tunnel dryer

The performance of the optimised solar tunnel dryer was evaluated by comparing data under the treatments (*NOSTD, OSTD, OS(a) and OS(b)*) as explained under Section 3.5.2. The first two Treatments considered evaluation of the system based on the energy harnessed and the drying of fish, while only the drying of fish could be assessed in the latter two Treatments. Further, the relative humidity and the temperature of the air during drying under the four Ttreatments (Section 3.5.2) and the air flow velocity under both *NOSTD* and *OSTD* were recorded.

a) Performance in Harnessing of Energy

Figure 4.7 presents the mean of 5 day actual plenum, and ambient air temperatures for optimised and non–optimised dryer systems, which were acquired under *NOSTD, OSTD, OS(a)* and *OS(b)* (Section 3.5.2). In addition, the figure shows that the plenum chamber temperatures for the *OSTD* were higher than those for the *NOSTD*. This fact is further supported by the ratios of *OSTD* plenum chamber temperatures to those of the *NOSTD* (Table 4.3). In this table, it is shown that the ratio ranged from 0.91–2.13, and had a mean of 1.32. Further, the ratio was always greater than 1, except at 6.00 p.m. when it fell to 0.91. Furthermore, the ratio of temperatures for *OSTD* to those for *NOSTD* varied from 0.63–1.47 and 0.81–1.91, respectively. Additionally, the plenum chamber temperature increased from low values in the morning and attained maximum values between 13 and 15 hours, before reducing to a minimum, for the sets of temperatures under analysis.

The peak temperatures for the solar tunnel dryers corresponded to the maximum value of global solar radiation, and are in agreement with observations by Kaplanis (2006), Trabea (2000) and Pidwimy (2006). Moreover, plenum chamber temperatures were higher at the end of the day, than at the start of the day, which could be attributed to the continued re–radiation of absorbed heat from the ground. These observations imply that the optimisation process provided a superior design, which must have improved the performance of the dryer in energy harnessing.

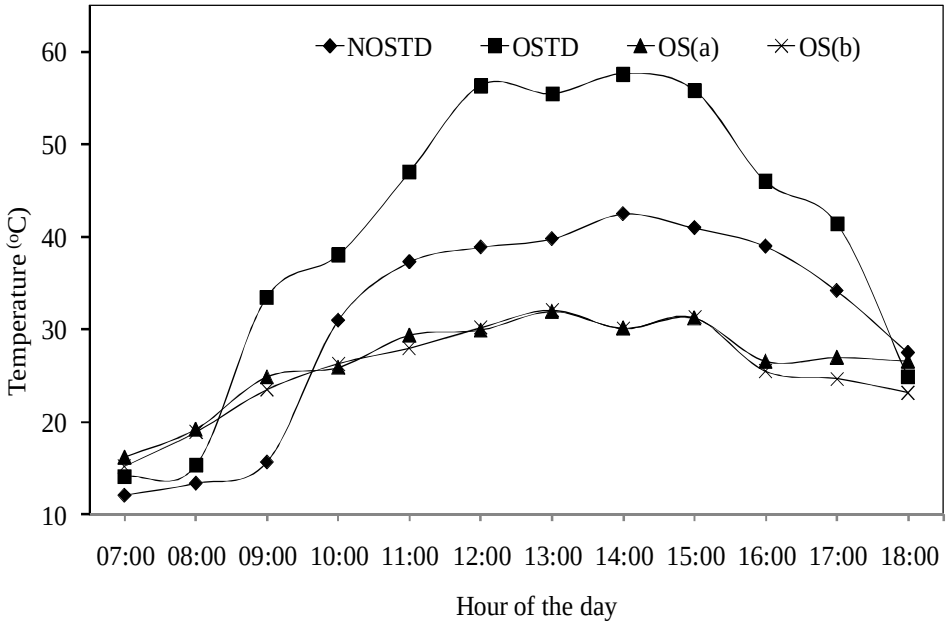

Figure 4.7: Daily ambient and plenum chamber temperatures.

Table 4.3: Post–Optimisation and pre–optimisation open sun and plenum chamber temperatures (^{o}C), and temperature ratios

Hour	$T_{i(OSTD)}$	$T_{p(OSTD)}$	$\frac{T_{p(OSTD)}}{T_{i(OSTD)}}$	T_i (NOSTD)	T_p (NOSTD)	$\frac{T_{p(NOSTD)}}{T_{i(NOSTD)}}$	$\frac{T_{p(OSTD)}}{T_{P(NOSTD)}}$	% T_p Increase
7	15.20	14.15	0.93	16.2	12.12	0.75	1.17	17%
8	18.90	15.30	0.81	19.3	13.40	0.70	1.14	14%
9	23.50	33.50	1.43	24.9	15.70	0.63	2.13	113%
10	26.30	38.00	1.44	25.9	31.00	1.20	1.23	23%
11	28.00	47.00	1.68	29.4	37.30	1.27	1.26	26%
12	30.20	56.35	1.87	30.0	38.90	1.30	1.45	45%
13	32.10	55.43	1.73	32.0	39.80	1.24	1.39	39%
14	30.10	57.60	1.91	30.2	42.50	1.41	1.36	36%
15	31.30	55.80	1.78	31.2	41.00	1.31	1.36	36%
16	25.50	45.98	1.80	26.6	39.00	1.47	1.18	18%
17	24.70	41.45	1.68	27.0	34.20	1.27	1.21	21%
18	23.20	24.90	1.07	26.6	27.50	1.03	0.91	–9%
Me			1.51			1.13	1.32	

In this table, T_i is open sun and T_p is plenum chamber temperature, respectively. Subscripts opt and nnopt represent optimised and non–optimised, respectively. The % increase is for plenum chamber temperatures only.

In order to establish the existence of difference between the drying temperatures under *NOSTD, OSTD, OS(a) and OS(b),* a two–factor Analysis of Variance (ANOVA) was performed. The results of the analysis confirmed the existence of highly significant difference between the temperatures under the stated treatments ($F = 16.37$, $F_{crit,\ 0.95} = 2.89$, $F_{crit,\ 0.99} = 2.89$). Further, using a two way Student's *t*–test, there was significant difference between temperures under *NOSTD* and those under *OSTD* ($t_{stat} = 9.62$; $t_{crit,\ 5\%} = 2.2$, $t_{crit,\ 1\%} = 3.11$). However, there was no significant difference between temperatures under *OS(a)* and *OS(b)* ($t_{stat}=0.005$; $t_{crit,5\%} = 2.2$, $t_{crit,1\%} = 3.11$). The results above show that the optimised solar tunnel dryer generated higher temperatures compared to the non–optimised solar tunnel dryer. In addition, these results show that there was a highly significant difference between the temperatures developed by the optimised solar tunnel dryer and those developed by the non–optimised solar tunnel dryer. Further, these results prove the ability of using Goal Genetic Algorithm in the optimisation of a solar tunnel dryer.

The best lines representing the variation of actual plenum chamber temperatures with ambient air temperatures, their respective regression equations and the corresponding coefficients of determination (R^2) are presented in Figure 4.8. The figure shows a linear relation between ambient and plenum chamber temperatures, with a strong correlation for the optimised dryer temperatures ($R^2=0.916$) and a weaker correlation for the non–optimised dryer temperatures ($R^2=0.816$). This implies that the optimised solar tunnel dryer was more sensitive to variations in ambient air temperatures, and therefore any changes in air temperatures would result in variations in plenum chamber temperatures. Thus there is an improvement in the

ability of the optimised solar tunnel dryer to harness energy in comparison with the non–optimised solar tunnel dryer.

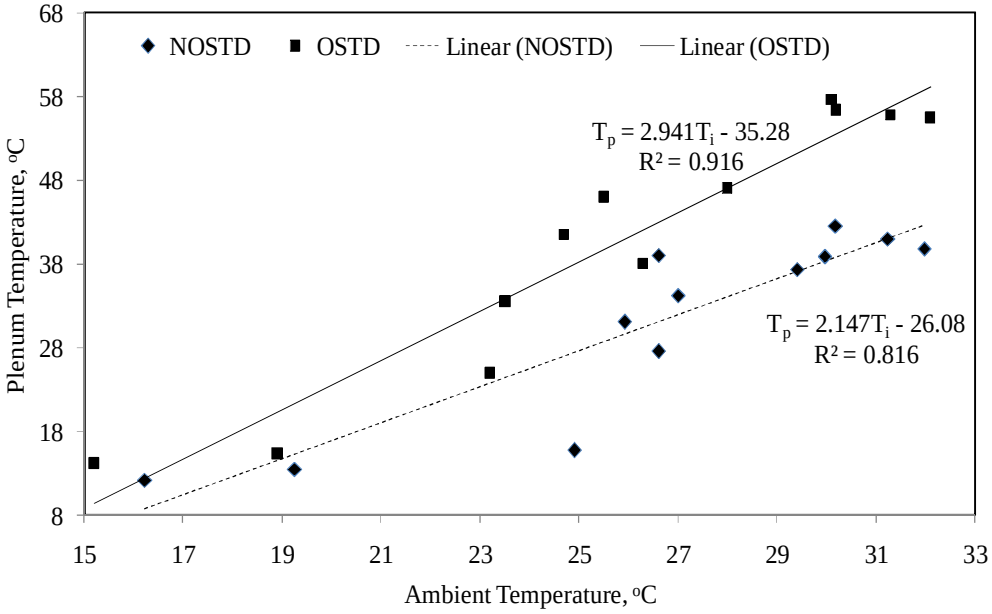

Figure 4.8: Variation of of actual plenum chamber temperature with inlet air temperature.

b). Performance in drying of fish

i) Moisture content

Figure 4.9 presents the variation of moisture ratio of tilapia fish with time under *NOSTD, OSTD, OS(s)* and *OS(b)* (section 3.5.2), while the relative humidity and air temperatures in the solar tunnel dryers at the time of drying of the fish under the four Treatments are presented in Figure 4.10. In this figure, *TiNOSTD* is ambient temperature for unoptimised solar tunnel dryer; *TpNOSTD*, is plenum chamber

temperature for un–optimised solar tunnel dryer; *TiOSTD*, ambient temperature during evaluation test for optimised solar tunnel; *TpOSTD*, optimised solar tunnel plenum temperature; *HNOSTD*, unoptimised solar tunnel dryer relative humidity; *HOSTD*, optimised solar tunnel dryer relative humidity. A similar trend was observed for the the moisture ratio of fish, and it reduced during drying for the four Treatments (Figure 4.9). In addition, the figure indicates that the reduction in moisture ratio with time was exponential. This agrees well with observations under Section 4.3.3. The figure also shows that the fish drying in the optimized solar tunnel dryer lost moisture more rapidly than that drying in the non–optimised solar tunnel dryer, while fish dried in the open sun had the lowest moisture loss rate. This could be attributed to the high drying air temperatures developed in the air heating chamber of the optimised solar tunnel dryer as a result of the optimization process. Further, it took the first 15, 22 and 28 drying hours, respectively, for the moisture content of the fish in the optimized and non-optimised solar tunnel dryers, and for fish drying in the open sun to be in equilibrium with the drying air, at 0.12kg/kg, dry basis. This shows the superiority of the solar tunnel dryer optimized with Goal GA in the drying of fish, compared to conventional solar tunnel dryer and open sun drying. Further, 18kg of fish can be dried under thin layer drying, with a thickness of 12.5mm, in 15, 22 and 28 hours respectively in the optimised, non-optimised and open sun drying, respectively.

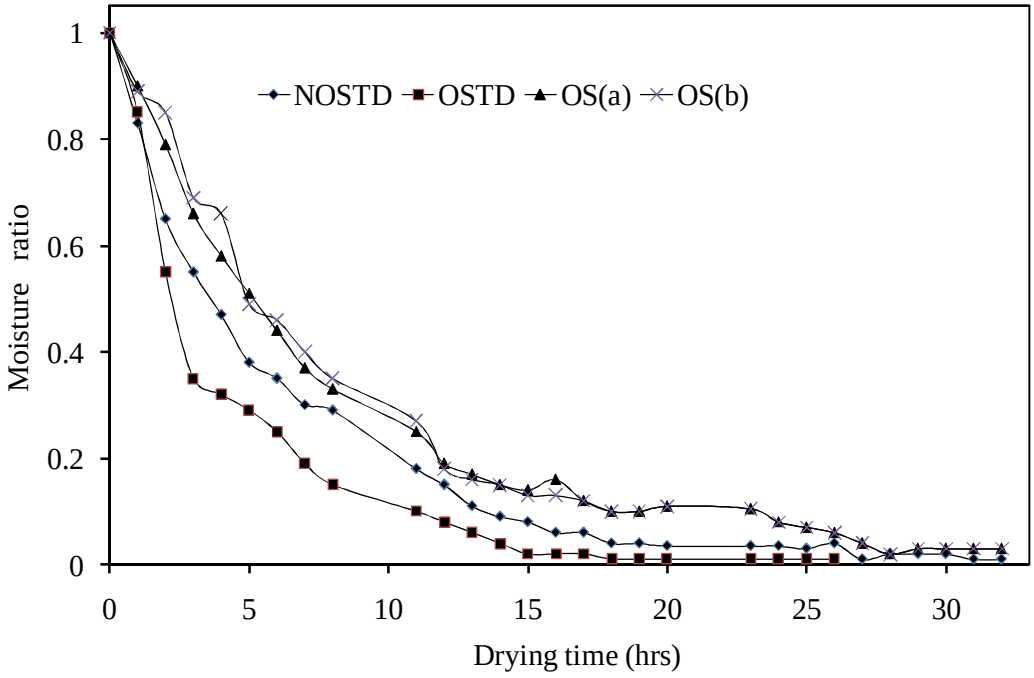

Figure 4.9: Moisture ratio for fish drying after optimisation.

Using analysis of variance (ANOVA) at 1% level of significance, there was a highly significant difference between moisture ratios for the fish dried under the four treatments ($F = 53.59$, $F_{crit,\ 1\%} = 4.09$). In addition, a two tailed Student's *t–test* proved the existence of a highly significant difference between MR for fish dried in the optimised solar tunnel dryer, and that dried in the non–optimised solar tunnel dryers ($t_{stat} = -6.828$; $t_{crit,5\%} = 2.048$, $t_{crit,1\%} = 2.763$). Further, similar Student's t–test showed the existence of a highly significant difference between the MR for fish dried in optimised solar tunnel dryer and that for fish dried under open sun drying ($t_{stat} = -8.392$; $t_{crit,5\%} = 2.074$, $t_{crit,1\%} = 2.819$), and the existence of a highly significant difference between the MR for fish dried in the non–optimised solar tunnel dryer and that for fish dried under open sun drying ($t_{stat} = -7.195$; $t_{crit,5\%} = 2.0739$, $t_{crit,1\%} =$

2.819). However, based on the Student's t–test, there was no significant difference between the MR of the fish dried in sun simultaneously with that dried in the optimised solar tunnel dryer and that dried in open sun at the same time with that dried in the non–optimised solar tunnel (t_{stat} = *–1.427;* $t_{crit,5\%}$= *2.0739,* $t_{crit,1\%}$ = *2.819*).

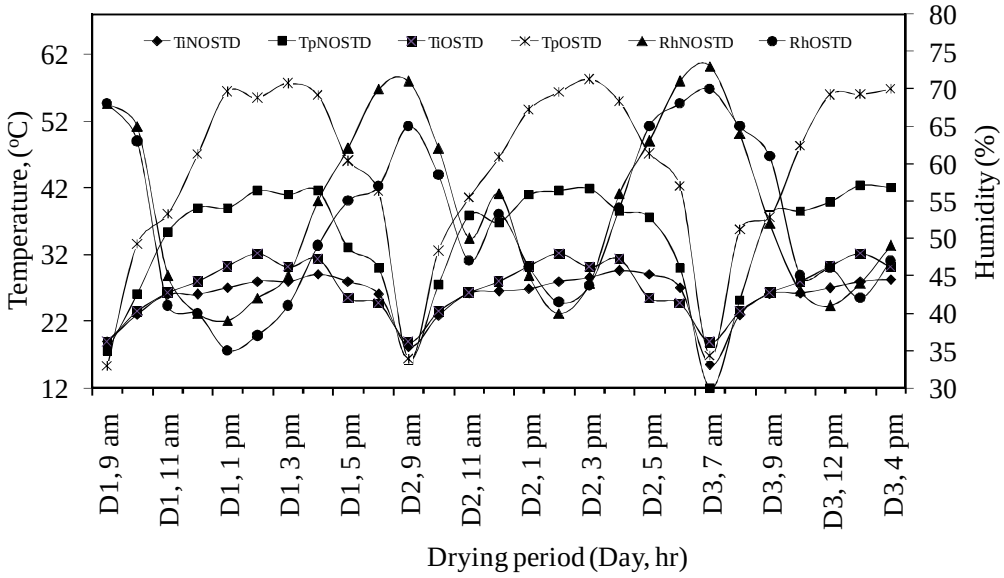

Figure 4.10: Ambient and plenum chamber air temperatures, and plenum relative humidites during evaluation of optimised solar tunnel dryer. In the figure, *TiNOSTD* is ambient temperature for unoptimised solar tunnel dryer; *TpNOSTD*, is plenum chamber temperature for un–optimised solar tunnel dryer; *TiOSTD*, ambient temperature during evaluation test for optimised solar tunnel; *TpOSTD*, optimised solar tunnel plenum temperature; *RhNOSTD*, unoptimised solar tunnel dryer relative humidity; *RhOSTD*, optimised solar tunnel dryer relative humidity.

ii) Quality attributes for solar dried fish

Proximate analysis

The protein, fat, carbohydrates and ash nutrients composition in the fish dried under the four Treatments is presented in Table 4.4. The table shows that the protein, fat, carbohydrates and ash content varied between 69.60–71.50%, 5.92–8.00, 0.68–1.01μg/g and 17.60–18.41%, respectively. These results agreed well with observations by Duyar and Eke (2009) when studied the production and quality of Marinade from different fish species. Therefore, drying of fish in either of the methods of drying did not have any effect on the nutrient composition of fish.

Table 4.4: Proximate composition

Sample	Protein (%)	Fat (%)	Carbohydrates (Sugar conc.) (μg/g)	% Ash Content	Moisture content, kg/kg, d.b
NOSTD	69.60	8.00	1.01	18.41	0.118
OSTD	69.70	7.92	1.00	17.60	0.122
OS(a)	71.50	7.45	0.68	18.27	0.120
OS(b)	70.70	7.15	0.78	17.95	0.119

Rancidity and putrefaction

The mean values of total volatile base nitrogen, TVB–N, for the fish after drying under the four Treatments are presented in Table 4.5. From the table, the mean TVB–N (mg/100g) ranged between 11.14–12.74mg/100g. In addition, the quality categorization of fish and fishery products according to TVB–N values is determined as in Table 3.6. Thus, based on TVB–N, the quality of the fish dried under the four

Treatments was considered excellent. This implies that the level of putrefaction in the fish dried under the four Treatments was insignificant. Further, the values of TBARS for the fish dried under the four Treatments are also presented in Table 4.5. Furthermore, based on Owaga (2009) and Robles–Martinez *et al*. (1982) the quality of fish under TBARS classification is categorised as in Table 3.7.

Table 4.5: TVB-N and TBARS values for the dried fish

Sample	TVB–N (mg/100g)	TBARS (Malonaldehyde (µg/kg))
NOSTD	12.74	5.30
OSTD	11.14	2.30
OS(a)	11.45	7.95
OS(b)	11.61	8.45

Using thiobarbituric acid reactive substances, TBARS, values in Table 4.5, and the quality guidelines in Table 3.7, it is evident that the fish dried under the four Treatments was of good quality. The value of 8.2 µg/kg obtained for open sun drying was slightly above the non–rancid quality and the slightly rancid quality. The *OSTD* achieved an extremely low value of TBARS (2.3 µgMA/kg) in comparison with the values obtained by the other Treatments. This demonstrates a system that can maintain fish in an extremely good condition during drying, compared to *NOSTD* and the *OS*. However, the quality of the dried fish could be termed good to excellent. Thus, the drying of fish under the four treatments within the drying periods did not have any significant effect on the rancidity of the fish.

iii) Colour

The values of L^*, a^*, b^* and the Hue (H) for fish dried under the four treatments are presented in Table 4.6. The initial values of L^*, a^*, b and H^* for the fish dried under the non–optimized and optimized tests were 45.83 and 45.64, –0.18 and –0.15, 13.21 and 12.25, and 90.78 and 90.69, respectively. These values are in agreement with observations by Corzo *et al*. (2006). In addition, based on the hue angle (H^*) and the lightness values (Figure 3.18), the colour of raw fish are considered very light yellow or brown colour.

Table 4.6: Parameters describing colour of fish during drying

	Sample	*OS(a)*	*NOSTD*	*OS(b)*	*OSTD*
L^*	Initial	45.83	45.83	45.64	45.64
	Dry	31.88	45.22	30.67	42.84
a^*	Initial	–0.18	–0.18	–0.15	–0.15
	Dry	3.13	2.89	3.15	1.76
b^*	Initial	13.21	13.21	12.25	12.25
	Dry	13.53	12.82	12.87	10.34
$H^*(^o)$	Initial	90.78	90.78	90.69	90.69
	Dry	76.98	79.65	79.75	80.34

The L^*–values for dry fish *OS(a)* and *NOSTD* were under the non–optimized were 36.88 and 45.22, respectively, while for *OS(b)* and *OSTD* were 30.67 and 42.84, respectively. In addition, the a^*–values (redness/greenness) for the fish samples showed a positive *a* value which ranged from 1.51–3.13 (Table 4.6) indicating that the samples were in the redness side of the scale. Further, the *b**–values varied from

10.34 to 15.82 indicating yellowness. The H^*–values varied from 79.85 to 80.34^o, which implies that the colour of the fish was yellow. A combination of the H^*–values (about 80^o) and the L^*–values was used to classify the colour of the fish as very light yellow for samples under the four treatments. This is in agreement with observations by Huda *et al.* (2010). These observations imply that the drying process did not effect noticeable change in the colour of the solar tunnel dried fish both in the optimised and non–optimised solar tunnel dryer.

4.6. Impact and Contribution of the study to Society

This study aimed at providing clear scientific procedures for artificially breeding optimal solar tunnel dryer design, using genetic algorithm (GA). In the study, mathematical relationships linking solar energy reception, solar energy harnessing by a solar tunnel dryer (incorporating both dryer design material and environmental factors), characteristics of the drying fish and the final quality attributes of the dried fish were established as requisite requirements in the design and optimisation of solar tunnel fish dryers. In addition, computer simulation models were developed and validated to simulate the established relations above. This model is an important tool for use in establishing the conditions of a fish drying environment in a solar tunnel dryer during design stage, in order to avoid overheating or under–heating, which lead to spoilage. The studies further demonstrated the application of genetic algorithm, using the developed simulation model to artificially breed an optimised solar tunnel dryer. Furthermore, the study provides clear procedures on how effective and efficient solar tunnel dryers can be developed using basic scientific principles, and

heuristic approach in optimisation. The study is useful to engineers, scientists, decision makers and the fishing fraternity as an important study and decision making tool, to reduce the prevailing wastage and produce high quality solar dried fish.

CHAPTER FIVE

CONCLUSIONS AND RECOMMENDATIONS

5.1. Conclusions

1. The developed computer simulation models satisfactorily predicted global solar radiation, the energy harnessed by a solar tunnel dryer and the drying of fish in the dryer given that their respective performances were 78.4, 83.3 and 81%, based on an absolute 10% residual error interval. Regression analysis showed that there existed a strong linear relationship between the simulated and actual data for the three models (R^2 = 0.788 for global solar radiation, 0.962 for the harnessed energy and 0.995 for drying of fish).

2. The optimisation process resulted in the reduction of the air heating chamber depth by 4.91. The validation results show that higher plenum chamber temperatures were obtained for the optimised dryer (2.44m long, 1.22m wide and 0.11m) than for the non–optimised dryer (2.24m long, 1.22m wide and 0.54m), and these were found to be significantly different.

3. It was also noted that the fish drying process took 15 hours for the drying to reach equilibrium moisture content of 0.12 kg/kg for the optimised dryer as compared to 22 hours for the non–optimised one. In addition, Student's t–test results established that there existed significant difference between the moisture ratios for fish dried in the optimised and non–optimised solar tunnel dryer (t_{stat}=–6.828; $t_{crit,5\%}$=2.048, $t_{crit,1\%}$ =2.763).

4. Quality analysis showed that fish dried in the optimised solar tunnel dryer did not develop rancidity (2.30μgMA/kg) or undergo significant putrefaction (11.14 μgMA/kg). However, although the rancidity for fish dried in the non–optimised solar tunnel dryer was within the acceptable limits (5.3 μgMA/kg) it was higher that that for fish dried under OSTD, and therefore, poorer in quality level. Further, it was observed that the fish dried in open sun experienced sligh levels of rancidity (7.95–8.45 μgMA/kg) , though still considered good in quality.

5. These studies demonstrate the ability of genetic algorithms to artificially breed optimised solar tunnel dryer for drying of fish.

6. The above results show that the developed simulation models can successfully be utilised to predict; global solar radiation, energy harnessed by a solar tunnel dryer and the drying process of fish in a solar tunnel dryer. Therefore, developed design and optimisation principles and models for solar dryers should be utilised in order to effectively and efficiently harness energy and improve the drying process.

5.2. Recommendations

1. The performance of the solar energy reception model of about 78% was evaluated based on solar radiation data from NASA. The possibility of using locally measured data with a view of establishing whether such data would improve the performance of the model should be investigated.

2. In the development of the harnessed solar energy model, it was assumed that the walls of the dryer are adiabatic and of negligible heat capacities, and that the energy was harnessed under steady state conditions. The properties of the heated air were also assumed to be only dependent on temperature. It was further assumed that the process of air heating is convective. However, the process of air heating is complex and depends on several factors including humidity and air flow rate among other factors, while the mode of heating could include other processes such as radiation. The influence of moisture content, internal walls radiation and the adiabatic nature of the solar tunnel dryer on the energy harnessed by the solar tunnel dryer should be investigated in future studies.

3. In the development of the fish drying model, it was assumed that the system was adiabatic, and that ambient temperatures and air flow around the dryer are constant. Further, it was assumed that thermal and physical properties of fish are homogeneous at any given time. Fish muscles, like those of other animals do not show homogeneity in their properties, and have different

concentrations of lipid and proteins at different parts of the body. The influence of inhomogeneous muscles and the possibility of energy leaks as sources of errors in this model should be investigated.

4. The analysis detailed in this thesis was for thin layer drying. The possibility of incorporating deep bed analysis in solar drying of fish in a solar tunnel dryer should be investigated.

5. The material used in the drying models was Tilapia Fish (*Oreochromis Niloticus*). However, the model design was such that it can take properties of other biological materials. Since no other material was used to evaluate the simulation and optimisation models, it is recommended that the simulation and optimisation process is carried out with other biological materials, to establish the ability of the model to simulate and the drying solar tunnel dryer for other biological materials.

REFERENCES

Abila R.O. (2003) “Food safety in food security and food trade: Case study: Kenyan fish exports”. 2020 Vision for Food, Agriculture and Environment. International Food Policy Research Institute, Washington D.C USA.

Akotsi E.F.N., M. Gachanja and J.K. Ndirangu (2006) “Changes in forest cover in Kenya’s five “water towers” 2003–2005”. Ministry of Environment and Natural Resources, Nairobi, Kenya.

Ajam H., S. Farahat and F. Sarhaddi (2005) “Exergetic optimization of solar air heaters and comparison with energy analysis”. International Journal of Thermodynamics, 8(4): 183–190.

Alam M.S., S.K. Saha, M.A.K. Chowdhury, M.D. Saifuzzaman and M. Rahman (2005) “Simulation of solar radiation system”. American Journal of Applied Sciences, 2(4): 751–758.

Al–Ajlan S.A., H. Al–Faris, H. Khonkar (2003) “A simulation modeling for optimization of flat–plate collector design in Riyadh, Saudi Arabia”. Renewable Energy, 28: 1325–1339.

Alfayo R. and C.B.S. Uiso (2002) “Global solar radiation distribution and available solar energy potential in Tanzania”. Physica Scripta (T), 97: 91–98.

Antoine F.R., C.I. Wei, W.S. Otwell, C.A. Sims, R.C. Littell, A.D. Hogle and M.R. Marshall (2002) “TVB–N correlation with odor evaluation and aerobic plate count in Mahi–Mahi (Coryphaena hippurus)”. Journal of Food Science, 67(9): 3210–2314.

Bala B.K. (1997) “Drying and storage of cereal grains”. Science Publishers, Inc, Plymouth, U.K.

Bala B.K. and M.R.A. Mondol (2001) “Experimental investigation on solar drying of fish using solar tunnel dryer”. Drying Technology, 19(2):427–436

Ball R.A., L.C. Purcell and S.K. Carey (2004) “Evaluation of solar radiation prediction models in North America”. Agronomy Journal, 96(2): 391–397

Balsa–Canto E., A. Alonso and J. Banga (2002) “A novel, efficient and reliable method for thermal process design and optimization. Part I. Theory”. Journal of Food Engineering, 52: 227–234

Batista L.M., C.A. da Rosa and L.A.A. Pinto (2007) “Diffusive model with variable effective diffusivity considering shrinkage in thin layer drying of chitosin”. Journal of Food Engineering, 81(1): 127–132.

Bennamoun L. and A. Belhamri (2003) “Design and simulation of solar dryer for agriculture products”. Journal of Food Engineering, 59: 259–266.

Bille P.G. and H.M. Shemkai(2006) “Process development, nutrition and sensory characteristics of spiced–smoked and sun–dried *Dagaa* from Lake Victoria, Tanzania”. African Journal of Food, Agriculture, Nutrition and Development, 6(2): 1–12.

Bindi M. and F Miglietta (1991) “Estimating daily global radiation from air temperature and rainfall measurements”. Climate Research, 1: 117–124.

Bolaji B.O. and A.P. Olalusi (2008) “Performance evaluation of a mixed–mode solar dryer”. AU. J.T, 11(4): 225–231.

Castro T., B. Mar, R. Longoria and L.G. Ruiz-Saurez (2001) “Surface albedo measurements in Mexico city metropolitan area”. Atmosfera, 14:69–74

Charron, R. and A. Athienitis (2006) “The use of genetic algorithms for a net–zero energy solar home design optimisation tool”. Paper presented at the 23rd Conference. Passive and Low Energy Architecture (PLEA2006). 6–8 September, 2000. Geneva, Switzerland.

Chavan B.R., S. Basu and S. R. Kovale (2008) “Development of edible texturised dried fish granules from low–value fish Croaker (*Otolithus argenteus*) and its storage characteristics”. CMU. J. Nat. Sci, 7(1): 173–182.

Chemkhi S., F. Zagrouba and A. Bellagi (2005) “Modeling and simulation of drying phenomena with rheological behaviour”. Brazil Journal of Chemical Engineering, 22(2): 153–162.

Chen R., E. Kang, X. Ji, J. Yang and J. Wang (2007) “An hourly solar radiation model under actual weather and terrain conditions: A case study in Heihe river basin”. Energy, 32(7): 1148–1157

Chukwu O. and I.M. Shaba (2009) “Effects of drying methods on proximate compositions of catfish (Clarias gariepinus)”. World Journal of Agricultural Sciences, 5(1): 114–116.

Codex Alimentarius (1979) “Recommended international code of practice for smoked fish”. CAC/RCP –25. Joint FAO/WHO Food Standards Programme, FAO, Rome, Italy.

Condori, M., R. Echaz and L. Saravia (2001) “Solar drying of sweet pepper and garlic using the tunnel greenhouse drier”. Renewable Energy, 22: 447–460.

Coops N.C., R.H. Waring and J.B. Moncrieff (2000) “Estimating mean monthly incident solar radiation on horizontal and inclined slopes from mean monthly temperatures extremes”. International Journal of Biometeorology, 44(4):204-11.

Correia, D.S., C.V. Gonçalves, S. Sebastião, C. Junior and V.A. Ferraresi (2004) “GMAW welding optimization using genetic algorithms”. Journal of the Brazillian Society of Mechanical Science and Engineering, 26(1).

Corzo O., N. Bracho and N. Marjan (2006) “Colour change kinetics of sardine sheets during vacuum pulse osmotic dehydration”. Journal of Food Engineering, 75: 21–26.

Corzo O., N. Bracho and C. Alvarez (2008) “Water effective diffusion coefficient of mango slices at different maturity stages during air drying”. Journal of Food Engineering, 87: 479–484.

Dai A. and K.E. Trenberth (2003) “Diurnal Variations in the Community Climate System Model”. AMS 14th Symposium on Global Change and Climate Variations, 9-13 Feb. 2003, Long Beach, CA, USA.

Delgado J, L.M. Martinez, T.T. Sanchez, A. Ramirez, C. Iturria and G. Gonzalez–Avila (2005) “Lung cancer pathogenesis associated with wood smoke exposure”. Chest, 128: 124–131.

De Souza J.L., R.M. Nica´cio and M.A.L. Moura (2004) “Global solar radiation measurements in Maceio, Brazil”. Renewable Energy 30: 1203–1220

Doyle J.W. (2007) “An agricultural future through sustainability”. Paper Presented at the IFF–FAO Global Feeds and Food Congress, April 2007, San Paulo, Brazil.

Duyar H.A. and E. Eke (2009) “Production and quality determination of marinade from different fish species”. Journal of Animal and Veterinary Advances, 8(2): 270–275.

Ebuy H.T. (2007) “Simulation of solar cereal dryer using TRNSYS”. MSc Thesis, Addis Ababa University, Addis Ababa, Ethiopia.

Ekechukwe O.V. and B. Norton (1999) “Review of solar energy drying systems II: An overview of solar drying technology”. Energy Conversion and Management, 40: 616–55.

El–Adawi M.K (2002) “New approach to modelling a flat plate collector: the Fourier transform technique”. Renewable Energy, 26(3): 489–506.

El–Sebaii A.A and A.A. Trabea (2005) “Estimation of global solar radiation on horizontal surfaces over Egypt”. Egypt Journal of Solids, 28(1).

Ezekoye B.A and O.M Enebe (2006) “Development and performance evaluation of modified integrated passive solar grain dryer”. The Pacific Journal of Science and Technology, 7(2).

Franke R. (1998) “Modelling and optimal design of a central solar heating plant with heat storage in the ground using Modelica”. Paper presented at the Eurosim '98 Simulation Congress, Espoo, Finland, April 1998.

Fudholi A., K. Sopian, M.H. Ruslan, M.A. Alghoul and M.Y. Sulaiman (2010) "Review of solar dryers for agricultural and marine products". Renewable and Sustainable Energy Reviews, 14: 1–30.

Garg H.P. and J. Prakash (2000) "Solar energy: Fundamentals and applications, 1st Revised Edition". Tata MCgraw Hill Publishers, New Delhi, India.

Gewali M.B., C.B Josh and R. Bhandari (2005) "Performance evaluation of hybrid solar biomass cabinet dryer". European Journal of Scientific Research, 4(1).

Ghiaus A.G, D.P Margaris and D.P Papanikas (1997) "Mathematical modelling of the convective drying of fruits and vegetables". Journal of Food Science, Engineering and Processing, 62(6).

Gitonga N.K., L. Okal and E .Mutegi (2003) "Effects of the EU ban on Lake Victoria fish export on Kenyan fisheries". Report and papers Presented at the 7th FAO Experts Consultation on Fish, FAO Document Depository, FAO, Italy.

Gram L. and P. Dalgaard (2002) "Fish spoilage bacteria–problems and solutions". Current Opinion in Biotechnology, 13: 262–266.

Hadrich B., N. Boudhrioua and N. Kechaou (2008) "Drying of Tunisian sardine (Sardinella aurita): Experimental study and three-dimensional transfer modelling of drying kinetics". Journal of Food Engineering, 84 (1): 92–100.

Hamdami N.J, Y. Monteau and A.L. Bail (2006) "Moisture diffusivity and water activity of part–baked bread at above and sub–freezing temperatures". International Journal of Food Science and Technology, 41: 33–44.

Hansen, R.C. and H.M. Keener (1993) "Thin layer drying of cultivated Taxus clippings". Transactions of the ASAE, 36 (6), 1873–1877

Hasan A. (2007) “Review of Solar Thermoelectric Energy Conversion and Analysis of a Two-Cover Flat-Plate Solar Collector”. B.Sc. Project Report, Massachusetts Institute of Technology, Massachusetts, USA.

Hassini L. (2006) “Estimation of the moisture diffusion coefficient of potato during hot–air drying”. Drying Equipment Sub Association. China General Machinery Drying Equipment Association, Beijing, China.

Himelbloom B.H. and C.A. Crapo (1998) “Factors influencing the microbial quality of cold-smoked salmon strips”. Journal of Food Science, 63(2): 356–358.

Horner W.F.A. (1992) “Preservation of fish by curing”. Fish Processing Technology. Chapman and Hall, London.

Ikeme A.I. and C.S. Bhandary (2001) “Effect of spice treatment on the quality of hot–smoked Mackerel (Scomber Scombrus)”. Reports and papers presented at the 7th FAO expert consultation on fish technology in Africa, FAO, Rome, Italy.

Jian D. and P. B. Pathare (2007) “Study the drying kinetics of open sun drying of fish” Journal of Food Engineering, 78(4): 1315–1319.

Jairaj K.S., S.P. Singh and K. Srikant (2009) “A review of solar dryers developed for grape drying”. Solar Energy, 83: 1698–1712

Jin Z. W. Yezheng and Y Gang (2005) “General formula for estimation of monthly average daily global solar radiation in China”. Energy and Conservation Management, 46: 257–268

Joshi C.B., M.B. Gewali and R.C Bhandari (2005) “Performance of solar drying systems: A Case of Nepal”. IE(I) Journal–ID, 85.

Kadam D.M. and D.V.K. Samuel (2006) “Convective flat–plate solar heat collector for cauliflower drying”. Biosystems Engineering, 93(2): 189–198.

Kalua I.P. (2008) “Biofuel (Jatropha) development in Kenya”. Green Africa Foundation, Nairobi, Kenya.

Kalogirou S.A. (2004) “Solar thermal collectors and applications”. Progress in Energy and Combustion Science, 30: 231–295.

Kanali C.L. (1997) “Prediction of axle loads induced by sugarcane transport vehicles using statistical and neural–network models”. Journal of Agricultural Engineering Research, 68(3): 207–213.

Kaplanis S.N. (2006) “New methodologies to estimate the hourly global solar radiation; Comparisons with existing models”. Renewable Energy, 31(6): 781－790.

Karekezi S. and W. Kithyoma (2003) “ Renewable energy in Africa: Prospects and limits”. In the proceedings of the Workshop for African Energy Experts on Operationalizing the NEPAD Energy Initiative; 2–4 June, 2003, Novotel, Dakar, Senegal

Kaushika N.D. and K. Sumathy (2003) “Solar transparent insulation materials: a review”. Renewable and Sustainable Energy Reviews, 7: 317–351.

Ke P.J., E. Cervantes and C.R. Martinez (1984) “Determination of thiobarbituric acid reactive substances (TBARS) in fish tissue by an improved distillation spectrometric method”. Journal of Science, Food and Agriculture, 35:1248–1254.

Ke J. and M. Ogura (2003) “Optimization models of sound systems using genetic algorithms”. Computational Linguistics, 29(1): 1–18

Kerr B. (1998) “ A review of solar food drying” The Solar Cooking Archive, The Sustainable Living Centre, 3310 Paper Mill Road, Taylor, Arizona 85939, USA (downloadable at http://solarcooking.org/dryingreview.htm).

Khoukhi M. and S. Maruyama (2005) “Theoretical approach of a flat plate solar collector with clear and low–iron glass covers taking into account the spectral absorption and emission within glass covers layer”. Renewable Energy, 30: 1177–1194.

Kiaye E. (2004) “Effect of improved processing techniques on the quality and storage stability of Tilapia from L. Victoria in Kenya”. MSc Thesis, Jomo Kenyatta University of Agriculture and Technology, Juja, Kenya.

Kingsly R.P., R.K. Goyal, M.R. Mankantan and L.M. Ilyas (2007) “Effect of pre–treatments and air temperature on drying behaviour of peach slices”. International Journal of Food Science and Technology, 42: 65–69.

Kituu G.M., D. Shitanda, C.L. Kanali, J.T. Mailutha, C.K. Njoroge, J.K.Wainaina and P.M.O. Ondote (2009) “Influence of Brining on the Drying Parameters of Tilapia (*Oreochromis Niloticus*) in a Glass-Covered Solar Tunnel Dryer”. Agricultural Engineering International: the CIGR Ejournal. Manuscript number. EE 1349, Vol. XI.

KNBS (2008) “Economic survey, 2008”. Kenya National Bureau Statistics, Nairobi, Kenya.

KNBS (2010) “Kenya Census, 2009”. Kenya National Bureau of Statistics, Nairobi, Kenya (downloadable at *www.knbs.or.ke/Census%20ResuIts/KNBS%20Brochure.pdf)*

Konishi Y. and M. Kobayashi (2003) “Characteristic innovation of a food drying process revealed by the physicochemical analysis of dehydration dynamics”. Journal of Food Engineering, 59: 277–283.

Krokida M. and Maroulis Z. (2001) “Structural Properties of dehydrated products during rehydration”. Internationa Journal of Food Science and Technology, 36: 529–538.

Kustever J.M. (2010) “NASA surface meteorology and solar energy”. Atmospheric Science Data Centre, Washington, USA.

Lalitha K.V.and P.K. Surendarn (2002) “Occurrence of Clostridium botulinum in fresh and cured fish in retailtrade in Cochin (India)”. Intenational Journal of Food Microbiology, 72: 169–174.

Lienhard J.H.IV and J.H. Lienhard (2006) “A heat transfer textbook, 3rded”. Phlogiston Press, Cambridge, Massachusetts, USA.

Malo M., M. Chipeta and M. Laverdiere (2008) “Visioning the energy dimension of Kenya: Changing forest landscape under vision 2030”. in Forest landscapes and Kenya’s Vision 2030; Proceedings of the 3rd Annual Forestry Society of Kenya (FSK) Conference and Annual General Meeting held at the Sunset Hotel, Kisumu, Kenya. 30th September–3rd October, 2008

Mechlouch R.F. and A.B. Brahim (2008) “A global solar radiation model for the design of solar energy systems”. Asian Journal of Scientific Research 3 (1): 231–238.

Menoyo D., C.J. López-Bote, A. Obach and J.M. Bautista (2005) “Effect of dietary fish oil substitution with linseed oil on the performance, tissue fatty acid profile, metabolism, and oxidative stability of Atlantic salmon”. Journal of Animal Science, 83:2853–2862.

Miguel Angel Olveira Novoa, Carlos A Martinez Palaccos, Elisabeth Real De Leon (1994) “Nutrition of fish and crustaceans: A laboratory manual, 3. Proximate Analysis” FAO Corporate Documentary Depository, Fisheries Department, FAO, Mexico City, Mexico.

Mohammadi A., S. Rafiee, Z. Emam-Djomeh and A. Keyhani (2008) “Kinetic models for colour changes in Kiwifruit slices during hot air drying”. World Journal of Agricultural Sciences, 4 (3): 376–383.

Mohan C.O., C.N. Ravishankar and T.K. Srinivasagopal (2008) “Effect of O_2 scavenger on the shelf-life of catfish (*Pangasius sutchi*) steaks during chilled storage”. Journal of the Science of Food and Agriculture, 88:442–448

Montastruc L., C. Azzaro–Pantel, L. Pibouteau and S. Domenech (2004) “Use of genetic algorithms and gradient based optimisation techniques for calcium phosphate precipitation” Chemical Engineering and Processing, 43(10): 1289–1298.

Mudgal V.D. and V.K. Pande (2007) "Dehydration characteristics of cauliflower". International Journal of Food Engineering, 3(6).

Mujaffar S. and C.K. Sankat (2005) “The mathematical modelling of the osmotic dehydration of shark fillets at different brine temperatures”. International Journal of Food Science and Technology, 41: 405–416.

Mujumdar S. and S. Dehavastin (2000) “Fundamentals and principles of drying” pp 1–22, in: S. Dehavastin (Ed), Mujumdar’s Practical Guide to Industrial Drying, Exergex, Montreal, Canada, 2000.

Naeher L.P, M. Brauer, M. Lipsett, J.T. Zelikoff, C.D. Simpson, J. Q. Koenig and K.R. Smith (2007) “Woodsmoke Health Effects: A Review”. Inhalation Toxicology, 19:67–106.

Ng P.P., S.M. Tasirin and C.L. Law (2006) “Thin layer method analysis of spouted bed dried Malaysian paddy – characteristic drying curves”. Journal of Food Process Engineering, 29: 414–428.

Oduor–Odote P.M., B.O. Ohowa and M. Obiero (2008) “Performance of improved and traditional fish smoking kilns introduced in the Tana Delta Area of Kenya”. Samaki News, 5: 23–28

Ogunja J.C, K.O. Werimo and E.N. Okemwa (1992) “A case study on high valued Nile–Perch products”. Proceedings of the symposium on post–harvest fish technology, Food and Agricultural Organisation (FAO), Rome, Italy.

Ogunjobi A.A., B.C. Adebayo-Tayo and A. A. Ogunshe (2001) “Microbiological, proximate analysis and sensory evaluation of processed Irish potato fermented in brine solution”. African Journal of Biotechnology, 4 (12): 1409-1412.

Ojutiku R.O., R.J. Kolo and M.L. Mohammed (2009) “Comparative study of sun drying and solar tent drying of Hyperopisus bebe occidentalis”. Pakistan Journal of Nutrition, 8(7): 955–957.

Oluwasesan O.T. (2008) “Determination of maximum number of layers of solar collector for fish solar dryer”. Journal of Engineering and Applied Sciences, 3(7): 553–559.

Omiti J., D. Otieno, E. McCullogh and T. Nyanamba (2007) “Strategies to promote market–oriented smallholder agriculture in developing countries: A case study of Kenya” in the proceedings of The Second International African Association of Agricultural Economics, August 20–22, 2007,Accra, Ghana.

Orengoh P. and A. Kisumo (2007) “Kenya: Countries Fish sector poised for boom”. East African Bussiness Week, 18th June 2007, Kampala, Uganda

Osei–Opara F. and A. Kukah (1988) “Improving the quality of dried fish through solar drying”. FAO. Fisheries Report, 400: 164–166.

Owaga E.E., C.A. Onyango and C.K. Njoroge (2010) “Influence of selected washing treatments and drying temperatures on proximate composition of dagaa (*Rastrineobola argentea*), a small pelagic fish species”. African Journal of Food, Agriculture, Nutrition and Development (AJFAND), 10(7): 2834-2847.

Oyero J.O., S.O.E. Sadiku, E.S.A. Ajisegiri and A.A. Eyo (2007) “Biochemical evaluation of enclosed solar dried and salted *Oreochromis niloticus*”. Reserach Journal of Animal Sciences, 1(3): 97–101.

Özoğul F. and Y. Özoğul (2000) "Comparision of methods used for determination of Total Volatile Basic Nitrogen (TVB–N) in Rainbow Trout (Oncorhynchus mykiss)". Turkish Journal of Zoology, 24: 113–120.

Palaniappan C. (2009) "Perspectives of solar food processing in India". International Solar Food Processing Conference, 2009.

Perumal R. (2007) "Comparative performance of solar cabinet, vacuum assisted solar and open sun drying methods". MSc Thesis, McGill University, Montreal, Canada.

Pidwimy M. (2006) "Daily and annual cycles of temperature: Fundamentals of physical geography, 2nd ed". British Columbia, Canada.

Pinto L.A.A. and S. Tobinaga (2006) "Diffusive model with shrinkage in the thin layer drying of fish muscle". Drying Technology, 25(4): 509–516.

Phoungchandang S. and J. L Woods (2000) "Solar drying of banana: Mathematical model, laboratory simulation and field data compared". Journal of Food Science, 65(6).

Purohit P., A. Kumar and T.C. Kandpal (2006) "Solar drying vs. open sun drying: A framework for financial evaluation". Solar Energy, 80(12): 1568–1579.

Rabah K.V.O (2005) "Integrated solar energy systems for rural electrification in Kenya". Renewable Energy, 30: 23–42.

Panduro T.B., Y.G. Vasquez, M.M Vivanco and O.M Taboada (2004) "Air drying of Clams (*Anodontites trapesialis*) and Tilapia (*Oreochromis niloticus*) Fillet". Drying 2004-Proceedings of the 14th International Drying

Symposium (IDS 2004), San Paulo, Brazil, August 2004, Vol C, pp 1977-1983

Rahman M.S., C.O. Perera, X.D. Chen, R.H. Driscoll and P.L. Potluri, (1996) "Density, shrinkage and porosity of calamari mantle meat during air drying in a cabinet dryer as a function of water content". Journal of Food Engineering, 30: 135 – 145.

Reza S., A.J. Bapary, N. Islam and M.D. Kamal (2009) "Optimization of marine fish drying using solar tunnel dryer". Journal of Food Processing and Preservation, 33: 47–59.

Robles–Martinez C., E. Cervantes and P.J. Ke (1982) "Recommended Method for Testing the Objective Rancidity Development in Fish Based on TBARS Formation". Canadian Technical Report of Fisheries and Aquatic Sciences No.1089

Sablani S.S., M.S. Rahman, O. Mahgoub and A.S. Al–Marzouki (2002) "Sun and solar drying of fish sardines". Drying' 2002–Proceedings of the 13th International Drying Symposium (IDS' 2002).

Sablani S.S., M.S. Rahman, I. Haffar, O. Mahgoub, A.S. Al–Marzouki, M.H. Al–Ruzeiqi, N.H. Al–Habsi and R.H. Al–Belushi (2003) "Drying rates and quality parameters of fish sardines processed using solar dryers". Agricultural and Marine Sciences, 8(2):79–86.

Sacilik K. and G. Unal (2005) "Dehydration characteristics of Kastamonu garlic slices". Biosystems Engineering, 92(2): 207–215.

Sacilik K., R. Keskin, A.K. Elicin (2006) “Mathematical modelling of solar tunnel drying of thin layer organic tomato”. Journal of Food Engineering, 73: 231–238.

Sano Y and H. Kita (2002) “ Optimization of noisy fitness functions by means of genetic algorithms using history of search with test of estimation”. *In Proceedings of the 2002 Congress on Evolutionary Computation CEC02 Cat No02TH8600*, *1917*(1), 360-365. Ieee. Retrieved from http://ieeexplore.ieee.org/lpdocs/epic03/wrapper.htm?arnumber=1006261

Seiki A., Y.N. Takayabu, T. Yasuda, N. Sato, C.Takahashi, K. Yoneyama and R. Shirooka (2011) “Westerly wind bursts and their relationship with ENSO in CMIP3 models”. Journal of Geophysical Research, 116, D03303, doi:10.1029/2010JD015039.

Senadeera W., B.R. Bhandari, G. Young and B. Wijesinge (2005) “Modelling dimensional shrinkage of shaped foods in fluidised bed drying”. Journal of Food Processing and Preservation, 29: 109–119.

Senadeera W. and I. Kalugalage (2004) “Performance evaluation of an affordable solar dryer for crops”. In *Biennial Conference of the Society of Engineers in Agriculture 2004*, 14-16 September, Dubbo, Australia.

Shitanda D. (2006) “Development of an intergraded solar tunnel drier for fish drying along Lake Victoria” Project Proposal submitted to Victoria Research (Vicres) Project, SAREC, Sida Funded Programme.

Shitanda D. and N.V. Wanjala (2006) “Effect of different drying methods on the quality of Jute (*Corchorus Olitorius L)”*. Drying Technology, 24: 95–98.

Sigurd A.N. (1994) “Strain gage selection in loads equations using a genetic algorithm”. NASA Contractor Report 4597; Edwards, California, USA.

Silvoso M.M., E.M.R. Fairbairn, R.D.T. Filho, N.F.F. Ebecken and J.L.D. Alves (2003) “Optimization of dam construction costs using genetic algorithms “. 16th ASCE Engineering Mechanics Conference, July 16th–18th, 2003, University of Washingtonn, Seattle, USA.

Simate I.N. (2003) “Optimization of mixed–mode and indirect–mode natural convection solar dryers”. Renewable Energy, 28: 435–53.

Smitabhindua R., S. Janjai and V. Chankong (2008) “Optimization of a solar–assisted drying system for drying bananas”. Renewable Energy, 33(7): 1523–1531.

Southall R. (2005) “The Ndungu report: Land and graft in Kenya”. Review of African Political Economy, 103: 142–51.

Spokas K. and F. Forcella (2006) “Estimating hourly incoming solar radiation from limited meteorological data”. Weed Science, 54(1): 182–189

Sukhatme P.K. (2003) “Solar energy: Principles of thermal collection and storage”. 2ndEd, Tata McGraw–Hill Publishing, New Delhi.

Supranto M., H. Ruslan, M.A. Alghoul, M.Y. Sulaiman, A. Zaharim and K. Sopian (2008) “Estimating the solar assisted drying system capacity for marine products”. Proceedings of the 3rd WSEAS int. conf. on renewable energy resources, University of Cambridge, Cambridge, U.K, February 23-25th, 2008.

Suzuki H., S. Hayakawa, E. Okazaki and M. Yamazawa (1988) “Effect of solar drying on vitamin D3 and provitamin D3 contents with fish meat”. Journal of Agriculture and Food Chemistry, 36(4): 803–806.

Talla A., J.R Puiggali, W. Jomaa and Y. Jannot (2004) “Shrinkage and density evolution during drying of tropical fruits: application to banana”. Journal of Food Engineering, 64: 103–109

Tidwell J.H. and G.L. Allan (2001) “Fish as foods: Aquacultures contribution”. Oxford Online Journals, EMBO Reports, 2(11): 958–963.

Tiwari G.N., T. Das and B. Sarkar (2006) ‘‘Experimental study of greenhouse prawn drying under natural convection”. Agricultural Engineering International: the CIGR Ejournal. Manuscript FP 06 016, Vol. VIII.

Trabea A.A. (2000) “Analysis of solar radiation measurements at Al–Arish area, North Sinai, Egypt”. Renewable Energy, 20: 109–125

Trujillo F.J, C.Wiangkaew and Q.T. Pham (2007) “Drying modeling and water diffusivity in beef meat”. Journal of Food Engineering, 78: 74–85

Uluko H., C.L. Kanali, J.T. Mailutha and D. Shitanda (2006) “A finite element model for the analysis of temperature and moisture distribution in a solar grain dryer”. The Kenya Journal of Mechanical Engineering, 2(1): 47–56,.

Wamwachai M.M.A. (2009) “A call to save the Mau”. Ministry of Foresty and Wildlife, Nairobi, Kenya

Waje S.S., M.W. Meshram, V. Chaudhary, R. Pandey, P.A. Mahanawar and B.N. Thorat “Drying and shrinkage of polymer gels”. Brazil Journal of Chemical Engineering, 22(2): 209–216.

Whitfield D.E.V. (2000) “Solar dryer systems and internet: important resources to improve food preparation”. Paper presented at the International Conference on Solar Cooking; Kemberly, South Africa, between 26th–29th November, 2000.

Zhang N, Y. Yamashita and Y. Nozaki (2002) “Effect of protein hydrolysate from Antarctic krill meat on the state of water and denaturation by dehydration of lizard fish myofibrils”. Fisheries Science, 68: 672–679.

APPENDICES

Appendix A: Solar tunnel drying simulation code

Appendix A1: The simulation code

```
'Declaration of variables and constants
Public Latitude As Single, DryingTime As Double, I As Double, U_L, Tp, I_c, Br
Public PartialVapourPressure, P_s, CoverPlate As String, MaterailThickness
Dim HydrualicradiusT As Double, hcv_tunnel As Double, Ga_z, MassFlowRate_z
Dim Lc As Double, Result As Double, StartHour, EndHour, DryingHours,
NumberOfTrays, Mcz
Dim Dryingperiod, t_f, K7 As Double, DryingLayers, t_f_tray, Tf, Qp_chimney,
n_Trays, dryingdepth
Dim Counts, HoursInADay, DryingDays, Albedo, R_sub_b, Delta_Tf_over_Deltat,
Fx
Dim Humidity_Z, ShrinkageCoeffi, rho_b_initial, SpecificVolume,
linearShrinkageCoefficient
Dim cosOmega_s, sinOmega_s, Omega_s, Io As Double, h_r, Ho, Ir, Ksky, a_a, b_b,
Id, Ib
Dim DeltaCa, DeltaCb, DeltacL, DeltaE, caZ, cbZ, cLz, DeltaEz, caz1, cbz1, cLz1,
caz2, cbz2, cLz2
Dim DeltaCaz, DeltaCbz, DeltacLz, I_oZ, I_dz, I_T, T_z, ha_eff
Dim InsolationTotal, InsolationDiffuse, R_b, R_d, R_r, InsolationSurface,
InsolationEffective
Dim lnPsOverRs, a_d, cao, ca, cbo, cb, cLo, cL, ca1, ca2, cb1, cb2, cL1, cL2
Dim InitialSpecificVolume, rho_w, rho_s, rho_p, rho_bo, rho_b, dayhours, td, Tamb,
InsolationDirect
Dim I_scApostrophy, I_o, S_p, S_a, H_o, a_kisangani, b_kisangani, K_t, a_Actual,
b_Actual, I_actual
Dim I_d, I_direct, I_Tt, CosTheta_h, SinTheta_h, Tantheta_h, Theta_h, H_act
Dim Ta, h_fp, h_fb, h_w, f_ut, U_t, k_b, t_b, U_b, L_1, L_2, L_3, k_e, t_e,
Efficiency
Dim U_e, T_av, E_e, h_eq, h_e, F_apost, T_fpn, TemperatureDiff, Countloss
Dim T_fp, epsilon_p, epsilon_g, epsilon_r, Tfp As Single, TiltAngle_radians,
AirColumnHeight
Dim Tpm, mu, K_v, D_h, V, Pr, Re, h_cv, C, N_c, h_p, f_p, F_aposr, Tbm, U_tn, B,
Z_o
Dim TiltAngle As Single, FirstDate As Date, StartDate As Integer, HourAngle As
Double
Dim EndDate As Integer, DateCount As Integer, n As Integer, EnergyDate As Date,
Declination As Double
Dim CosThetaZ As Double, SunsetAngle As Double, SunriseAngle As Double, Hr
As Single, Azimuth As Double
```

```
Dim CosAngleOfIncidence As Double, sinThetaZ As Double, SolarFactor As
Double, DeltaMc As Double
Dim RefractiveIndex As Double, SinTheta2, CosTheta2 As Double, ThetaTwo As
Double
Dim ThetaZ As Double, rho_subP As Double, rho_subS As Double,
MaterialThickness As Double, Nu As Double
Dim Tau As Double, Absorptivity As Double, TauALphaSubEe  As Double, x As
Double
Dim CollectorLength As Double, CollectorWidth As Double, CollectorArea  As
Double, massflowrate As Double
Dim Cpa As Single, Humidity, Txexp As Double, D_eff_M As Double, Mf As
Single, DeltaTfx  As Double
Dim InletAirTemperature As Single, Tx As Double, Qax As Double, Qi As Double,
Eff As Double, B_t As Double
Dim InstEff  As Single, FR As Double, UL  As Double, TL As Double, Qa As
Double, WaterViscosity
Dim CollectorHeight  As Double, AirVelocity  As Single, AirDensity As Single,
ThermalEfficiency As Single
Dim QL As Double, Mo, Eqm, Mc, hcv_Chimney As Double, A As Double,
ChimneyArea As Single
Dim DryingRateConst As Double, del_M_over_Del_t As Single, AirViscocity As
Double, MR_t  As Double
Dim DryingTime_Eqm As Double, Tz As Double, Chimneybreadth As Double,
HydrualicradiusC  As Double
Dim Z_t As Single, Z As Single, DryingRateConstant As Double, mu_air As
Double, rho_a As Double
Dim ReyNumber As Double, AirConductivity As Double, Prandtl As Double,
Nusselt  As Double
Dim Cpv As Single, Ga, A1 As Double, A2 As Double, P1 As Double, P2 As
Double
Dim hfg   As Double, CpW As Single, F As Double, Cpf, P1_C As Double, P2_C As
Double, DeltaHTz
Dim P3_C As Double, CIntDryingTimeEqm As Single, t, DeltaH As Double
Dim K5 As Double, K6 As Double, del_T_f_over_del_t As Double, Delta_Tz As
Double, K1 As Double
Dim K2 As Double, K3 As Double, K4 As Double, dM_over_dt, dz As Double, L_c,
D_eff
Dim D_o As Single, E_a As Single, InstEff_subZero As Single, H As Date
Dim Ti As Single, Tax As Double, hcv As Double, P3 As Double,
CollectorCross_Section As Double
Dim B_t_o

Const MonolayerSpacing As Double = 0.0000000003, gamma As Single = 290, nd
As Single = 0.7838
Const ad As Single = 0.16, W_M As Single = 18, R As Single = 8.31447, EW As
Single = 4.055, ED As Single = 16.7
```

```
Const SolarConstant As Single = 1367, K = 5, rho_D As Single = 0.15, f_l As Single
= 2385.76
Const rho_f As Single = 1250, L As Single = 2502535.259, pi As Single = 3.1459

Private Sub cmdBegin_Click()
Call Chimney
End Sub

Private Sub column_headers()
  ' With lvwDisplay.ColumnHeaders
    .Clear
    .Add , , "Energy Date", 700
    .Add , , "n", 200
    .Add , , "Hr", 200
    .Add , , "Angle of Incidence", 1000
    .Add , , "Declination", 700
    .Add , , "Insolation", 750
    .Add , , "Qix", 500
    .Add , , "x (cm)", 400
    .Add , , "Tax", 400
    .Add , , "Qcx", 500
    .Add , , "% Eff", 300
    .Add , , "QL", 700
    .Add , , "TL", 500
     .Add , , "Tz", 500
  End With
End Sub

Private Sub Column_Header2()
   With lvwDrying.ColumnHeaders
   .Clear
   .Add , , "Date", 700
   .Add , , "n", 100
   .Add , , "Hr", 100
    .Add , , "Hrs", 100
    .Add , , "Insol", 500
   .Add , , "x", 170
   .Add , , "I_b", 250
   .Add , , "Ti(C) ", 400
   .Add , , "Tx", 400
   .Add , , "Tplen", 500
   .Add , , "Eff.", 500
   .Add , , "Pv", 500
   .Add , , "Ps", 500
   .Add , , "Mc(db)", 370
   .Add , , "Part. dens ", 500
```

```
    .Add , , "Bulk.dens", 500
    .Add , , "Tm (C)", 500
    .Add , , "Tf (C)", 430
    .Add , , "H", 250
     .Add , , "Tz (C)", 500
    End With
End Sub

Private Sub cmdHalt_Click()
End
End Sub

Private Sub cmdStop_Click()
'Unload Me
End
End Sub

  Private Sub Readings()
  Dim n_Trays   As Integer
    Absorptivity = Val(txtAbsorptance.Text)
    Latitude = Val(txtLatitudes.Text)  'in degrees
    TiltAngle = Val(txtTiltAngle.Text) 'in degrees
    FirstDate = "1 Jan 2007"
    StartDate = DateDiff("y", FirstDate – 1, txtStartMonthDate)
    EndDate = DateDiff("y", FirstDate – 1, txtEndmonthDate)
    Mf = CSng(txtTotalMass.Text)
    F = Val(txtFatCOntent.Text)
    CpW = CSng(txtSpecificHeatOfWater.Text)  'Specific heat of water vapour
    Mo = Val(txtInitialMoistureContent.Text)
    Eqm = CSng(txtEqM.Text)
    AirVelocity = Val(txtAirVelocity.Text)
    CollectorHeight = Val(txtCollectorHeight.Text)
    dz = CDbl(txtDryingSlabThickness.Text)
    Chimneybreadth = CSng(txtChimneyBreadth.Text)
    Humidity = Val(txtAirHumidity.Text)
    CollectorWidth = Val(txtCollectorWidth.Text)
    CollectorLength = Val(txtCollectorLength.Text)
    CollectorArea = CollectorLength * CollectorWidth / 100
    Chimneybreadth = CSng(txtChimneyBreadth.Text)
    n_Trays = CSng(txtNumberOfTrays.Text)
    Z_t = CSng(txtChimneyHeight.Text)
  End Sub


‘SUBROUTINE FOR PLENUM CHAMBER TEMPERATURE
  Private Sub Chimney()
```

```
Call Readings    'Calling a sub program
Call txtBrine_Change  'Brine concentration decision box
'DECLARING VARIABLES
Dim HydrualicradiusT As Double, hcv_tunnel As Double, Ga_z, MassFlowRate_z
Dim Lc As Double, Result As Double, StartHour, EndHour, DryingHours,
NumberOfTrays, Mcz
Dim Dryingperiod, t_f, K7 As Double, DryingLayers, t_f_tray, Tf, Qp_chimney,
n_Trays, dryingdepth
Dim Counts, count, HoursInADay, DryingDays, Albedo, R_sub_b,
Delta_Tf_over_Deltat, Fx
Dim Humidity_Z, ShrinkageCoeffi, rho_b_initial, SpecificVolume,
linearShrinkageCoefficient
Dim cosOmega_s, sinOmega_s, Omega_s, Io As Double, h_r, Ho, Ir, Ksky, a_a,
b_b, Id, Ib
Dim DeltaCa, DeltaCb, DeltacL, DeltaE, caZ, cbZ, cLz, DeltaEz, caz1, cbz1,
cLz1, caz2, cbz2, cLz2
` Dim DeltaCaz, DeltaCbz, DeltacLz, I_oZ, I_dz, I_T, T_z, ha_eff
Dim InsolationTotal, InsolationDiffuse, R_b, R_d, R_r, InsolationSurface,
InsolationEffective
Dim PartialVapourPressure, P_s, lnPsOverRs, a_d, cao, ca, cbo, cb, cLo, cL, ca1,
ca2, cb1, cb2, cL1, cL2
Dim InitialSpecificVolume, rho_w, rho_s, rho_p, rho_bo, rho_b, dayhours, td,
Tamb, InsolationDirect
Dim I_scApostrophy, I_o, S_p, S_a, H_o, a_kisangani, b_kisangani, K_t,
a_Actual, b_Actual, I_actual
Dim I_d, I_direct, I_Tt, I_c, CosTheta_h, SinTheta_h, Tantheta_h, Theta_h, H_act
 Dim Ta, h_fp, h_fb, h_w, f_ut, U_t, k_b, t_b, U_b, L_1, L_2, L_3, k_e, t_e, Tp As
Double
Dim U_e, U_L, T_av, E_e, h_eq, h_e, F_apost, T_fpn, TemperatureDiff,
Countloss
 Dim T_fp, epsilon_p, epsilon_g, epsilon_r, Tfp As Single, TiltAngle_radians,
AirColumnHeight
Dim Tpm, mu, K_v, D_h, V, Pr, Re, h_cv, C, N_c, h_p, f_p, F_aposr, Tbm, U_tn,
B, Z_o
 Dim CoverPlate As String, MaterailThickness  As Double
 Dim DeltaM, Delta_t

 'DECLARING CONSTANTS
Const Tsun = 5762, stefan_boltzman = 0.00000056697, StephanBoltmanConstant
= 0.00000005669
Const A_s = –27405.526, B_s = 97.5413, C_s = –0.146244, D_s = 0.00012558,
E_s = –0.000000048502,
 Const G_s = 0.0039381, R_s = 22105649.25, F_s = 4.34903

‘EVALUATING GLOBAL SOLAR RADIATION AND PLENUM CHAMBER
TEMPERATURE
```

```
 StartHour = 8
EndHour = 17
Albedo = 0.2
rho_w = 1000   'Desnity of water
rho_s = 1312  'Dry solid true density of tuna
CollectorArea = CollectorLength * CollectorWidth / 100      'Collector plate area
CollectorCross_Section = CollectorWidth * CollectorHeight
ChimneyArea = Chimneybreadth * CollectorWidth
Dim Insolation As Single
t_f = Mf / (rho_f * CollectorArea)  'Tray thickness
DryingLayers = 2                'Number of trays
t_f_tray = t_f / DryingLayers       'Thickness of trays
Z_o = t_f_tray
B_t_o = t_f_tray / 2              'Half thickness of tray
B_t = B_t_o
Z = Z_o                         'Initialising the thickness of drying material
Call txtBrine_Change
Counts = 1                      'Counter
   lvwDrying.ListItems.Clear
   Call Column_Header2
   lvwDrying.View = lvwReport

   'ENERGY HARNESSING IN THE TUNNEL SECTION
   '======================================
   Call Column_Header3            'A calling procedure
   lvwDrying.View = lvwReport       'Assigning display
   DryingDays = 0                 'Initialising
     Mc = Mo                       'Initialising Moisture content
      For n = StartDate To EndDate       'Loop for the drying dates
         Declination = (23.45 * Sin((360 / 365) * (284 + n) * pi / 180)) 'in degrees
         EnergyDate = DateAdd("d", n – 1, FirstDate)
         Lc = CollectorLength / 100      'Colletcor length
         For Hr = StartHour To EndHour   'Loop for the drying hours
         'Call AirTemperatures    'Air temperature procedures
            If Hr = 7 Then
               InletAirTemperature = 10 + 273.15
               ElseIf Hr = 8 Then
               InletAirTemperature = 20 + 273.15
               ElseIf Hr = 9 Then
               InletAirTemperature = 22 + 273.15
               ElseIf Hr = 10 Then
               InletAirTemperature = 25 + 273.15
               ElseIf Hr = 11 Then
               InletAirTemperature = 27 + 273.15
               ElseIf Hr = 12 Then
               InletAirTemperature = 30 + 273.15
```

```
    ElseIf Hr = 13 Then
    InletAirTemperature = 35 + 273.15
    ElseIf Hr = 14 Then
    InletAirTemperature = 36 + 273.15
    ElseIf Hr = 15 Then
    InletAirTemperature = 38 + 273.15
    ElseIf Hr = 16 Then
    InletAirTemperature = 36 + 273.15
    ElseIf Hr = 17 Then
    InletAirTemperature = 26 + 273.15
    Else
    InletAirTemperature = 20 + 273.15
  End If


Ti = InletAirTemperature        'Assigning the ambient air temperature value to
inlet air temperature
  'Tx = Ti                       'Initialising the value of Tx
  'Tf = Tx                       'Initialising the value of Tf
DryingHours = 12 * DryingDays + Hr – StartHour  'Evaluating the drying
period in hours
  dayhours = Hr – StartHour     'Evaluating the dayhours
  HourAngle = 15 * (12 – Hr)  'Hour angle in degrees
 ' For x = 0 To CollectorLength Step 240  'Loop for collector length
 x = CollectorLength
  Ti = InletAirTemperature         'Initialising value of Ti
  Humidity = Val(txtAirHumidity.Text) 'Assigning values to humidity
  Tx = Ti           'Initialising Tx
  Tf = Tx           'Initialising Tf
  'Evaluation of the angle of incidence
CosTheta_h = Sin(Latitude * pi / 180) * Sin(Declination * pi / 180) +
Cos(Declination * pi / 180) * Cos(HourAngle * pi / 180) * Cos(Latitude * pi /
180)
  SinTheta_h = Sqr(1 – CosTheta_h ^ 2)
  Tantheta_h = SinTheta_h / CosTheta_h
  Theta_h = (Atn(Tantheta_h)) * 180 / pi
CosThetaZ = Cos((Latitude – TiltAngle) * pi / 180) * Cos((Declination) * pi /
180) * Cos((HourAngle) * pi / 180) + Sin((Latitude – TiltAngle) * pi / 180) *
Sin((HourAngle) * pi / 180)

`   sinThetaZ = Sqr(1 – CosThetaZ ^ 2)
ThetaZ = Atn((sinThetaZ / CosThetaZ)) * 180 / pi    'Angle of incidence in
 degrees
  'Angle of refraction
  SinTheta2 = Sin(ThetaZ * pi / 180) / RefractiveIndex
  CosTheta2 = Sqr(1 – SinTheta2 ^ 2)
```

```
ThetaTwo = (Atn(SinTheta2 / CosTheta2)) * 180 / pi    'Angle of refraction in
degrees
  'Parameters for evaluating the transmissivity
rho_subP = ((Tan((ThetaZ – ThetaTwo) * pi / 180)) ^ 2) / (Tan((ThetaZ +
ThetaTwo) * pi / 180)) ^ 2
rho_subS = (Sin((ThetaZ – ThetaTwo) * pi / 180)) ^ 2 / (Sin((ThetaZ +
ThetaTwo) * pi / 180)) ^ 2
Tau = 0.5 * ((((1 – rho_subP) / (1 + rho_subP)) + ((1 – rho_subS) / (1 +
rho_subP)))) * Exp(–K * MaterialThickness / Cos(ThetaTwo * pi / 180))
  TauALphaSubEe = (Tau * Absorptivity) / (1 – (1 – Absorptivity) * rho_D)

'SOLAR ENERGY ON THE EARTHS SURFACE AT DAY N
I_scApostrophy = SolarConstant * (1 + 0.033 * (Cos((360 / 365) * n * pi /
180)))
  cosOmega_s = –(Tan(Latitude * pi / 180)) * Tan(Declination * pi / 180)
  sinOmega_s = (1 – cosOmega_s ^ 2) ^ 0.5
  Omega_s = (Atn(sinOmega_s / cosOmega_s)) * 180 / pi 'in Degrees
  I_o = I_scApostrophy * CosTheta_h
  I_oZ = I_scApostrophy * CosThetaZ
I_dz = I_oZ * Cos(60 * pi / 180)
  I_T = I_oZ + I_dz
R_b = CosThetaZ / (Cos(Latitude * pi / 180) * Cos(Declination * pi / 180) *
Cos(HourAngle * pi / 180) – Sin(Latitude * pi / 180) * Sin(Declination * pi /
180))
  R_d = (1 + Cos(TiltAngle * pi / 180)) / 2
  R_r = (1 – Cos(TiltAngle * pi / 180)) / 2
  I_Tt = (I_oZ * R_b) + (I_dz * R_d) + (I_T * R_r * Albedo)
  I_c = I_Tt * TauALphaSubEe


    'DRYING AIR PROPERTIES
    '====================
    Cpa = 999.2 + 0.143 * (Tx – 273.15)  'Specific heat of air
    mu_air = (0.041 * (Tx) + 0.5924) * 0.00001
    Cpv = 1513.1 * Exp(0.0007 * Tx)
    rho_a = 353.44 / (Tx)
    massflowrate = rho_a * AirVelocity * CollectorCross_Section
    Ga = massflowrate / CollectorCross_Section
   HydrualicradiusT = 2 * CollectorHeight * CollectorWidth / (CollectorWidth
   + CollectorHeight)
    WaterViscosity = 0.3382 * Exp(–0.0197 * Tx)
    ReyNumber = AirVelocity * HydrualicradiusT * rho_a / mu_air
    AirConductivity = (0.0069 * (Tx) + 0.5123) * 0.001
    Prandtl = mu_air * Cpa / AirConductivity
    Re = ReyNumber
    Nusselt = 0.01344 * Re ^ 0.75 / (1 – 1.586 * Re ^ –0.125)
```

```
  hcv_tunnel = Nusselt * AirConductivity / HydrualicradiusT
HydrualicradiusC = 2 * Chimneybreadth * CollectorWidth /
(CollectorWidth + Chimneybreadth)
  hcv_Chimney = Nusselt * AirConductivity / HydrualicradiusC
     B = Val(txtCollectorWidth.Text)
     CollectorHeight = Val(txtCollectorHeight.Text)
     L_c = Val(txtCollectorLength.Text) / 100
     TiltAngle = CDbl(txtTiltAngle.Text)
     TiltAngle_radians = TiltAngle * pi / 180
     Ta = InletAirTemperature
     AirColumnHeight = 0.6
     Humidity = 0.63
     k_e = 0.044   'Glass wool conductivity
     t_e = 0.0554   '1 inch thickness
     U_b = k_e / t_e
     U_e = (L_c / 100 + B) * CollectorHeight * k_e / 100 * t_e
     CpW = 1513 * Exp(0.0007 * Tx)   'Specific heat of water
     Tpm = Ta + 10
     mu = 0.00001718
     K_v = 0.0244
     D_h = 2 * B * CollectorHeight / (B + CollectorHeight)
     rho_a = 353.44 / Ta
     V = 1.2
     Pr = Prandtl
     Re = ReyNumber
     Nu = Nusselt
     h_cv = Nu * K_v / D_h
     C = 365.9 * (1 – 0.00883 * TiltAngle + 0.0001298 * TiltAngle ^ 2)
     N_c = 1    'Number of covers
     h_w = 2.8 + 3 * V
     h_p = Nu * K_v / D_h
     h_r = Nu * K_v / D_h
     f_p = (1 + 0.091 * N_c) * (1 – 0.04 * h_w + 0.0005 * h_w ^ 2)
     epsilon_p = 0.12   'For black nickel on galvanised iron
     'epsilon_g = 0.95
     epsilon_r = 0.05      'Alluminium, polished
     E_e = 1 / ((1 / epsilon_p) + (1 / epsilon_r) – 1)
   T_av = (Tpm + Ta) / 2  'At the start of the calculations, for small
   temperature change (about 10K)
  U_t = (((N_c / ((C / Tpm) * ((Tpm – Ta) / (N_c + f_p)) ^ 0.33)) + 1 / h_w)
    ^ –1) + (0.00000005669 * (Tpm ^ 2 + Ta ^ 2) * (Tpm + Ta)) / ((1 /
    (epsilon_p + 0.05 * N_c * (1 – epsilon_p)) + ((2 * N_c + f_p – 1) /
    epsilon_g) – N_c))

    Countloss = 0
```

```
h_eq = StephanBoltmanConstant * 4 * T_av ^ 3 * E_e   'Equivalent
 convective heat transfer coefficient

 Do                                        'Loop
 CpW = 1513 * Exp(0.0007 * Tx)                  'Specific heat of water
vapour
 rho_a = 353.44 / Tx                       'Density of air
Cpa = 999.2 + 0.143 * (Tx – 273.15)          'Specific heat capacity of
air
 Pr = Prandtl                             'Prandtl number
 Re = ReyNumber                            'Reynold Number
 Nu = Nusselt                              'Nusselt Number
 h_cv = Nu * K_v / D_h
 h_w = 2.8 + 3 * V
 h_p = Nu * K_v / D_h
 h_r = Nu * K_v / D_h
 f_p = 1.058 * (1 – 0.04 * h_w + 0.0005 * h_w ^ 2)
 U_L = U_t + U_b + U_e
 h_e = (h_p + (h_eq * h_r) / (h_eq + h_r))
 F_aposr = 1 / (1 + U_L / h_e)
 Tpm = (I_c + U_L * Ta + h_p * Tx) / (U_L + h_e)  'Top plate
temperature
 Tbm = (h_eq * Tpm + h_r * Tx) / (h_eq + h_r)     'Bottom plate
temperature
 T_av = (Tpm + Tbm) / 2
 h_eq = StephanBoltmanConstant * 4 * T_av ^ 3 * E_e
U_tn = (((N_c / ((C / Tpm) * (Abs(Tpm – Ta) / (N_c + f_p)) ^ 0.33)) + 1 /
h_w) ^ –1) + (0.00000005669 * (Tpm ^ 2 + Ta ^ 2) * (Tpm + Ta)) / ((1 /
(epsilon_p + 0.05 * N_c * (1 – epsilon_p)) + ((2 * N_c + f_p – 1) /
epsilon_g) – N_c))
 U_t = U_tn              'Top heat loss coefficient
 Countloss = Countloss + 1
 Loop Until Countloss = 8
 U_L = U_t + U_b + U_e     'Total heat loss coefficient
Tx = Ta + (I_c / U_L) – (I_c / U_L) * Exp((–B * F_aposr * (x / 100) *
U_L) / (massflowrate * (Cpa + Humidity * CpW)))
Tp = Ta + (I_c / U_L) – (I_c / U_L) * Exp((–B * F_aposr * (L_c) * U_L) /
(massflowrate * (Cpa + Humidity * CpW)))

'DRYING IN THE CHIMNEY SECTION
'============================
D_o = CDbl(txtInfiniteTimeDiffusivity.Text)      'Value of diffusion
coefficient for an infinite temperature (m/s/s)
      'Br = CSng(txtBrine.Text)
      E_a = CDbl(txtActivation.Text) 'Activation energy in J/mol
      'Ea fo dry cured ham is 50001
```

```
        D_eff = D_o * Exp(–E_a / (R * Tp))
        ShrinkageCoeffi = rho_s / (rho_s + Mo * rho_w)
        D_eff_M = D_eff * (1 / (1 + ShrinkageCoeffi * Mc)) ^ 2
        DryingRateConstant = (pi ^ 2) * D_eff_M / (Z ^ 2)
        dM_over_dt = –DryingRateConstant * (Mc – Eqm)
        DeltaM = dM_over_dt * Delta_t
        Mc=Mc+ DeltaM

'FISH TEMPERATURE
  '==================
t = DryingHours * 3600  'drying hours
Delta_t = 3600
   DeltaM = dM_over_dt * Delta_t
   td = dayhours * 3600
 K3 = hcv_Chimney / (Z * rho_f * (Cpf + Mc * CpW))  'Partial differential
 constant
  Tf = T_z – (T_z – Tf) * ((Exp(–K3 * t)))      'Fish temperature

  'MOISTURE CONTENT
  '==================
  If DryingHours = 0 Then
  Mc = Mo
  ElseIf Mc >= 0 Then
c = Mc * Exp(–DryingRateConstant * Delta_t) + Eqm * (1 – Exp(–
DryingRateConstant * Delta_t))
 Else
  Mc = 0
  End If

  PartialVapourPressure = 5144 / Tx    'Vapour pressure
 nPsOverRs = (A_s + B_s * Tx + C_s * Tx ^ 2 + D_s * Tx ^ 3 + E_s * Tx ^ 4)
/ (F_s * Tx – G_s * Tx ^ 2)
  P_s = R_s * Exp(lnPsOverRs)  'Saturation partial pressure
  rho_b_initial = 1050
 rho_w = 1000
 rho_s = 1312
 rho_bo = 1216
 a_d = rho_s / rho_w
 rho_p = rho_s * rho_w * (1 + Mc) / (rho_w + rho_s * Mc)
 rho_b = rho_bo * rho_w * (1 + Mc) / (rho_w + rho_bo * ShrinkageCoeffi *
 Mc)
  'For NumberOfTrays = 0 To n_Trays
    Mcz = Mo
   caZ = cao
   cbZ = cbo
   cLz = cLo
```

```
        With lvwDrying
      .ListItems.Add , , EnergyDate
      .ListItems(Counts).SubItems(1) = n
      .ListItems(Counts).SubItems(2) = Hr
      .ListItems(Counts).SubItems(3) = DryingHours
      .ListItems(Counts).SubItems(4) = Round(I_c, 2)
      .ListItems(Counts).SubItems(5) = x
      .ListItems(Counts).SubItems(6) = Round(I_oZ, 2)
      .ListItems(Counts).SubItems(7) = Round((Ti – 273.15), 2)
      .ListItems(Counts).SubItems(8) = Round((Tx – 273.15), 2)
      .ListItems(Counts).SubItems(9) = Round((Tp – 273.15), 2)
      .ListItems(Counts).SubItems(10) = Round((Efficiency), 2)
      .ListItems(Counts).SubItems(11) = Round(PartialVapourPressure, 2)
      .ListItems(Counts).SubItems(12) = Round(P_s, 2)
      .ListItems(Counts).SubItems(13) = Round(Mc, 5)
      .ListItems(Counts).SubItems(14) = Round(rho_p, 2)
      .ListItems(Counts).SubItems(15) = Round(rho_b, 2)
      .ListItems(Counts).SubItems(16) = Round((Tpm – 273.15), 2)
      .ListItems(Counts).SubItems(17) = Round((Tf – 273.15), 2)
      .ListItems(Counts).SubItems(18) = Round(Humidity, 2)
      .ListItems(Counts).SubItems(19) = Round((T_z – 273.15), 2)
      End With

 Counts = Counts + 1
            'Next NumberOfTrays
  Next x
   DryingHours = DryingHours + 1
   Next Hr
   DryingDays = DryingDays + 1
   Next n
   End Sub

   'SUBROUTINE FOR CALLING THE SIMULATION
Private Sub HeatLossCoefficients()
Call Chimney
Dim Ta, h_w, h_fp, h_fb, h_eq, h_e, F_apost, U_L, U_t, U_b, U_e, T_pm,
T_bm, epsilon_p
Dim epsilon_r, E_e, B, stefan_boltzman, N_u, K_v, m_u, R_e, D_h
End Sub

Private Sub cmdStart1_Click()
Call FishDryerAnalysis  'Call programme for execution
End Sub

Private Sub cmdStop1_Click()
```

```
Unload Me  'Terminate programme
End Sub

Private Sub cmdSave_Click()
Dim Counts As Integer, Br As Single
If Br = 0 Then
Counts = 1
Do While Counts <= lvwDrying.ListItems.count
Adodc1.Recordset.AddNew
With lvwDrying
      Adodc1.Recordset.Fields("Date").Value = .ListItems.Item(Counts)
      Adodc1.Recordset.Fields("n").Value = .ListItems(Counts).SubItems(1)
      Adodc1.Recordset.Fields("Hr").Value = .ListItems(Counts).SubItems(2)
      Adodc1.Recordset.Fields("Hrs").Value =
.ListItems(Counts).SubItems(3)
      Adodc1.Recordset.Fields("Insol").Value =
.ListItems(Counts).SubItems(4)
      Adodc1.Recordset.Fields("x").Value = .ListItems(Counts).SubItems(5)
      Adodc1.Recordset.Fields("UL").Value =
.ListItems(Counts).SubItems(6)
      Adodc1.Recordset.Fields("Ti").Value = .ListItems(Counts).SubItems(7)
      Adodc1.Recordset.Fields("Tx").Value = .ListItems(Counts).SubItems(8)
      Adodc1.Recordset.Fields("Tp").Value = .ListItems(Counts).SubItems(9)
      Adodc1.Recordset.Fields("Eff").Value =
.ListItems(Counts).SubItems(10)
      Adodc1.Recordset.Fields("Pv").Value =
.ListItems(Counts).SubItems(11)
      Adodc1.Recordset.Fields("Ps").Value =
.ListItems(Counts).SubItems(12)
      Adodc1.Recordset.Fields("Mc(db)").Value =
.ListItems(Counts).SubItems(13)
      Adodc1.Recordset.Fields("Part dens").Value =
.ListItems(Counts).SubItems(14)
      Adodc1.Recordset.Fields("Bulk dens").Value =
.ListItems(Counts).SubItems(15)
      Adodc1.Recordset.Fields("Tm").Value =
.ListItems(Counts).SubItems(16)
      End With
      Counts = Counts + 1
      Adodc1.Recordset.Update
   Loop
   MsgBox "Updated complete, Number of records are " &
  Adodc1.Recordset.RecordCount
   End If
   End Sub
```

```
Private Sub txtCoverPlate_Change()
CoverPlate = CStr(txtCoverPlate.Text)

'Notation for GlassCover
 'GLA=Glass
 'ACR=Acrylic
 'PVC=PVC
 If CoverPlate = "GLS" Then
 RefractiveIndex = 1.518
 MaterailThickness = 0.003175
 epsilon_g = 0.94
 ElseIf CoverPlate = "ACR" Then
  RefractiveIndex = 1.49
  MaterailThickness = 0.003175
  epsilon_g = 0.86
 ElseIf CoverPlate = "PVC" Then
 RefractiveIndex = 1.5
 MaterailThickness = 0.001016
 epsilon_g = 0.93
 ElseIf CoverPlate = "FBG" Then
 RefractiveIndex = 1.54
 MaterailThickness = 0.00635
 epsilon_g = 0.75
 ElseIf CoverPlate = "LEXAN" Then
    RefractiveIndex = 1.586
      epsilon_g = 0.97
      MaterailThickness = 0.003175
      ElseIf CoverPlate = "TEFLON" Then
      RefractiveIndex = 1.343
     MaterailThickness = 0.00508
      epsilon_g = 0.97
      ElseIf CoverPlate = "TEDLAR" Then
      RefractiveIndex = 1.46
      MaterailThickness = 0.001016
   epsilon_g = 0.93
   ElseIf CoverPlate = "MYLAR" Then
   RefractiveIndex = 1.64
   MaterailThickness = 0.00127
   epsilon_g = 0.97
     ElseIf CoverPlate = "KYNAR" Then
     RefractiveIndex = 1.413
     MaterailThickness = 0.001016
     epsilon_g = 0.97
     End If
     End Sub
```

```
‘SUBROUTINE FOR DECLARING MEAN INLET AIR
TEMPERATURES
Private Sub AirTemperatures()
Dim Hr As Integer, InletAirTemperature As Single
If Hr = 7 Then
InletAirTemperature = 10 + 273.15
ElseIf Hr = 8 Then
InletAirTemperature = 18 + 273.15
ElseIf Hr = 9 Then
InletAirTemperature = 20 + 273.15
ElseIf Hr = 10 Then
InletAirTemperature = 25 + 273.15
ElseIf Hr = 11 Then
InletAirTemperature = 27 + 273.15
ElseIf Hr = 12 Then
InletAirTemperature = 30 + 273.15
ElseIf Hr = 13 Then
InletAirTemperature = 35 + 273.15
ElseIf Hr = 14 Then
InletAirTemperature = 27 + 273.15
ElseIf Hr = 15 Then
InletAirTemperature = 25 + 273.15
ElseIf Hr = 16 Then
InletAirTemperature = 20 + 273.15
ElseIf Hr = 17 Then
InletAirTemperature = 16 + 273.15
Else
InletAirTemperature = 10 + 273.15
End If
End Sub
```

Appendix A2: The sample simulation results

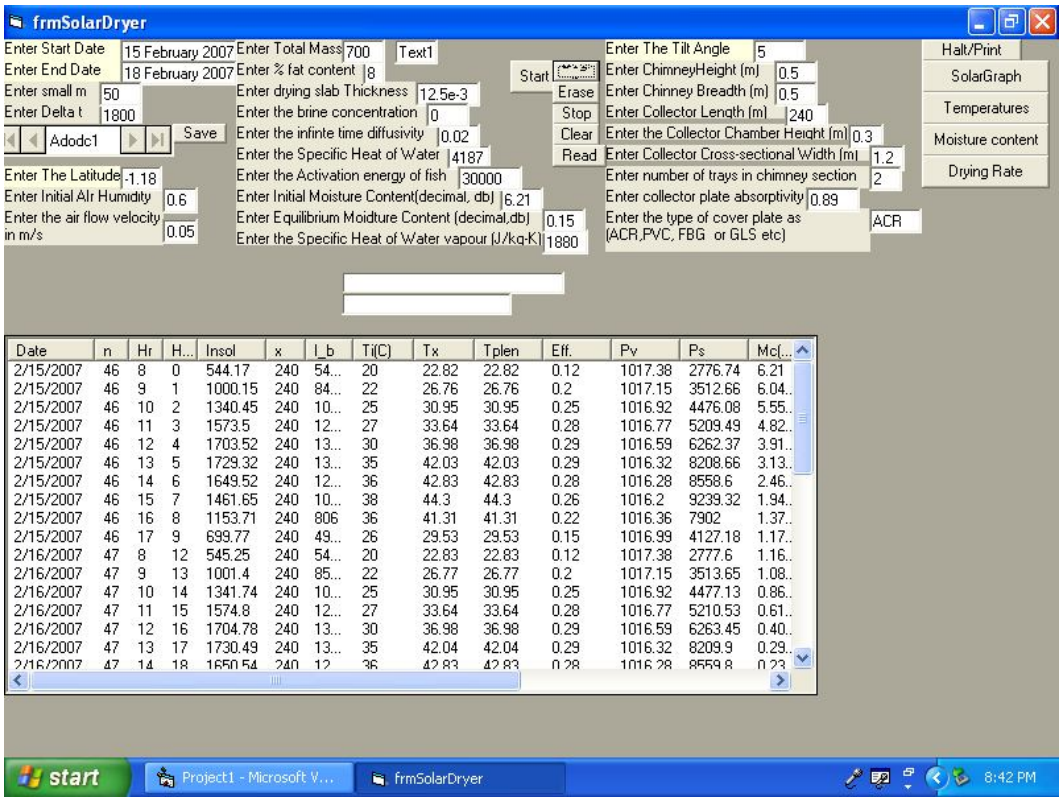

Figure A1: Graphics user inter–phase for the simulation algorithm

Appendix B: Emissivity and Thermal Conductivity Tables

Table B1: Emissivity for different material

Material	Emmisivity
Aluminium: anodised	0.77
Aluminium: polished	0.05
Chromium: polished	0.10
Fabric: Hessian, green	0.88
Fabric: Hessian, uncoloured	0.87
Fibreglass	0.75
Fibre board: porous, untreated	0.85
Fibre board: hard, untreated	0.85
Firebrick	0.68
Formica	0.94
Galvanized Pipe	0.46
Glass	0.92
Hardwood: across grain	0.82
Hardwood: along grain	0.68–0.73
Mortar: dry	0.94
P.V.C.	0.91–0.93
Paint: aluminium	0.45
Paint: oil, black, flat	0.94
Paint: oil, black, gloss	0.92
Paint: oil, grey, flat	0.97
Paint: oil, grey, gloss	0.94
Paint: oil, various colours	0.94
Paint: plastic, black	0.95
Paint: plastic, white	0.84
Paper: black	0.90
Paper: black, dull	0.94
Paper: black, shiny	0.90
Paper: cardboard box	0.81
Paper: green	0.85
Paper: red	0.76
Paper: white	0.68
Paper: white bond	0.93
Paper: yellow	0.72
Plaster	0.86–0.90
Plaster: rough coat	0.91
Plasterboard: untreated	0.90
Plastic: acrylic, clear	0.94
Plastic: black	0.95

Plastic: white	0.84
Plastic paper: red	0.94
Plastic paper: white	0.84
Plexiglass: Perspex	0.86
Plywood	0.83–0.98
Plywood: commercial, smooth finish, dry	0.82
Plywood: untreated	0.83
Polypropylene	0.97
Redwood: wrought, untreated	0.83
Redwood: unwrought, untreated	0.84
Rubber	0.95
Rubber: stopper, black	0.97
Sand	0.90
Stainless Steel	0.59
Stainless Plate	0.34
Steel: galvanized	0.28
Steel: rolled freshly	0.24
Styrofoam: insulation	0.60
Tile: glazed	0.94
Tin: burnished	0.05
Tin: commercial tin–plated sheet iron	0.06
Wood: planed	0.90
Wood: panelling, light finish	0.87
Wood: spruce, polished, dray	0.86

Source: Thermoworks

Table B2: Thermal conductivity of common materials and products

Material/substance	Thermal conductivity, k, (W/mK)
Acrylic	0.2
Clay, saturated	0.6 – 2.5
Cobalt	69
Constantan	22
Copper	401
Corian (ceramic filled)	01.Jun
Corkboard	0.043
Cork, regranulated	0.044
Cork	0.07
Cotton	0.03
Carbon Steel	54

Cotton Wool insulation	0.029
Diatomaceous earth (Sil–o–cel)	0.06
Earth, dry	01.May
Ether	0.14
Epoxy	0.35
Felt insulation	0.04
Fiberglass	0.04
Fiber insulating board	0.048
Fiber hardboard	0.2
Fireclay brick 500^{o}C	01.Apr
Foam glass	0.045
Freon 12	0.073
Gasoline	0.15
Glass	01.May
Glass, window	0.96
Glass, wool Insulation	0.04
Hardboard high density	0.15
Hardwoods (oak, maple..)	0.16
Insulation materials	0.035 – 0.16
Iron	80
Iron, cast	55
Leather, dry	0.14
Magnesia insulation (85%)	0.07
Mica	0.71
Mineral insulation materials, wool blankets ..	0.04
Molybdenum	138
Monel	26
Nickel	91
Plaster, gypsum	0.48
Plaster, metal lath	0.47
Plastics, foamed (insulation materials)	0.03
Plastics, solid	
Plywood	0.13
Polyethylene HD	0.42 – 0.51
Polypropylene	0.1 – 0.22
Polystyrene expanded	0.03
Polyurethane	0.02
Porcelain	01.May

PVC	0.19
Pyrex glass	1.005
Rock, solid	02.Jul
Rock Wool insulation	0.045
Sand, dry	0.15 – 0.25
Sandstone	01.Jul
Silica aerogel	0.02
Silver	429
Steel, Carbon 1%	43
Stainless Steel	16
Straw insulation	0.09
Styrofoam	0.033
Wood across the grain, white pine	0.12
Wood across the grain, balsa	0.055
Wood across the grain, yellow pine	0.147
Wood, oak	0.17
Wool, felt	0.07

Table B3: Actual Five Day Ambient and Plenum Chamber Temperature, ^{o}C for Evaluation of Solar Energy Harnessing by the Optimised Solar Tunnel Dryer

	Inlet Temperature, *OS(a)*						Inlet Temperature, *OS(b)*						Plenum Temperature, *NOSTD*						Plenum Temperature, *OSTD*					
Hr	Day 1	Day 2	Day 3	Day 4	Day 5	Mean	Day 1	Day 2	Day 3	Day 4	Day 5	Mean	Day 1	Day 2	Day 3	Day 4	Day 5	Mean	Day 1	Day 2	Day 3	Day 4	Day 5	Mean
07:00	15.1	14.9	14.8	15.5	15.6	15.2	15.4	15.7	16.9	16.0	16.8	16.2	12.3	12.9	12.7	11.5	11.2	12.1	13.7	14.2	15.2	14.2	13.5	14.2
08:00	19.1	18.1	18.7	19.2	19.3	18.9	19.9	18.9	19.1	18.9	19.5	19.3	13.5	14.1	13.2	12.9	13.1	13.4	14.8	15.4	16.1	15.8	14.5	15.3
09:00	23.7	22.9	23.5	24.1	23.2	23.5	25.2	25.1	24.5	24.9	24.7	24.9	16.1	15.5	15.6	15.4	15.9	15.7	33.6	33.2	34.1	33.7	33.1	33.5
10:00	26.2	26.8	26.9	25.8	25.9	26.3	26.3	25.9	26.8	25.3	25.1	25.9	30.9	30.7	30.5	31.4	31.5	31.0	38.7	37.5	37.3	37.9	37.6	38.0
11:00	29.3	27.5	28.2	27.3	27.5	28.0	29.7	30.5	28.9	29.2	28.9	29.4	37.8	37.5	36.9	37.2	37.1	37.3	46.5	47.8	48	47.2	45.9	47.0
12:00	30.5	31.0	29.6	29.2	30.8	30.2	30.2	29.7	29.5	30.5	30.3	30.0	39.0	38.7	38.5	38.9	39.4	38.9	56.5	55.9	57.1	57.5	54.7	56.4
13:00	32.5	32.7	31.4	31.5	32.7	32.1	31.5	32.8	32.7	32.5	30.7	32.0	40.3	39.5	39.4	39.5	40.3	39.8	55.6	54.6	56.7	54.8	55.3	55.4
14:00	30.2	29.5	30.3	31.1	29.3	30.1	29.9	29.3	31.1	30.2	30.6	30.2	42.1	42.9	42.7	41.8	43.0	42.5	60.1	56.5	55.5	57.9	57.9	57.6
15:00	29.5	29.6	35.8	31.7	29.8	31.3	30.0	35.0	30.8	29.9	30.3	31.2	40.6	40.4	41.2	41.4	41.5	41.0	56.2	55.7	58.2	54.8	54.3	55.8
16:00	25.8	24.5	25.6	24.9	26.8	25.5	26.2	26.8	26.1	26.9	27.2	26.6	38.9	39.4	38.5	39.4	39.2	39.0	46.6	45.7	45.5	45.9	46.2	46.0
17:00	24.3	24.2	25.9	24.7	24.4	24.7	25.2	27.3	28.0	27.5	27.2	27.0	33.7	34.5	34.2	35.1	33.4	34.2	41.1	42.1	42.1	41.4	40.5	41.5
18:00	23.8	22.9	23.5	23.3	22.5	23.2	25.4	26.9	27.2	27.3	26.1	26.6	28.7	27.6	26.9	26.8	27.5	27.5	24.6	25.7	24.8	24.4	24.9	24.9

Appendix C: Fish drying and solar tunnel dryer plates

Plate A1: Drying fish inside the solar tunnel dryer

Plate A2: Fish sample after evisceration

Plate A3: Tilapia Fish before evisceration

Plate A4: Prepared fish samples ready for drying

Plate A5: Solar tunnel dryer undergoing modification after optimisation

Plate A6: Traditional Systems of fish drying

Appendix D: Publications

Appendix D1: Publications in peer reviewed journals

1. **Kituu** M.G, D. Shitanda, C. L Kanali, J. T Mailutha, C.K Njoroge and J. K Wainaina (2009) "The effect of brining on the drying parameters of Tilapia in a glass–covered solar tunnel dryer", Agricultural Engineering International, The CIGR Ejournal, Manuscript number EE 1349, Vol. XI.

2. **Kituu** M.G, D. Shitanda, C. L Kanali, J. T Mailutha, C.K Njoroge and J. K Wainaina, J. O Bonngyereire (2010) "A Simulation Model for Global Solar Radiation and Energy Harnessing By a Solar Tunnel Dryer Agricultural Engineering International, The CIGR Ejournal, Manuscript number 1553, Vol. XII.

3. **Kituu** M.G, D. Shitanda, C. L Kanali, J. T Mailutha, C.K Njoroge and J. K Wainaina (2010) "Thin layer drying model for simulating the drying of Tilapia fish (*Oreochromis Niloticus*) in a solar tunnel dryer", Journal of Food Engineering, Volume, 98(3): 325–331.

4. Oduor–Odote, P. M., Shitanda, D., Obiero, M., and **Kituu**; G .(2010) "Drying characteristics and some quality attributes of Restrineobola Argentea (Omena) and Stolephorus delicatulus (Kimarawali)", African Journal of Food, Agriculture, Nutrition and Development , 10 (8) .

5. G. M. **Kituu,** D. Shitanda, C. L. Kanali, J. Mailutha, C. K. Njoroge, P. M. O Peter Odote (2011) "Artificial Breeding of an Optimised Solar Tunnel Dryer using Genetic Algorithms", International Journal of Sustainable Energy, Volume 30, Issue 6, 1478-646X

Appendix D2: Manuscripts In conferences and workshop proceedings

6. **Kituu** M.G, D. Shitanda, C. L Kanali, J. T Mailutha, C.K Njoroge and J. K Wainaina (2009) "The effect of brining on the drying parameters of Tilapia in a glass–covered solar tunnel dryer" , Paper presented at the 3rd International Conference on Appropriate Technology, Serena Hotel, Kigali, Rwanda, November 2009.

7. **Kituu** M.G, D. Shitanda, C. L Kanali, J. T Mailutha, C.K Njoroge and J. K Wainaina (2009) "Effect of brining on the drying rate of tilapia in a solar tent dryer". Paper presented at the Third JKUAT Scientific, Technological and Industrialisation Conference held at JKUAT campus between 25th and 26th October 2007.

8. **Kituu** M.G, D. Shitanda, C. L Kanali, J. T Mailutha, (2008) "The effect of brining on the drying rate of Tilapia in a solar tunnel dryer" Paper Presented at the 3rd IASTED Conference on "Power and Energy Systems" (AfricaPES, 2008), held at Gaborone, Botswana.

9. **Kituu** M.G, D. Shitanda, C. L Kanali, J. T Mailutha, C.K Njoroge and J. K Wainaina (2009) "A Simulation Model For Global Solar Radiation And Energy Harnessing By A Solar Tunnel Dryer" . Paper presented at the at the 11th Mechanical Engineering Seminar held at the Jomo Kenyatta University of Agriculture and Technology, Juja, Kenya, 1st–3rd April, 2009.

10. G.M **Kituu**, D. Shitanda, C.L. Kanali, J.T. Mailutha, C. K Njoroge, J. K Wainaina, P.O. Odote (2011) "Performance of a Solar Tunnel Dryer Optimised Using Genetic Algorithm in Energy Harnessing and Thin Layer Drying of Fish" . Paper presented at the at the at The IEK Annual International Conference held on 11th - 13th May 2011 at Laico Regency Hotel, Nairobi, Kenya.